Consequences of secondary succession on water availability in Mediterranean areas: a study case in northeastern Spain

Master Thesis

Jeroen Bernhard

26-3-2013

Utrecht University

Faculty of Geosciences

First supervisor:

dr. D. Karssenberg

Second supervisor:

dr. N. Lana-Renault

Contents

List of figures

List of tables

List of Appendices

Preface

In this report, the results of the author's MSc research are discussed. This research is part of the second year of the Hydrology track within the Master program Earth Surface and Water at the Faculty of Geosciences, Utrecht University. The work consists of a literature study, followed by a half year modeling research, starting September first 2012. The study was supervised by dr. D. Karssenberg and dr. N. Lana-Renault.

The completion of this Master Thesis would not have been possible without the help of several people and I would like to take a moment to express my gratitude. First I would like to thank my two supervisors: Derek Karssenberg and Noemí Lana-Renault. From the first moment during our exploratory meeting I had a good feeling about this project. During the entire project you were always available for good advice when I got stuck or had some questions. Communication went very smoothly and despite your busy schedules, I never had to wait long before I got a reaction to my many emails. I remember I followed a bachelor course given by Derek. The course gave an introduction on spatial analysis and GIS, which involved modeling exercises with PC Raster. At first this was quite a frustrating course because my modeling skills were nonexistent. Although I thought I would never master it, I still got quite intrigued by the possibilities of spatial modeling. Little did I know that years later I would be working with a model written by Derek and actually be able to understand what the codes means and apply changes to it. Apart from all the thesis related help Noemí provided, she also helped me when my good friend Google Translate abandoned me and I got completely lost in inimitable Spanish websites. I will never forget the name of the village Jaca is pronounced as "Gaca" and not as "Jaca". To both I would like to say dankjewel and gracias.

Also I would like to acknowledge the help of Rens Van Beek and Yoshihide Wada. Rens has not just been my supervisor during my (somewhat postponed) Bachelor Thesis. I remember many times sitting besides Rens when he helped me with translating my thoughts to (at that time) unintelligible PC Raster code. This made me interested in spatial modeling and for the first time I actually found something about my study that made me enthusiastic. Since then, Rens has been a lecturer of a Master course and he has provided great advice and help with the construction of the vegetation model of this study. I have known Yoshi since my Bachelor project. He provided data on future climate and demand that are part of his PhD work and gave advice on how to implement them in future scenarios. It is too bad that the climate data turned out to be unusable but the demand data give a nice tough to this study. Thank you both.

Finally I would like to thank the people who might not have contributed to this work in a direct way, but still were indispensible in actually completing it. First and foremost my parents. Paps en mams, zonder jullie help en support door de jaren heen was dit natuurlijk nooit gelukt. Jullie staan altijd voor me klaar geven advies en aanmoediging als ik dat nodig heb. Ik heb geen flauw idee hoe ik het verder in woorden uit moet drukken maar ik ben jullie dus heel erg dankbaar. And last but not least I would like to thank my little brother, my roommates and all my friends. Allemaal bedankt voor het luisteren naar mijn geklaag over verschrikkelijke computers en weinig samenhangende verhalen over heel veel water en mooie plantjes en steentjes. Jullie bijdrage heeft vooral gezeten in de afleiding en het misbruiken van mijn niet al te stugge ruggengraat als het gaat om het afslaan van feestjes omdat ik eigenlijk moet studeren.

Allemaal bedankt!

Jeroen

Abstract

Mountainous areas in Europe, especially in Southern regions such as the Spanish Pyrenees, have undergone major depopulation during the past century, which has lead to the abandonment of agricultural fields. These abandoned fields have been colonized by natural species which changed the hydrological characteristics of the area. Studying the hydrological effect of secondary succession in abandoned fields on water yield can be helpful to determine future reservoir management strategies. This work uses a modeling approach to investigate the effects of secondary succession on monthly inflow into the Yesa reservoir (central Spanish Pyrenees). The study focuses on three major elements. First the change in hydrological relevant parameters of the vegetation and soil due to secondary succession is simulated from 1950 until 2050. This is done by simulating the change in aboveground carbon density and organic matter fraction with a logistic Markov-chain model. This Markov-chain model has spatially distributed transition probabilities that depend on terrain characteristics in order to simulate different transition rates depending on the suitability of the terrain. Vegetation and soil parameters are related to carbon and organic matter with equations from literature. Secondly, a hydrological model is used to calculate the discharge flowing into the Yesa reservoir during different stages of the succession. These modeled discharges are analyzed to determine trends in water yield on both monthly and decadal scale. Finally, the calculated future reservoir inflow is compared with reservoir outflow. Analysis of present and future monthly residuals of reservoir in an outflow allows for a simple way of assessing changes in water stress. Results of this study indicate that secondary succession in abandoned fields below 1600 m has been responsible for a decrease in river discharge of over 4% from 1950 to 2005. By 2050, the continuing vegetation growth is expected to cause river discharges to decrease further by more than 5% compared to 1950. Decreases are only noticed from autumn to spring and are not expected to cause a major shortage of water in the reservoir.

1 Introduction

1.1 Problem definition and objectives

Reservoirs store runoff from upstream catchments and take care of the water supply in the lowlands during periods with insufficient river flow and high water demand. Studying processes that affect water availability is helpful to determine future reservoir management strategies. This study is carried out in the Upper Aragón Basin, located in the Pyrenees in North Eastern Spain (Figure 1). Water availability during summer periods in Mediterranean regions is low and depends on the supply of water from upstream reservoirs (López-Moreno et al., 2011). One of these reservoirs is the Yesa reservoir, which stores the water from the Upper Aragón Basin. River discharges have decreased during the last century in the Pyrenees, leading to less inflow into reservoirs such as the Yesa reservoir (e.g. López-Moreno et al., 2004; García-Ruiz et al., 2010). The two major factors influencing fluvial discharge are climate and vegetation cover (Beguería et al., 2003).

Mountainous areas in Europe, especially in Southern regions such as the Pyrenees, have undergone major depopulation during the last century (e.g. Mottet et al., 2006; García-Ruiz &Lasanta, 1990; Lasanta-Martínez et al., 2005). This has resulted in the abandonment of lands that were used for agricultural purposes. These abandoned fields have been recolonized by natural species, which evolved to more mature vegetation stands (e.g. Molinillo et al., 1997; Pueyo & Beguería, 2007). This process is called secondary succession. Several studies have proposed that the hydrological properties of river catchments in the Pyrenees have been altered due to secondary succession in abandoned fields, which has led to decreased river discharge (López-Moreno et al., 2011; Beguería et al., 2003). These authors base this theory on the fact that climate variations alone could not explain the intense decrease in Pyrenean river discharges. Water consumption by urban areas and agriculture areas is not thought to have increased in the mountainous headwaters, which are responsible for the majority of the water supply of the rivers. This leaves revegetation as the most plausible explanation for the hydrological changes. The effect of vegetation on runoff is not fully understood, but the general consensus is that afforestation leads to less runoff due to increased evapotranspiration and infiltration (López-Moreno et al., 2011; Bosch & Hewlett, 1981; Zhang et al., 2001; Cerdà, 1998). Vegetation growth in mountain areas is constraint by abiotic factors, resulting in a spatially varying vegetation pattern of different stages in the succession (Pueyo & Beguería, 2007). This means that in the present, at some locations the vegetation can be expected to have already reached its full potential, while at other locations vegetation is still expanding (López-Moreno et al., 2011). If secondary succession is a still ongoing process, its effects will be noticed in the future.

During the last decades the climate in the region has changed to warmer temperatures and less precipitation (López-Moreno et al., 2008; López-Moreno et al., 2011). This led to higher evapotranspiration rates, different pattern of melt water supply and less runoff of rainwater to rivers (López-Moreno & García-Ruiz, 2004; López-Moreno et al., 2008; López-Moreno et al., 2011). Results of future climate studies indicate that temperatures will continue the rise and precipitation will keep on decreasing for the next century, implying a decrease in water supply to reservoirs (López-Moreno et al., 2008; López-Moreno et al., 2011). Water management is not just dependent on changes in water supply, it is also has to cope with changes in water demand. In case of the Yesa reservoir, the majority of the water is used for irrigation purposes (López-Moreno et al., 2004). Future climate change is expected to cause an increase in irrigation demand (López-Moreno et al., 2011). Other factors influencing demand are irrigation techniques and the amount and type of crops that need to be irrigated. Besides the increased demand due to climate, water demand for irrigation purposes is expected to increase slightly due to irrigation modernization (Lecina et al., 2010).

The combination of decreased water yield and increased water demand can cause water stress, which requires water management of reservoirs to adapt (López-Moreno et al., 2004). Water stress is

the result of changes in vegetation cover, climate conditions and water consumption in a complicated system of interrelated processes. Studying the individual contributions of processes that are related to changes in water stress should be helpful to determine strategies for future land and water management. The objective of this study is to assess the effects of secondary succession in abandoned farmlands on river discharge from 1950 to 2050. This allows determining of the decrease in future water supply to the Yesa reservoir that can be attributed to land abandonment and create a better understanding of processes that are responsible for water stress. This objective can be divided into three research questions:

- What is the reconstructed vegetation cover in abandoned farmlands from 1950 to 2050?
- What is the hydrological response of the system to vegetation growth in terms of infiltration, evapotranspiration and runoff?
- What is the effect of secondary succession on monthly residuals between reservoir inflow and outflow?

Descriptions in literature of land use in 1950 will be used to construct a land use map that is representative for the period of abandonment. Subsequently, secondary succession and soil development from the period of abandonment to 2050 is simulated with a logistic Markov-chain model (Pueyo & Beguería, 2007). In order to simulate the spatio-temporal pattern of succession, this model uses spatially varying transition probabilities that describe the probability that the vegetation of an abandoned field makes the transition to forest. These transition probabilities depend on terrain characteristics to simulate the effect of terrain suitability on vegetation growth. The transition from abandoned lands to shrubs or forest is expressed in changes in carbon biomass and organic matter. Subsequently, vegetation and soil parameters are related to carbon and organic matter with equations from literature. These parameters are then used as input for a hydrological model to calculate river discharge during different stages of the succession for a representative sub catchment of the Yesa reservoir. The modeled runoff, evapotranspiration and infiltration fluxes for the different stages in the succession will be used to analyze trends on both monthly and decadal scale. Finally the modeled discharges of the sub catchment are extrapolated to the entire Yesa catchment and compared with measured present outflow from the reservoir. Analyses of the monthly residuals allows for a simple way of assessing changes in water stress that can be contributed to secondary succession in abandoned fields. In addition to the above, also two scenarios are studied which consider future changes in climate and water demand. This is done in order to put the magnitude of changes in water stress due to land abandonment in the perspective of the changes due to climate variations.

2 Study area

2.1 Location and geomorphology

The study will be carried out in the Upper Aragón Basin, located in the Pyrenees in North Eastern Spain (Figure 1). The basin has an area of 2181 km2 and water that is collected in the basin is retained in the Yesa reservoir (García-Ruiz et al., 2010). Altitudes in the mountainous area range from 500 m in the Yesa reservoir up to 2886 m in the Collarada peak (Vicente Serrano et al., 2005). The Aragón river flows from East to West to the Yesa reservoir and several contributory streams flow in from North to South facing valleys. Modeling the discharge for the entire basin is not possible due to the model complexity and computation time limits. Therefore, a sub catchment is taken that is thought to be representative for the basin and results will be extrapolated to the entire Yesa catchment. This sub catchment is the most Western valley, situated between the village of Jaca and the high mountains North of Canfranc (Figure 1).

From North to South several parallel bands occur of morpho-structural units, which coincide with the general relief of the higher mountain ranges in the North to the lower Inner Depression (García-Ruiz

et al., 2010; López-Moreno et al., 2004; Vicente Serrano et al., 2005). In the most Northern high regions, the Paleozoic rocks of the Axial Pyrenees are located, which mainly consist of limestones, shales and clays. The highest mountains can be found in the more Southern located Inner Sierras, consisting of limestones and sandstones. Water flows from the Inner Sierras to the Eocene Flysch Sector which consists of alternating strongly folded and faulted thin beds of sandstone and marls. The Inner Depression is covered by large terrace deposits dating from the Quaternary Period. The most Southern regions are covered by the Outer Sierras of the pre-Pyrenees, consisting of limestone, sandstone and claystone.

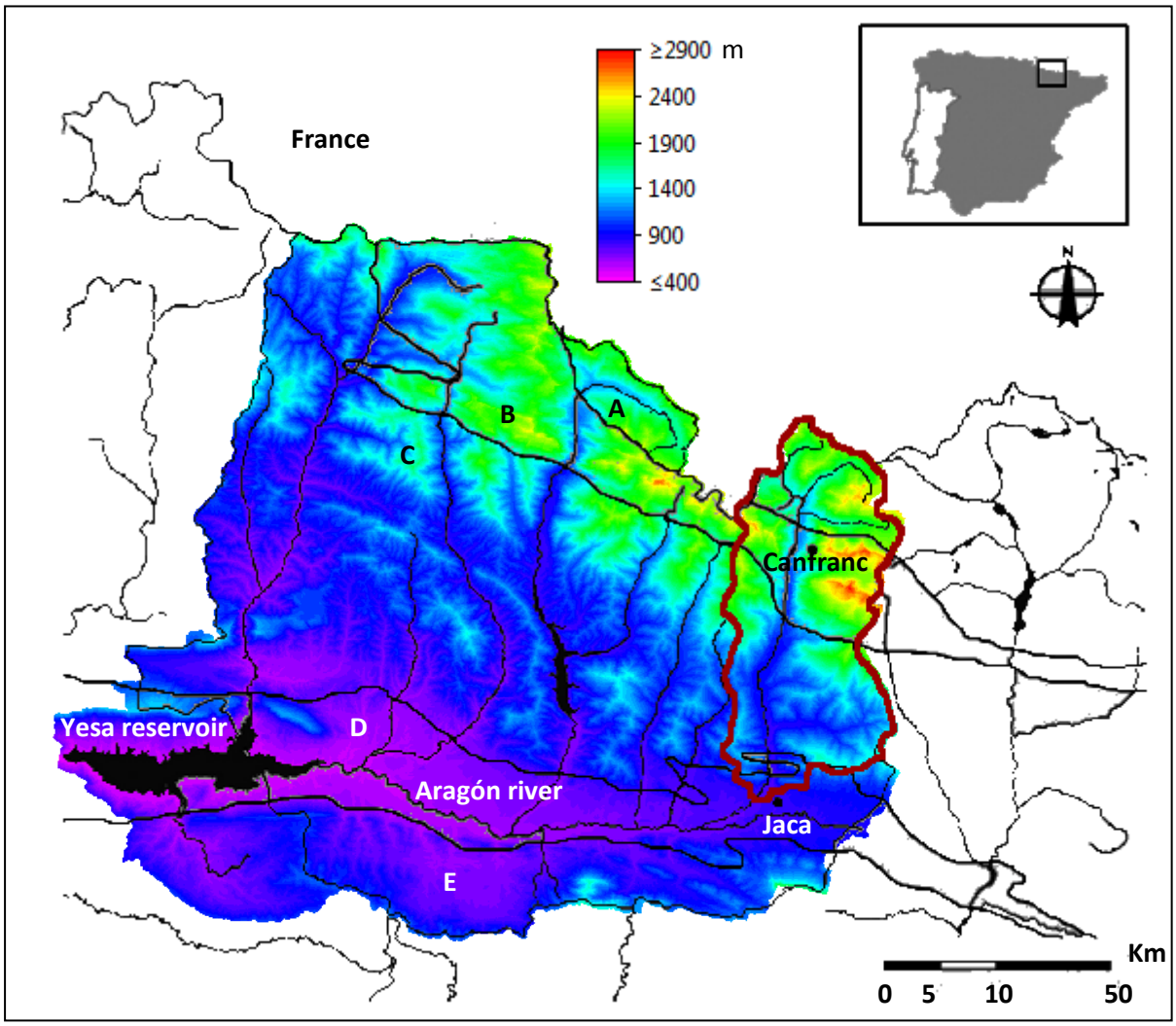

Figure 1 Location of the study area with elevations, the sub catchment used for the modeling is accentuated with the red line. Morpho-structural units are indicated with letters: Paleozoic rocks of the Axial Pyrenees (A),Inner Sierras (B), Flysch Sector (C), Inner Depression (D) and the pre-Pyrenean molasses (adapted from García-Ruiz et al., 2010).

2.2 Climate

In the Pyrenees, several factors cause great climatic heterogeneity over short distances (López-Moreno et al., 2008). The wide range of elevations causes a strong altitudinal gradient from South to North (García-Ruiz et al., 2010). Also the presence of a relatively cool water mass of the Atlantic Ocean on the one side and the relatively warm water mass of the Mediterranean Sea on the other induce a gradient from East to West (López-Moreno et al., 2008). Furthermore, the perpendicular location of the main divide to the predominant circulation of several air masses forms a boundary for several climatic processes (López-Moreno et al., 2008). Due to the altitudinal gradient, precipitation increases towards the North and due to the Atlantic influence it increases towards the West. The mean annual precipitation in the low elevations of the study area is 800 mm and above 1500 m it surpasses 1500 mm (García-Ruiz et al., 2010). The wet season occurs between October and June

(Figure 2). Occasionally intense rainstorms can occur of over 100 mm d^{-1} (Vicente-Serrano et al., 2005). These events happen most frequently in autumn but they can occur year round.

The mean annual temperature in the low altitudes of the Inner Depression is 12 °C and decreases towards the higher elevations in the North (Vicente-Serrano et al., 2005). Summers are relatively warm and winters are cold (Figure 2). The location of the 0 °C isotherm differs in literature (López-Moreno & García-Ruiz, 2004) but for April it was located between 1600 and 1700 m (García-Ruiz et al., 1986 in López-Moreno & García-Ruiz, 2004). This means that above 1600 m, snow can accumulate for a long period. Figure 3 shows a frequency histogram of average snow depth and regional anomalies of snow stakes in the Pyrenean mountain range from the end of April to the beginning of May (López-Moreno, 2005). Several of the snow stakes are located within the Upper Aragón Basin. A decline in snow depth can be noticed from 1985 to 1999 (Figure 3).

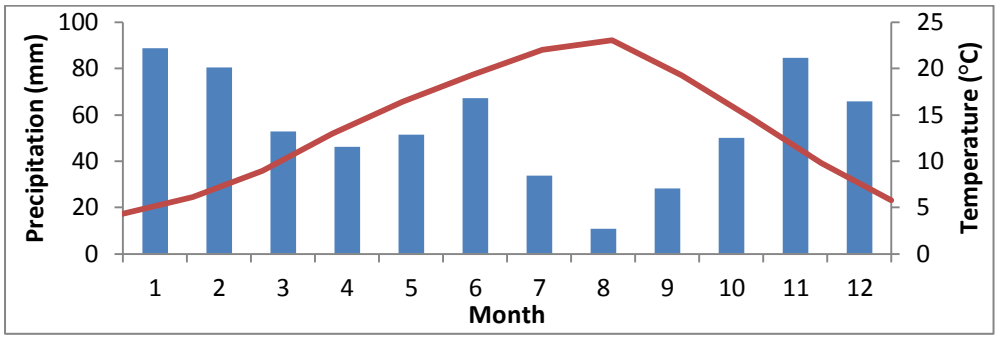

Figure 2 Monthly average mean temperature (red line) and precipitation (blue bars) for the Yesa reservoir over the period from 2009 until 2011 (SAIH Ebro).

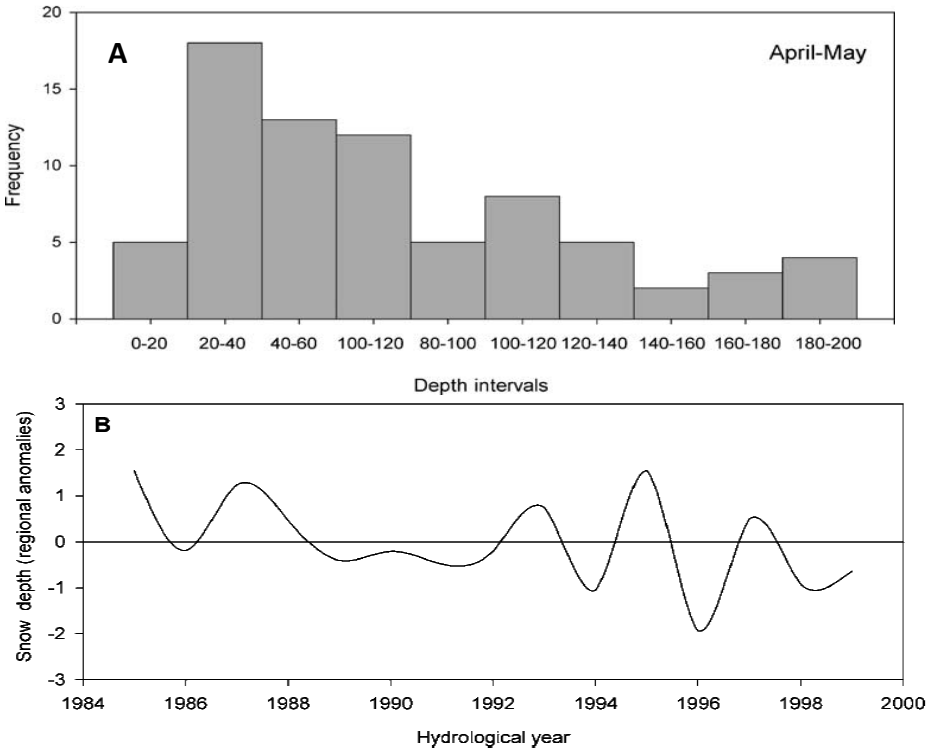

Figure 3 Frequency histogram of average snow depth (A) and regional anomalies (B) of snow stakes in the Pyrenean mountain range from the end of April to the beginning of May (López-Moreno, 2005).

Beguería et al. (2003) studied the effect of climate oscillations and land use changes on stream flow in the Central Spanish Pyrenees. Trends in precipitation, temperature and runoff over the period

from 1940 until 2000 are presented in Figure 4. The results show an initial increase in precipitation and runoff until 1960 after which a decrease can be observed. Temperature shows the opposite pattern, a general decrease until 1970, followed by an increase. Studies have also tried to predict the climate change for the next century with the help of global climate models. Considering IPCC (Intergovernmental Panel for Climate Change) scenarios A2 and B2, temperatures are thought to increase by 2.8 and 4 °C respectively in the 2100 and precipitation is thought to decrease by 10.7% and 14.8% (López-Moreno et al., 2008). These scenarios are based on two different hypotheses on future greenhouse gas emissions, where scenario A2 assumes more emissions than B2. The Southern slopes and highest mountains of the Pyrenees are expected to experience the most pronounced effects of climate change (López-Moreno et al., 2008).

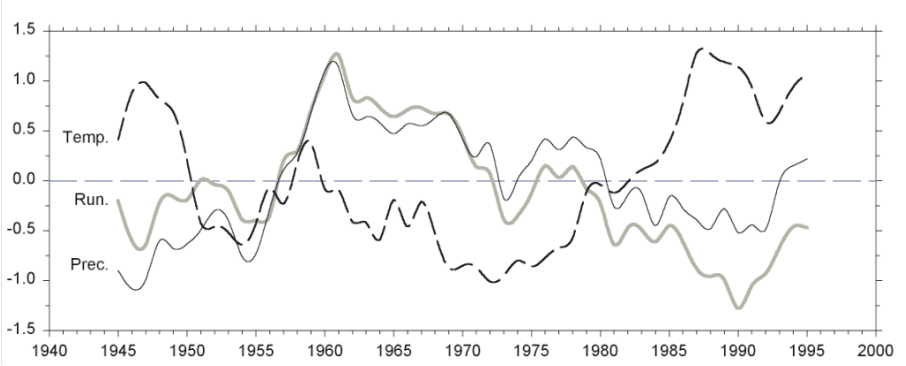

Figure 4 Temperature (Temp), runoff (Run) and precipitation (Prec) indices over the period from 1940 until 2000 in the Spanish Pyrenees. Positive values indicate an increase and negative values a decrease compared to the average (Beguería et al., 2003).

2.3 Land Abandonment and vegetation recovery

2.3.1 Land use change

From the Middle Ages up to the years 1840 to1860, population has constantly grown in the Spanish Pyrenees (Ayuda & Pinilla, 2002 in Lasanta, 2006). The agriculture driven economy was self-supplying and exchanges with areas outside of the system were scarce (Vicente-Serrano et al., 2005). The increased population required more food production and thus more agricultural land and livestock. Natural forests were cut down and replaced by cultivation areas and pastures for livestock, even on steep slopes and high elevations, far removed from villages. Many marginal areas with steep sunny slopes were cultivated under a shifting culture system (Lasanta, 2006). These plots with shifting culture were relatively unproductive compared to permanently farmed fields. However, the best locations were already occupied, leaving the people no choice but to exploit the unfavorable steep slopes with poor physical properties and low nutrient content. Shifting agriculture implied the cutting and burning of natural vegetation on a slope, after which the ashes were plowed into the soil. Subsequently, the field could be cultivated for 1 to 3 years after which a fallow period of 15 to 25 years was needed to restore the nutrient content of the soil. An imbalance between resources for summer pasturing for livestock production on the one hand and cultivatable land for human food supply on the other, led to the development of the transhumance system (García-Ruiz & Lasanta, 1990; Lasanta-Martínez et al., 2005). Mountain and valley production were complementing each other in this system, which was focused on livestock raising. Sheep flocks grazed in highly productive mountain pastures in the summer and during winter months, they were fed with fodder from cultivated land in the Ebro basin (Molinillo et al., 1997). Some of the fields that were suitable for cereal cultivation were cropped, whereas on others, sheep were allowed to graze and fertilize the land.

Drastic economic changes have occurred in the Pyrenees since the 20th century. Depopulation and aging hampered the maintenance of the labor-intensive traditional agriculture system (García-Ruiz & Lasanta, 1990). Better communications introduced competition from other areas such as the plains

of the Ebro valley (Vicente Serrano et al., 2005). This area has better connections to other regions and higher soil fertility. Also, irrigated lands and slopes are gentler, which makes mechanization easier. Other factors that lead to the disruption of the old system in the Pyrenees were tourism and the construction of dams (García-Ruiz & Lasanta, 1990). Tourism caused abandonment of pastures by cattle farmers because they devoted their work to the tourism business.

Depopulation caused the abandonment of agricultural land on steep slopes and high elevations. The traditional self-supplying system changed to a system with very dynamic interactions with the outside world (García-Ruiz & Lasanta, 1990; Lasanta-Martínez et al., 2005). The old, complicated system, directed at supporting large populations of humans and livestock, changed to the recent more simple system that aims at only exploiting the more profitable areas. These profitable areas are the flat valleys bottoms that can be cultivated with tractors (Vicente Serrano et al., 2005).

2.3.2 Spatial distribution of abandonment

A summary of literature with information on fractions of agricultural and abandoned land in the Upper Aragón basin is presented in Table 1. Beguería et. al. (2003) states that at the beginning of the 20th century, cultivated areas accounted for about 30% of the total area below 1600 m in the Central Pyrenees. The same author also mentions that currently 22% of the Upper-Aragón basin is occupied by abandoned fields. These numbers are confirmed by García-Ruiz & Lasanta (1990) who studied air photographs dating from 1956 of several smaller valleys, of which three are located within the Upper-Aragón basin. They also find roughly 30% of land use in elevations below 1600 m devoted to agriculture. Around 17% of the whole area located below altitudes of 1600m was abandoned by 1957 and 20% by 1981. Molinillo et al. (1997) found a cultivated area of 19% of the Aísa Valley during the early 20th century. In total 14% of the valley, located within the Upper Aragón basin, has been abandoned since. The Ijuez river is a small river located in the Upper Aragón basin, North of Jaca. Results of Pueyo & Beguería (2007) show that for the catchment area of this river, initially 61% of the area was cultivated and this part had decreased to 14% by the year of 1977. No more land was abandoned since then. This percentage is much higher than the overall average of percentages of cultivated land in the valleys of the Upper Aragón area for the year 1900. This can be explained by the fact that the study area of Pueyo & Beguería (2007) is relatively small and could have a higher than normal suitability for cultivation. In addition, García-Ruiz & Lasanta (1990) mention that their values are probably underestimations. Where there is information available, over 75% of abandoned land was already left by 1981 and presumably also by 1977. Pueyo & Beguería (2007) state that no land was abandoned after 1977.

Molinillo et al. (1997) describe that the abandoned fields can generally be found on South facing hills with a slope between 20% and 40% and at elevations between 900 and 1200 m. The highest abandoned fields have been found at 1450 m. The fact that abandoned fields can be found at sunny and steep hill slopes at higher elevations is confirmed in other literature (García-Ruiz & Lasanta, 1990; Pueyo & Beguería, 2007; Ruiz-Flano et al., 1991). Ruiz-Flano et al. (1991) mentions that areas facing East and West were also heavily farmed and steepest slope of an abandoned plot was 46%. The abandoned fields in the study area of Pueyo & Beguería (2007) can be found at slightly higher elevations than 1450 m but the majority is found between 800 and 1400 m (figure 1 Pueyo & Beguería, 2007). In Ortigosa et al. (1990) it is described that 44% of reforestation projects in the Pyrenees and Pre-Pyrenees are located in the belt that was formerly exploited, at elevations between 800 and 1100m. The areas below 1100 m also cover 70% of the total reforested area in the Pre-Pyrenees. The distribution of different land use types of the 30% total cultivated area in 1957 found by García-Ruiz & Lasanta (1990) in relation to slope, exposure and elevation is presented in Figure 5. It can be seen that the percentage of abandoned lands increases with slope, elevation and exposure to the South. However, the figure gives no information on the distribution of the terrain characteristics in the total cultivated area. Therefore the figure can only be used as an indicator for unfavorable areas, namely steep sunny slopes in high altitudes.

Study	Where	Cultivated land located below 1600 m around the year 1900	Abandoned land below 1600 m (year if information is available)	Abandoned land below 1600 m by the year 1957
García-Ruiz&Lasanta (1990)	Hecho valley Aragüés valley Aísa valley Biescas valley (all lower than 1600m)	30.18% 22.10% 32.80% 24.39%	23.7% 17.94% 24.56% 13.8% (1981)	21.6% 15.76% 20.01% 11.13%
Molinillo et al. (1997)	Aísa valley	19%	14%	
Beguería et. al. (2003)	Upper Aragón (lower than 1600m)	30%	22%	
Puyeo et. al. (2007)	Ijuez valley (800-2200m)	61%	59% (1977)	45%

Table 1 Summary of literature with information on fractions of cultivated and abandoned land. Molinillo et al (1997) and Beguería et al. (2003) mention no specific year to which the abandoned land percenatges correspond.

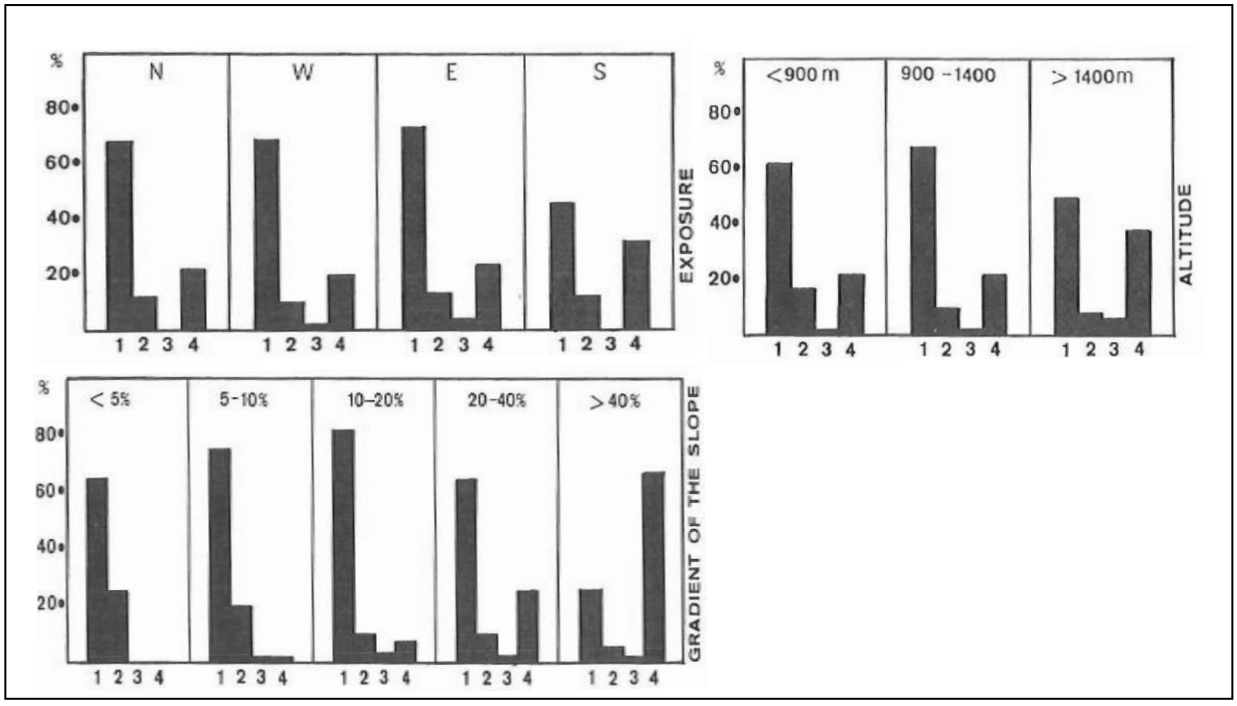

Figure 5 Distribution of agricultural land use types with respect to terrain characteristics in 1957. Top left shows the distribution for different exposure, top right for elevation and bottom left for slope. Considered land use types are cereals (1), cutting meadows (2), grazing meadows (3) and abandoned fields (4) (García-Ruiz & Lasanta, 1990).

2.3.3 Vegetation and secondary succession

Anthropomorphic activities have strongly impacted the vegetation cover. Potentially the montane community between altitudes of 800 and 1800 m should contain forests of *Quercus pubescens* and *Quercus faginea* on the sunny slopes and *Pinus Sylvestris* in the shaded and higher areas. Above 1800 m the subalpine community should mainly be cover by *Pinus uncinata* (Chauvelier, 1987; Rivas Martínez, 1987 in Lasanta-Martinez et al., 2005). The alpine belt begins around 2300 m (López-Moreno et al., 2004).

The sunny hillsides and the upper forestlands were, as previously discussed, deforested for cultivation and expansion of summer pastures since 1900. Most of these agricultural lands have been abandoned by 1981. The abandonment lead to secondary succession and this process is described in literature (Molinillo et al., 1997; Pueyo & Beguería, 2007). In brief, abandoned lands are colonized by herbaceous plants and weeds during the first years (*Brachypodium pinnatum* (L.) P. Beauv., *Carex flacca* Schreb., *Bromus erectus* Huds., *Medicago lupulina* L.). Around 10 to 15 years after abandonment, woody shrubs are introduced, which spread to a generalized cover in the next 20 years (*Genista scorpius* (L.) DC., *Juniperus communis* L., *Rosa* sp. and *Crataegus monogyna* Jacq.). When the plot has abandoned over 35 years woody shrubs start to retreat and herbaceous plants dominate (*Thesium divaricatum, Hippocrepis carnosa, Coronilla minima, Onobrychis hispanica, Rhynanthus mediterraneus, Thymus vulgaris, Cephalaria leucantha, Juniperus communis, Dorycnium pentaphyllum,* and *Linum apressum*). The final succession stage is reached during the colonization by *Pinus Sylvestris* trees and some *Quercus gr. faginea*. Generally this leads to the development of almost monospecific forests of *Pinus Sylvestris*. The years needed for the succession described above, are the generalized years as mentioned by Molinillo et al. (1997). In reality succession rate depends on suitability of the terrain and can take shorter or longer (Pueyo & Beguería., 2007). Molinillo et al. (1997) mentions that secondary succession of cereal fields and meadows can differ slightly in the first 15 years, but after that the succession is very similar.

Instead of the potential situation without human interference, the montane community is now dominated by shrubss with *Echinospartum horridum*, *Buxus sempervirens,Genista scorpius, Echinospartum horridum, Rosa gr. canina,* and *Juniperus communis* and small forests of *Pinus sylvestris*. The subalpine community contains mainly summer pastures with Trifolium *alpinum*, *Festuca rubra*, *Nardus stricta*, *Carex montana* and *Festuca eskia* (Remón, 1997 in Lasanta-Martinez et al., 2005; Molinillo et al., 1997). The land of the Inner Depression is still cultivated and cereal fields and hay meadows prevail.

2.4 Reservoir regime and water demand

The 74 m high Yesa dam was built in 1959 and had an original capacity of 470 hm^3. This capacity has decreased to 450 hm^3 due to siltation (López-Moreno et al., 2004). The Bardenas Canal was built to supply water to irrigated areas in Northeast Spain. It has a maximum capacity of 64 $m^3 s^{-1}$. The lower elevations in the study area experience heavy winter precipitation which produces high runoff and discharge into the reservoir. The accumulated snow above the 0℃ isotherm during winter months melts from April to June. During this period, the Yesa reservoir experiences the highest inflow. During the summer months, low discharges are produced due to little precipitation (Figure 2) and the exhausting of the snowpack. The annual average contribution of the Aragón river and the, much smaller, Esca river is 1327 $hm^3 yr^{-1}$ or 42 $m^3 s^{-1}$ (López-Moreno et al., 2004). The goal of the reservoir management is to reach the maximum stored volume of water by May or June and release this during the dry summer months. This is preferably done by retaining the high flows of the Aragón river during autumn and spring. Maximum storage is not reached during the winter, because a safety margin is kept as a precaution against flooding (López-Moreno et al., 2004). Two storage regimens can be identified in the Yesa reservoir over the past half century. Between the 1960s until the 1970s the reservoir was filled during autumn and spring. The second pattern prevailed during the 1980s and 1990s, when the reservoir was filled more gradually from October to May and more winter

discharge was used. The storage volumes of the second pattern were lower than that of the first. The change in storage pattern is caused by a decrease in reservoir inflow (Figure 6)(López-Moreno et al., 2004). This decrease in river discharge is confirmed by literature (Beguería et al., 2003; García-Ruiz et al., 2010). When river discharge decreases, more water should be stored during winter in order to reach high storage volumes at the end of the spring, explaining the change in storage regimen (López-Moreno et al., 2004). A shift in the month with the highest river discharge from May to April indicates a decrease in snowmelt discharge (López-Moreno & García-Ruiz, 2004). However, the serious decrease in discharge cannot be explained by trends in climate (Beguerí et al., 2003). The diminished water yield has been associated with the increase in evaporation rates in natural vegetation due to secondary succession in abandoned farmlands (López-Moreno et al., 2011; Beguería et al., 2003).

Figure 6 shows that the outflow in the Bardenas Canal has remained fairly constant with a slight positive trend. Since the water resources have decreased, this means that the outflow through the Aragón river has decreased and the water supply to irrigation areas has slightly increased. The water needed for irrigation will increase in the future due to irrigation modernization, despite an increase in irrigation efficiency (Lecina et al., 2010). This is because the intensified productivity of the lad requires more water. The increase in irrigation water demand will be aggravated in the future because climate changes to warmer temperatures and less precipitation (López-Moreno et al., 2011; López-Moreno et al., 2008). The dependence of the Ebro Basin on water supply by the Pyrenees is expected to increase, while the water yield capacity of the Pyrenees is expected to decrease (López-Moreno et al., 2011).

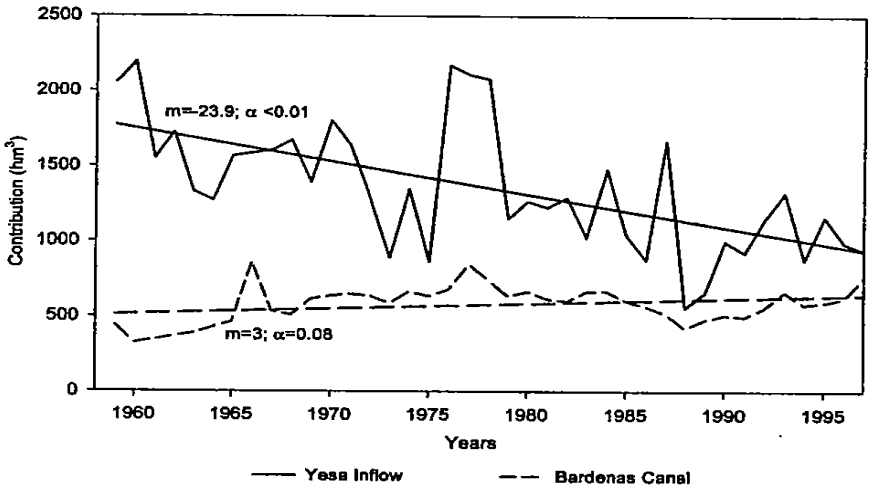

Figure 6 Inflow into the Yesa reservoir and outflow into the Bardenas Canal over the period from 1959 to 1999 (López-Moreno et al., 2004).

3 Methods

3.1 Study methodology

This study focuses on three major elements. First the secondary succession and soil development from the period of abandonment to the future is simulated. Second, the change in hydrological relevant parameters of the vegetation and soil are used to model the effect on the discharge that flows into the Yesa reservoir. Finally the calculated reservoir inflow is compared with outflow for the present and the future to determine periods with water stress. The evolution of the vegetation and soil is simulated with a logistic Markov-chain model. The transition of vegetation from abandoned lands to shrubs or forest is simulated and connected to carbon biomass and organic matter. Subsequently, vegetation and soil parameters are related to carbon growth and organic matter with equations and parameters from literature. Runoff that is gathered into rivers flowing from the upstream catchment is calculated with a hydrological model (Lana-Renault et al., 2010). Climate input is based on measurements from Lana-Renault et al. (2010). Reservoir outflow is obtained from the Centre of Hydrographic Studies (CEH). Future climate and water demand for the extra scenarios with climate change are based on a hypothetical climate scenario and future water demand data from Wada et al. (2012). A schematic overview of the study structure is presented in Figure 7.

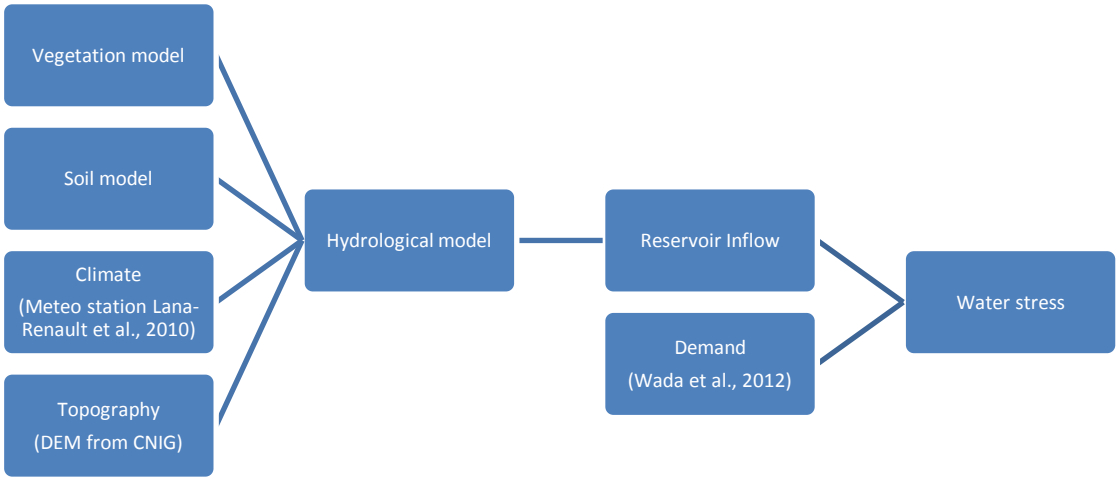

Figure 7 Schematic overview of the study structure. Rectangles indicate the major components and text between brackets shows the source of the data.

3.2 Vegetation model

3.2.1 Model approach

The hydrological model requires several vegetation parameters in order to represent the effect of vegetation cover on rainfall interception and evapotranspiration. A schematic overview of the vegetation model is presented in Figure 8. Vegetation growth is simulated from 1950 until 2050. The starting year of 1950 was chosen because information for the vegetation model is available from 1950, as will be discussed later. The simulation of secondary succession since 1950 requires an initial land cover map representing the situation during that time. This land use map is reconstructed based on information in literature and assumptions. The use of a full process based physical vegetation model would require too much time to develop and also is not required to reach the actual goal of this study. There is no need for a complete description of specific vegetation species and all interrelated mechanisms such as competition and carbon uptake properties. This study is only interested in the evolution of hydrological relevant parameters over time. A Markov chain model is used to model vegetation succession stages, based on transition matrices and logistic model specifications from Pueyo & Beguería (2007). Subsequently, these succession stages will be linked to carbon biomass and parameter values (Figure 10).

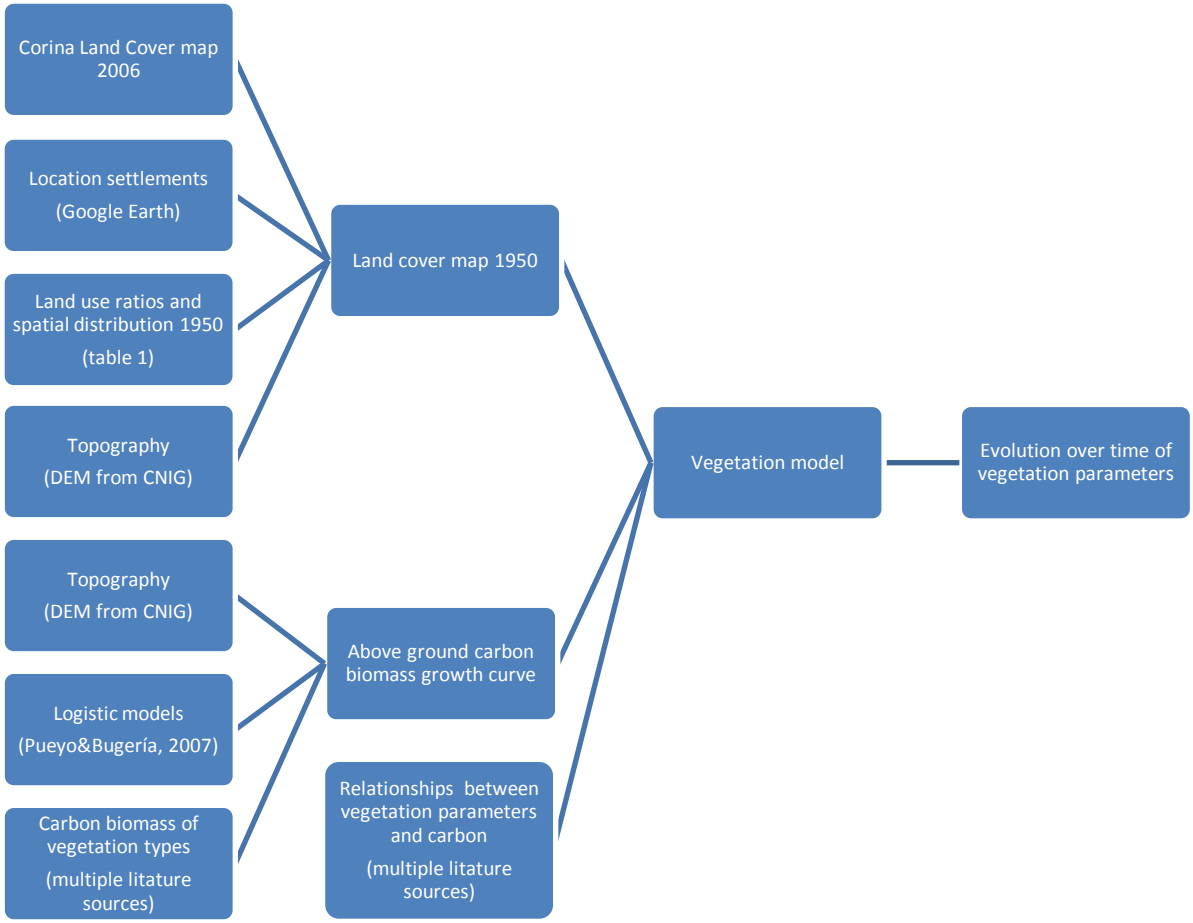

Figure 8 Schematic overview of the vegetation model. Rectangles indicate the major components and text between brackets shows the source of the data.

3.2.2 Land use map

Digital land cover maps, such as the modern Corina Land Cover maps (CLC, 2006), are not available for the year 1950. Air photographs are available for 1957 (Pueyo & Beguería, 2007), but are not an option either due to the considerable size of the catchment and the therefore needed large amount of photographs. To circumvent these problems, the reconstructed land use map will be based on assumptions and descriptions of land use during 1950 from literature (Table 2). Land abandonment of former farmlands is assumed to have been the only changing factor since 1950. The present land use map (CLC, 2006) is used to describe land use in the unchanged areas. Locations of formerly abandoned farmlands are determined based on present land use, elevation, slope and distance to nearest settlement. The information on elevation and slope is retrieved from the DEM from the National Centre of Geographical Information (CNIG). Locations of settlements are retrieved from Google Earth.

Description	Assumption	Source or explanation
Year of abandonment of Agricultural lands	1950	As can be seen in Table 1, the majority of agricultural lands were already abandoned before 1957. For simplicity reasons, all fields are assumed to be abandoned at the start of the simulation period.
Remainder of the area that is not assumed to have been formerly abandoned farmland	Equal to CLC 2006	The remainder of the area is assumed to have remained unchanged. Pueyo & Beguería, (2007) mention that the fraction of natural areas that have been transferred to farmland is negligible. Hence a land use map of the present can be used to describe land use in 1950.
Present land use of formerly abandoned farmland	Natural shrubs and forest	Abandoned areas are all assumed to have been revegetated. Hence they are covered with shrubs or forest in the present.
Maximum slope of abandoned farmland	46%	Ruiz-Flano et al. (1991) mention that the steepest found slope of an abandoned plot was 46%.
Determining factor for the exact location of abandoned farmland when all conditions are met.	Nearest to settlement	The least favorable areas were abandoned first, followed by areas that were better suitable (García-Ruiz & Lasanta, 1990). This means that the best locations are still exploited and the areas located closest to settlements will have higher chance of being traditionally cultivated than further removed slopes (Mottet et al., 2006). It is assumed that flat slopes would be cultivated before steep slopes (Mottet et al., 2006). However, when the distance to town was shorter, steeper slopes became cultivated too. Therefore, distance to settlement is assumed to be more important than slope, as long as slopes are below 46%.
Total percentage of abandoned farmland below elevations of 1600 m since 1950	24%	Agricultural lands cover 6% of the area below 1600 m on CLC 2006. Based on the information in Table 1, agricultural lands are assumed to have covered 30% before 1950. The difference between the present situation and 1950 must be the percentage of abandoned lands.
Percentage of abandoned farmland below elevations of 1200 m	18%	The majority of abandoned agricultural lands are, as previously mentioned, located in altitudes between 800 and 1200 m. This study assumes this majority to be 75% of total abandoned area.
Percentage of abandoned farmland between elevations of 1200 m and 1400 m	4.8%	Cultivation above 1400 m was scarce because these areas are far removed from roads and settlements (García-Ruiz & Lasanta, 1990). This study assumes that 95% of agricultural land was located below 1400 m.
Percentage of abandoned farmland between elevations of 1400 m and 1600 m	1.2%	This study assumes that 95% of agricultural land was located below 1400 m. This leaves 5% for above 1400 m.

Table 2 Overview of the conditions and assumptions used to reconstruct a land use map that includes a representative spatial distribution of abandoned farmlands for 1950.

The workflow for the reconstruction of the locations of formerly abandoned farmland for the land use map of 1950 is presented in Figure 9. The present land use map (CLC, 2006) is used as a starting map. Some currently uncultivated areas on CLC 2006 are assigned as abandoned farmland until a total of 30% of the area below 1600 m is either cultivated or abandoned. Slopes of farmlands cannot be steeper than 46%. In succession, the cells with the shortest distance to any settlement will be selected. Furthermore, 75% of the abandoned area must lie below 1200 m, 20% between 1200 m and 1400 m and 5% between 1400 m and 1600 m. The result of this method might not be the exact land use of 1950, but the spatial distribution of the land cover is thought to be representative for 1950. The fact that most abandoned areas are located in South facing slopes turns out by itself since Southern exposures are overrepresented in the Flysch sector, located between altitudes of about 800 and 2200 m.

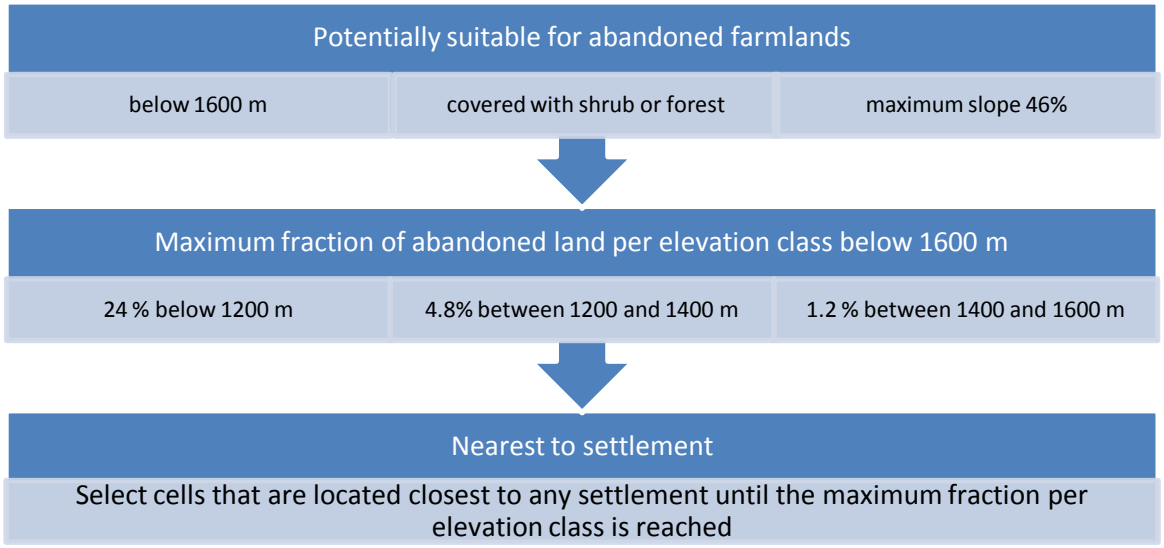

Figure 9 Workflow for determining the locations of formerly farmlands. Explanations for the conditions can be found in Table 2.

3.2.3 Secondary succession model

An overview of the used workflow to model secondary succession is presented in Figure 10. Pueyo & Beguería (2007) use Markov chains and logistic multivariate regression to model secondary succession after farmland abandonment in a small river catchment within the Upper Aragón basin. Where Pueyo & Beguería calculate probabilities and transition times to succession stages, in this study these succession stages are assumed to represent aboveground carbon densities. The model is run many times and the average carbon biomass from many runs gives a carbon biomass growth curve over time. Subsequently vegetation parameters required by the hydrological model are calculated with relationships between these parameters and the estimated carbon biomass. The logistic models of the succession model only consider naturally revegetated areas. However, the reforestation projects are mostly located in suitable locations where the pioneer stage will be relatively short. Also the dominant planted trees were pines (Ortigosa et al., 1990), the same as the considered tree type in the model. Therefore, it is assumed that the growth of natural and planted trees in abandoned areas is relatively similar and both can be simulated by the same model.

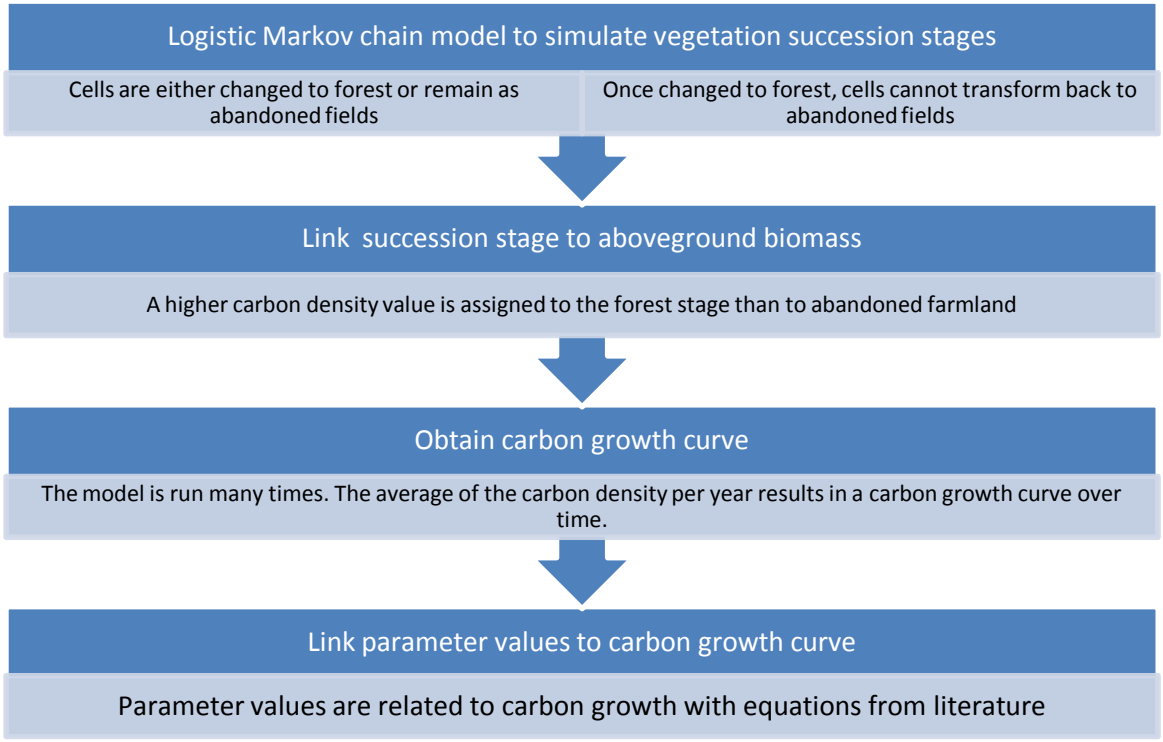

Figure 10 Workflow of the secondary succession model.

3.2.4 Aboveground carbon estimation

Secondary succession in mountain areas is limited by abiotic factors. Such factors are nutrient availability, radiation , temperature , soil moisture and slope (Picon-Cochard et al., 2006; Davis et al., 1999 and Pueyo & Beguería, 2007). In suitable places, succession is fast, land is progressively occupied and the forest state is reached in relatively short time compared to unsuitable places, where the forest state might even never be reached. Pueyo & Beguería (2007) developed a method to calculate the expected transition time from abandoned land to forest, based on terrain characteristics in a small catchment within the upper Aragón basin. The used variables that are explanatory for the suitability for succession are elevation, slope, topographic index and potential radiation. The elevation is an important factor for precipitation and temperature as higher altitudes generally have higher amounts of rainfall and lower temperatures (Beniston, 2006). Hydrological and erosion mechanisms are controlled by slope gradients, which influence the potential energy at a location (Florinsky et al., 1996). The slope and topographic index determine the availability of nutrients and soil moisture at a location. The topographic index is calculated by:

$$TI = \ln\left(\frac{A_s}{\tan\beta}\right) \qquad \text{Eq. 3.2.4.1}$$

Where TI is the topographic index, A_s is the upslope catchment area of a pixel divided by the area of the specific pixel and β the slope (°). Topographic index is used in numerous studies that try to explain spatial distribution of vegetation by terrain characteristics (Moore et al., 1993; Gessler et al., 2000). It can be seen as a kind of wetness index that describes the amount of water that can be accumulated by an area. Potential radiation determines temperature and evaporation, which affects on its turn the availability of soil moisture. It can be influential on growth speed since *Pinus Sylvestris* trees grow slower on sunny slopes (Gracia et al., 2002). In order to determine the potential radiation, Pueyo & Beguería use the Potrad 5.1 model (Van Dam, 2000) which is written in PCRraster dynamic modeling language. Potrad 5.1 (Van Dam, 2000) is also used in this study to estimate the potential radiation for the succession model.

Pueyo & Beguería analyzed air photographs dating from 1957, 1977 and 2002 to determine the percentages of land that were cultivated, abandoned, covered with shrub, planted forest and natural forest. Based on this analysis vegetation maps and transition matrices were made that describe the ratios of abandoned land that are covered by shrubs and forest in three time intervals. Logistic regressions were performed for the transitions between two consecutive maps. The logistic models with the relevant variables are presented in Table 3. The β parameter that results from one of the logistic models can be used to create a transition probability map for the corresponding time interval. The transition probability (tp_t) of the transition from shrubs to forest per cell is calculated by the formula similar to Augustin et al. (2001):

$$tp_t = \frac{\exp(\beta)}{1+\exp(\beta)} \qquad \text{Eq. 3.2.4.2}$$

This transition probability corresponds to the entire time interval between two vegetation maps by Pueyo & Beguería (2007), which is about 20 years. In Pueyo & Beguería (2007), the yearly transition probability is calculated by dividing the period probability by the amount of years. When using this method, the probability is overestimated due to the effect of compounding (Briggs & Sculpher, 1998). Hence, in this study the yearly transition probability (tp_1) is calculated with the formula given by Briggs & Sculpher (1998):

$$tp_1 = 1 - (1 - tp_t)^{\frac{1}{t}} \qquad \text{Eq. 3.2.4.3}$$

Where t is the amount of years corresponding to the observation interval of the period transition probability. Pueyo & Beguería (2007) used solely logistic model b (Table 3) for the stochastic simulation of the secondary succession from 1950 to 2002 (pers. com. Pueyo & Beguería, 2012). Model b corresponds to the transition from shrubs to forest in the observation period from 1957 to 1977. The fact that the model describes transition from shrubs to forest while it is used to describe the transition from abandoned land might seem confusing. This is because the authors initially set all abandoned fields to shrubs at the start of their simulation (pers. com. Pueyo & Beguería, 2012). The model is, however, used to simulate the transition of vegetation from the moment of abandonment. The probabilities obtained with model b were also thought to be representative for the years beyond 1977. In this study logistic model c (Table 3) is incorporated in the stochastic simulation as well. The yearly transition probability following from logistic model b is taken as representative for the period 1950 to 1977 and for the period from 1977 to 2050, model c is taken as representative. As vegetation growth continues, transition probabilities should decrease because the vegetation in the more suitable locations has already approached the end stage of the succession. In Pueyo & Beguería, (2007) this change in transition probability after 1977 is neglected while there is information available. In this study it is assumed that incorporating model c for the period beyond 1977 should result in more accurate results.

Variable	β
Part (b)	
Intercept	9.711
Slope gradient	−7.036
Topographic index	0.05
Potential radiation	−0.870
Part (c)	
Intercept	7.539
Slope gradient	−6.328
Topographic index	−0.123
Potential radiation	−0.622

Table 3 Logistic models with explanatory variables for parameter β, used to calculate the probability maps for the periods from 1950 to 1977 (b) and 1977 to 2002 (c). Adopted from Pueyo & Beguería (2007).

The probability maps show the probability of a certain cell to transform from the initial state to forest. Random fields containing values drawn from a uniform distribution between zero and one for each cell are created for each timestep of a year. The random value of each cell is compared with the transition probability. When the random value is lower than or equal to the transition probability, the cell is transformed to forest. When it is higher, the cell is left unchanged. Once a cell has changed to forest it will not change back. In this study estimated average aboveground carbon biomass densities are assigned to the succession stages of abandoned land and forest. Subsequently, the simulation is repeated 100 times in order to obtain the average outcome. For each cell the average aboveground carbon biomass (C_a) (Kg m^{-2}) is taken per year in order to create a carbon growth curve. Initially, the cells will have a carbon density corresponding to grass (0.3 Kg m^{-1}). Subsequently the cells will transform to a *Pinus Sylvestris* forest (6.5 Kg m^{-1}), which is the end vegetation type of the succession (Pueyo & Beguería, 2007). Carbon densities of different succession stages with corresponding literature source are presented in Table 5. Plots are, as previously mentioned, either abandoned as pastures or cereal fields (Molinillo et al, 1997). Grasses and weeds are either already present, or they colonize within the first few years. Therefore, grass is taken as the cover of abandoned land.

3.2.5 Vegetation parameters

The hydrological model requires several vegetation parameters in order to represent the effect of vegetation cover on rainfall interception and evapotranspiration (Table 4). The parameters values are calculated using equations that relate the specific parameter value to aboveground carbon density. An exception to this method is the calculation of maximum stomatal conductance, as will be explained later on. The pioneer vegetation types during the early stages of the succession will have different growth characteristics than the trees that settle later on. Considering only one single growth equation for trees would result in unrealistic parameter values during the early stages of succession. Therefore, the equations and parameter values in a cell change once the carbon density value surpasses the threshold value of 3 Kg C m^{-2} for shrubs (Table 5). As long as vegetation in a cell has not surpassed the shrub stage, the vegetation parameter is solely calculated with the shrub equation. Once the cell has reached the forest stage, the remainder of the carbon is used for the growth of trees and the calculated parameter value is added to the parameter value of shrubs. This method allows the representation of the effect that understory has on a parameter value. Also, it helps to prevent the occurrence of huge abrupt changes in parameter values at the transition point between the shrubs and forest stage.

	Parameter	Symbol (unit)
Hydrological model	Leaf Area Idex	LAI (m^2 m^{-2})
	Maximum Interception Storage	I_c (mm)
	Albedo	A (-)
	Vegetation Height	H (m)
	Maximum Stomatal Conductance	g_s (mm s^{-1})

Table 4 Overview of the required vegetation parameters by the hydrological model.

Parameter (unit)	Succession stage	Value	Source or explanation
C_a (Kg m^{-2})	Grass (abandoned farmland)	0.3	Maximum carbon density found in subalpine grasslands in Pyrenees (M. T. Sebastià, personal communication, 2006 in Montane et al., 2007)
	Shrubs	3	Average between conifer and legume type shrub in Pyrenees and Central System mountains of Iberian peninsula (Montané et al., 2007)
	Forest	6.5	Stem carbon mass of a 49 year old *Pinus Sylvestris* in the Upper Ebro basin (Bravo et al., 2008). Aboveground carbon density for trees is almost equal to Stem carbon mass (Arora & Boer, 2005)
g_s (mm s^{-1})	Grass (abandoned farmland)	6	Rounded average of values for crops and grasses (Breuer et al., 2003)
	Shrubs	4	Rounded average of values for dry shrub species (Breuer et al., 2003)
	Forest	2.5	The average value for *Pinus Sylvestris* trees (Breuer et al., 2003)
a_{wl} (Kg C m^{-2})	Shrubs	0.3	Chosen because this results in a value of 4 for LAI for full grown shrubs (C_a = 3)
	Forest	0.65	Cox (2001)
a_{00} (-)	All	0.18	Cox (2001)
k (-)	All	0.5	Cox (2001)
$a_{0\infty}$ (-)	Shrubs	0.2	Cox (2001)
	Forest	0.1	Cox (2001)
a_{s0} (-)	Shrubs	0.8	Cox (2001)
	Forest	0.3	Cox (2001)
$a_{s\infty}$ (-)	Shrubs	0.5	Cox (2001)
	Forest	0.15	Cox (2001)

Table 5 Parameter vales for different succession stages with corresponding literature source.

Vegetation height (H), is directly related to aboveground carbon mass with equations from Arora & Boer (2008). For crops (shrubs) the equation yields:

$$H = (C_a)^{0.385} \qquad \text{(Eq. 3.2.5.1)}$$

Where H is the vegetation height (m) and C_a above ground carbon density (Kg m^{-2}). For trees, the equation for vegetation height changes slightly to (Arora & Boer, 2005)):

$$H = 10 \cdot {C_a}^{0.385} \qquad \text{Eq. 3.2.5.2}$$

Leaf area index, LAI (m^2 m^{-2}), is calculated with an equation from the physically based vegetation model TRIFFID (Cox, 2001):

$$LAI = \left(\frac{C_a}{a_{wl}}\right)^{\frac{3}{5}} \qquad \text{Eq. 3.2.5.3}$$

Where a_{wl} (Kg C m^{-2}) is a plant functional type (PFT) dependent parameter. Maximum interception storage (I_c) (mm) can be linearly related to LAI (De Jong & Jetten, 2007). De Jong & Jetten (2007) performed an extensive literature research and came up with the relationship between LAI and I_c for a combination of grass and shrubs:

$$I_c = 0.3063 \cdot LAI + 0.5753 \qquad \text{Eq. 3.2.5.4}$$

For a mix of pine species under which *Pinus Sylvestris* De Jong & Jetten (2007) found:

$$I_c = 0.282 \cdot LAI \qquad \text{Eq. 3.2.5.5}$$

Also snow-free albedo of the vegetation (a_0) (-) can be related to LAI by an equation from the TRIFFID model (Cox, 2001):

$$a_0 = a_{00} \exp\{-k \cdot LAI\} + a_{0\infty}(1 - \exp\{-k \cdot LAI\}) \qquad \text{Eq. 3.2.5.6}$$

Where a_{00} (-)is the soil albedo, $\exp\{-k \cdot LAI\}$ (-)represents the fraction of incident light which passes through the soil surface and $a_{0\infty}$) (-) maximum canopy albedo. Due to the shape of this equation, a gentle transition in albedo from shrubs to trees is impossible. When snow is present, the equation changes slightly and the snow covered vegetation (a_s) (-) is calculated by (Cox, 2001):

$$a_s = a_{s0} \exp\{-k \cdot LAI\} + a_{s\infty}(1 - \exp\{-k \cdot LAI\}) \qquad \text{Eq. 3.2.5.7}$$

In this case, both the snow covered soil albedo (a_{s0}) (-) as well as the maximum snow covered vegetation albedo ($a_{s\infty}$) (-) are dependent of the plant type.

Maximum stomatal conductance describes the maximum amount of water that passages through the stomata of plant leaves over time. It is dependent on environmental conditions such as CO_2 partial pressure and soil moisture and therefore hard to measure (Breuer et al., 2003). No relations have been found that describe a change in stomatal conductance of a species during the different growth stages of a plant. Stomatal conductance for herbs, forbs and grasses is generally higher than that of trees. Maximum stomatal conductance is simulated in the same way as carbon mass is simulated. In case a cell is transformed to forest, it is assigned a value of 2.5 mm s^{1} and otherwise it is left to 6 mm s^{-1} (Table 5). The hydrological model uses stomatal conductance to calculate canopy (or surface) resistance. The values obtained from Breuer et al. (2003) represent stomatal conductance of the leaves. This means that the stomatal (or leave) resistance first has to be corrected for the active LAI in order to get canopy (or surface) resistance (FAO. 56). Robinson & Ward, (2000) give values for canopy resistance for several land covers. In order to get values for canopy resistance in the same range as Robinson & Ward, (2000), stomatal conductance is multiplied by 4. Considering soil moisture content at or above limiting point, this results in canopy resistance values of 41, 62.5 and 100 s m^{-1} for covers with grass, shrubs and forest respectively.

3.2.6 Parameterization for the remaining area

The areas that are not classified as abandoned fields also need to be parameterized. Parameter values are assigned in a relative similar way to the abandoned fields, except for that there is no variation over time. In other words, this area is assumed to have remained unchanged since 1950. The spatial variation in parameter values depends on the vegetation cover on the CLC 2006 land use map. Values for C_a and g_s are assigned to each class on the CLC. Subsequently, parameter values are calculated with the same equations as used in the succession model. The table with used values for C_a and g_s per land cover class on CLC 2006 can be found in Appendix 1.

3.2.7 Simplifications and assumptions

Changes in subalpine regions are not considered and no differentiation is made between naturally revegetated areas and reforestation projects. The disappeared shifting culture also has resulted in a change in vegetation cover above the lowered tree line. A warmer climate could result in a shift of the tree line as well. Some information is available on abandoned land in (sub) alpine regions (e.g. Tappeiner & Carnusca, 1993), but not enough in order to make accurate assumptions on how to model vegetation changes in this area. Reforestation projects have been numerous in the area and the emergence of these new forests should have a similar hydrological impact as that of the natural secondary succession. The majority of these planted forests are situated in the belt that was previously exploited, between elevations of 800 and 1100 m (Ortigosa et al., 1990). Generally the more suitable locations with smooth slopes were chosen and the most common tree types were pines such as *Pinus Sylvestris*. No information has been found that could be used to make estimates on the percentage of forestation projects that were located in formerly cultivated or natural areas. Forestation projects in areas that were not formerly exploited are not considered in this study.

3.2.8 Reproducing results of Pueyo & Beguería (2007)

Reproducing the results of Pueyo & Beguería (2007) with the data that was provided by the authors through email correspondence proved to be difficult. When calculating the potential radiation with the Potrad 5.1 model and the DEM of the Ijuez catchment (provided by the authors), the values did not match with those of the potential radiation map used as input for the logistic models used by the authors. For example, when the output of the Potrad 5.1 model is expressed in GJ instead of kJ (as reported in Pueyo & Beguería, 2007) and multiplied by 2, the values did match (except for some decimals) with the potential radiation map used by the authors. Other explanatory variables needed some correction as well before values were in acceptable accordance (Table 6). These corrections were determined with a trial and error method. It is assumed that the logistic models in Pueyo & Beguería (2007) are correct and usable, as long as input variables are scaled to the values of the maps used by the authors.

Variable	Correction
Potential radiation	Multiplied by factor 2 and values expressed in GJ instead of kJ.
Slope	Divided by 1.85
Topographic index	Added a value of 0.8

Table 6 Corrections made to the calculated explanatory variables before used in the logistic models.

3.3 Soil model

3.3.1 Model approach

The soil parameters that are required by the hydrological model are presented in Table 7. Several parameters are assumed to change with the vegetation transition in abandoned farmlands, while others are kept constant. Parameters are kept constant because modeling their change in relation to vegetation cover would be to complex and time consuming, or not enough reliable information is available on how to model the change. The change in the vegetation dependent parameters is based on the organic matter fraction of the soil. Soils covered with forests tend to have higher organic matter content than soils with less vegetation (Navas et al., 2005). Soil porosity is correlated to organic matter and this relation is used to model the change in soil parameters with secondary succession in abandoned farmlands. An overview of this approach is presented in Figure 11.

In this study several hydrological parameters of the soil are estimated with the help the European Soil Database version 2.0 (ESDB v2), Navas et al. (2005) and the model ROSETTA version 1.0 (1999). The European Soil Database (ESDB v2) provides a soil map containing information on textural classes, Van Genuchten parameters (1980) and soil depth on a scale of 1 km. The work of Navas et al. (2005) provides information on two soil types present in a nearby catchment with shrub and forest cover. The soil model ROSETTA consists of five hierarchical pedo transfer functions for the estimation of Van Genuchten (1980) parameters, saturated and unsaturated hydraulic conductivity (Schaap et al., 2001). Pedo transfer functions translate basic soil data into hydraulic properties. The hierarchical approach allows a broad range of estimates with very limited input data. As more input data is available, estimations of the hydraulic properties become more accurate. ROSETTA can already estimate the hydrological parameters of the soil with only the use of textural classes of the ESDB v2. Percentages of sand, silt clay as well as bulk density are added to the input of textural classes, in order to improve accuracy the estimations. Subsequently the Van Genuchten parameters can be used to calculate water retention at certain suction pressures, required by the hydrological model.

Parameter	Symbol	Change or Constant
Saturated conductivity	Ksat	+
Saturated conductivity for infiltration	Kinf	-
Field capacity	$\theta_{(333)}$	+
Limiting point	$\theta_{(500)}$	+
Wilting point	$\theta_{(15000)}$	+
Porosity	θ_s	+
Soil depth	DR	-

Table 7 Overview of the soil parameters that are required by the hydrological model. The column on the right indicates whether the parameters change with vegetation cover (+) or are kept constant (-).

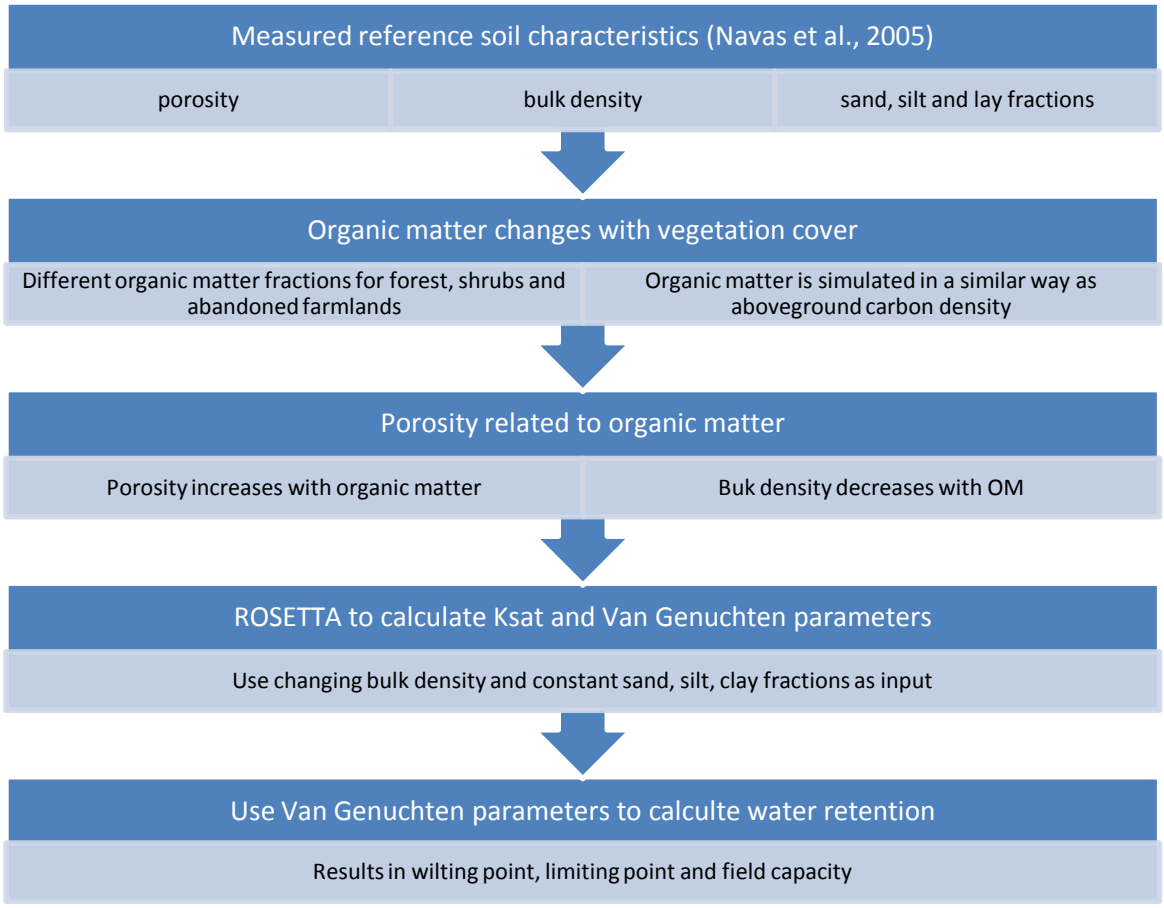

Figure 11 Workflow for the calculation of the change in soil paramters with vegetation cover.

3.3.2 Changes in hydraulic properties due to vegetation growth

The estimations of hydraulic properties of the soil by ROSETTA are independent of the vegetation cover. A change in vegetation cover however, has consequences for the soil characteristics as well. One of the ways vegetation influences soil properties is through the increase of organic matter (OM) which affects the soil through aggregation. An increase in organic matter means a decrease in bulk density and hence porosity (Soane, 1999). The organic matter is predicted in the same way as aboveground carbon with percentages (Table 9) of OM for land covered by abandoned crops and land where the vegetation cover has made the transition to forest.

Vegetation cover	Soil Organic Matter (%)	Source
Forest	5.9	Navas et al. (2005)
Shrubs	5.4	Navas et al. (2005)
Abandoned farmland	5.0	Lasanta et al. (2006)

Table 8 Soil Organic Matter (OM) percentages and corresponding literature sources for different vegetation covers.

The hydrological soil and erosion model Caleros adapts relationships from Soane (1999), Chaney & Swift (1984) and Rachman et al. (2003) to describe the change of porosity with change in organic matter. This is done by varying the OM between zero and ten percent and assuming a tentative mean for OM of 4%:

$$f = 1 + \tan\left(\frac{OM}{0.04} - 1\right) \qquad \text{Eq. 3.3.2.1}$$

Subsequently the obtained factor f is multiplied with both the intersect (y_o) and slope b of the models in Table 9. This yields the relative change in porosity compared to the porosity when OM is 4% (C_{rel}):

$$C_{rel} = (f \cdot b \cdot OM) + (f \cdot yo) \qquad \text{Eq. 3.3.2.2}$$

	Porosity θs [m3·m-3]
y0	0.809
b	0.048

Table 9 Intercept (y_0) and slope (b) of relative change in soil porosity with organic matter content (%). Adapted from Van Beek et al. (in prep.). Values are based on Soane (1999).

In this study the difference in porosity between the two soils is assumed to be solely caused by the change in OM. Eq. 3.3.2.3 implies that C_{rel} equals 1 (no change) when OM is 4%. This means that when the porosity is known for a soil with 4% OM($\theta_{OM4\%}$), porosity (θ_s) values for soils with different OM can be calculated by multiplyingC_{rel}:

$$\theta_s = C_{rel} \cdot \theta_{OM4\%} \qquad \text{Eq. 3.3.2.4}$$

Table 2 in Navas et al. (2005) presents average values for soil properties of soils covered with shrubs and forest. The average porosity of the shrub and forest soil is 0.5605, the average OM is 5.65% and the average bulk density is 1.15 g cm^{-3}. These averages can be seen as a kind of reference values for the soil properties. Using these reference values, Eq. 3.3.2.5, Eq. 3.3.2.6 and Eq. 3.3.2.7 can be solved for $\theta_{OM4\%}$ and subsequently porosity can be calculated for every OM. The differences between sand, silt and clay fractions of the shrub and forest soils in Table 2 of Navas et al. (2005) are neglected in this study. The soil texture is assumed to consist of the average of the two soils and not to change with vegetation cover. When the soil texture is assumed to remain unchanged and the porosity does, the bulk density of the soil is altered. Bulk density (ρ_b) is dependent on the density of the soil grains (ρ_s) and the porosity:

$$\rho_b = (1 - \theta_s) \cdot \rho_s \qquad \text{Eq. 3.3.2.8}$$

A value of 2.65 g cm^{-3} for ρ_s follows from the reference average bulk density and porosity of the shrub and forest soils in the equation above (Eq. 3.3.2.9). A change in porosity due to a change in OM means a changed bulk density. The average sand, silt and clay fractions together with bulk density values are used as input for ROSETTA to calculate Van Genuchten water retention parameters and hydraulic conductivity. The parameters are used to calculate water retention at field capacity, wilting point and limiting point with Van Genuchten (1980):

$$\theta(h) = \theta_r + \frac{\theta_s - \theta_r}{[1 + \alpha h^n]^{1-1/n}} \qquad \text{Eq. 3.3.2.10}$$

Here $\theta(h)$ (cm^3/cm^3) is the water content at a certain pressure head (cm), θr and θs (cm^3/cm^3) are residual and saturated water contents, respectively. Variables α (1/cm) and n are curve shape parameters. Wilting point ($\theta_{(15000)}$) describes the minimum water content beyond which plants are

no longer capable of subtracting moisture from the soil. Field capacity ($\theta_{(333)}$) describes the maximum amount of water a soil can hold against gravity forces after excess water has drained away. Finally, limiting point ($\theta_{(500)}$) is the water content at pressure head h=500 cm, from this point water uptake by plants declines linearly to zero at wilting point.

The above described method allows the storage capacity and the saturated hydraulic conductivity of the soil to change with a transition in vegetation cover. The input parameters for ROSETTA for different OM fractions are presented in Appendix 2 and the resulting soil parameters for the hydrological model in Appendix 3. Porosity and bulk density values for soils covered with shrubs and forest correspond fairly well with the values found by Navas et al. (2005).

3.3.3 Parameterization for the remaining area

Similar to the vegetation parameters, soil parameters for the areas that are not assigned as formerly abandoned areas are assumed to have remained constant over time. The spatial variation is dependent on the ESDB V2 texture map, elevation as well as vegetation cover. First the texture map of the ESDB V2 divides the catchment in two classes, roughly coinciding with locations of high mountains and lower valleys. No useable information is available on soils at high altitudes in the study area. Therefore, the rough relation is emphasized and all soils above 2000 m are assumed to consist of texture class 2 of the ESDB V2 (medium grainsize). Below 2000 m the soil parameters are assumed to be dependent on the vegetation cover. The CLC map is divided into three classes: forest, shrubs and grasses and bare soil. Subsequently, OM fractions from Table 8 are assigned to each class where bare soil is considered to have low OM, comparable to abandoned crops. Sand, silt and clay fractions are thought to be equal to those used in the soil model for abandoned areas. Subsequently soil parameters are calculated with the same method as the soil parameters of the abandoned areas. The resulting soil parameters values are presented in Appendix 3.

3.3.4 Soil depth

Soil depth (SD) can be retrieved from the ESDB V2 but this soil map is at a very large scale and soil classes cover a wide range of soil depths. It is assumed that very steep slopes and elevations far above the tree line have shallow soils. Due to the course scale and large depth classes of the ESDB V2, the variation in soil depth on local slopes is not included. Also, soils that are covered with forest are generally deeper than soils with shrub cover (Navas et al., 2005). Therefore, new classes are made and added to the soil depth map of the ESDB V2, based on the smaller scaled DEM and CLC map. Classes are based on slope, elevation and present land use on CLC 2006 (Table 10).

Description of the soil class	Soil depth	Source or explanation
Slopes steeper than 200%, bare rock cover on CLC 2006 or elevations above 2000 m	5 cm	Images from Google Earth show that the high elevations and very steep slopes generally are covered with rocks, mosses and scarce grass. This leads to the assumption of little or no soil present in these conditions.
Slopes between 40 and 200%	25 cm	The work of Navas et al. (2005) shows that soil depths in locations with slopes steeper than 40%, all belonged in the shallowest soil class (less than 25 cm)
North facing slopes with forest cover on CLC2006 with slopes less than 40%	75 cm	North facing soils with forest cover are generally deeper than 50 cm and sometimes exceed depths of 75 cm (Navas et al., 2005)
Elevations below 800m and slopes less than 5%	140 cm	Valley bottoms have very deep soils (García-Ruiz & Lasanta, 1990).Valley bottoms are assumed to be located below 800 m and have shallow slopes of less than 5% based on Google Earth. Depths are set to 140 cm, conform the very deep soil class of the ESDB V2.
Remainder of the area	50 cm	Soil profiles taken North of Jaca at elevations between 1000 and 1200 m generally had a depth of 50 cm (Navas et al., 2002)

Table 10 Descriptions of the soil depth classes, used to create the soil depth map.

3.3.5 Assumptions and simplifications

No useable information has been found on the hydraulic conductivity for infiltration in the area, let alone on how it changes during vegetation transition from abandoned fields to forest. There are studies that conclude infiltration must change due to changes in stoniness, OM and roots. but no values are provided (Ruis-Flaño et al., 1992). Therefore, the value for hydraulic conductivity for infiltration used by Lana-Renault et al. (2010) is adopted and remained constant. Lana-Renault et al. (2010) obtained this value by calibration of the same hydrological model as is used in this study.

Soil depths can change due to lateral transport of sediment by erosion and deposition. These processes are definitely altered when vegetation cover changes after abandonment (e.g. Lasanta et al., 2006; García-Ruiz, 2010; Sauer & Ries, 2008). Also the process of soil formation by bedrock weathering influences the soil depth (Van Beek et al., in prep.). These processes are not included in this study because their complexity makes it too time consuming to model. Instead soil depth is assumed to be constant over time. Later transport of sediment could have been modeled with the revised Morgan, Morgan and Finney method (Morgan, 2001). The model of Cox (1980) could have been used for bedrock weathering, as is done by the model Caleros (Van Beek et al., in prep).

3.4 Hydrological model

In order to calculate the inflow into the reservoir, an existing hydrological model is used (Lana-Renault et al., 2010). The input parameters for soil and vegetation have already been discussed. The used model is a process-based distributed hydrological model that predicts surface runoff. The model is written in the PCRaster Python scripting language (Karssenberg et al., 2007). Hydrological processes are simulated by several stores that are interconnected by water fluxes. Evapotranspiration is modeled with the Penmann-Monteith method (Allen et al., 1998), infiltration with Green-Ampt, subsurface flow trough soil storage with Darcy's law and overland flow is routed though the local drainage network. The effect of topography on radiation and a maximum surface storage are included as well. Grid size is 25 m and the model works with an hourly timestep.

3.4.1 Snow

Snow accumulation was not incorporated in the original model, while there is snow present in the study areas during winter time (López-Moreno, 2005). Therefore, a snow model was added to the hydrological model. Accumulation and melting of snow are simulated with a degree-day method and parameter values from Seibert, (1997) (Table 11). When the temperature at timestep t ($T_{(t)}$) (h) is lower than freezing point (TT)(˚C), precipitation that has passed interception (P) (m), will not be available as surface water (SW) (m), but stored as snow and added to the snow cover that was already present ($SC_{(t-1)}$)(m). Snow cover in water equivalent at a certain timestep ($SC_{(t)}$) (m) is calculated by:

$$SC_{(t)} = \begin{cases} [SC_{(t-1)} + P + Refreezing] & if\ T_{(t)} \leq TT \\ [SC_{(t-1)} - Snowmelt] & if\ T_{(t)} > TT \end{cases} \quad \text{Eq. 3.4.1.1}$$

Where $Snowmelt$ (m) is the amount of molten snow and $Refreezing$ (m) is the amount of refrozen water that was stored in spaces between the snow crystals. When the temperature is higher than the freezing point, the snow will be subjected to melting. $Snowmelt$ is linearly dependent on a melting factor ($CFMAX$)(m °C^{-1} h^{-1}) and the difference between TT and $T_{(t)}$. $Snowmelt$ cannot exceed the amount of snow present at the beginning of the timestep:

$$Snowmelt = \begin{cases} \begin{cases} CFMAX \cdot (T_{(t)} - TT) & if\ Snowmelt \leq SC_{(t-1)} \\ SC & if\ Snowmelt > SC_{(t-1)} \end{cases} & if\ T_{(t)} > TT \\ 0 & if\ T_{(t)} \leq TT \end{cases} \quad \text{Eq. 3.4.1.2}$$

In case the temperature is below freezing point, the liquid water that was stored in spaces between the snow during the previous timestep ($SF_{(t-1)}$) (m) partly refreezes. This refreezing depends on the refreeze coefficient (CFR) (-):

$$Refreezing = \begin{cases} [CFR \cdot SF_{(t-1)}] & if\ T_{(t)} \leq TT \\ 0 & if\ T_{(t)} > TT \end{cases} \quad \text{Eq. 3.4.1.3}$$

In case the combination of molten snow and precipitation is smaller than the water holding capacity of the snow that is still present, both are potentially subject to evaporation. The amount of liquid water that is stored in spaces between the snow at a certain timestep ($SF_{(t)}$) (m) is calculated by:

$$SF_{(t)} = \begin{cases} [SF_{(t-1)} + P + Snowmelt - Refreezing - E] & if\ SF \leq CWH * SC \\ [CWH * SC] & if\ SF > CWH * SC \end{cases} \quad \text{Eq. 3.4.1.4}$$

Not more water can be stored than the water holding capacity of the snow, which is dependent on SC and a capacity coefficient (CWH) (-). If the water holding capacity of the snow is exceeded, the remainder of the water is available for infiltration as surface water (SW) (m):

$$SW = \begin{cases} [P + Snowmelt - (CWH * SC)] & if\ SW \geq 0 \\ 0 & if\ SW < 0 \end{cases} \quad \text{Eq. 3.4.1.5}$$

No information on parameter values have been found for the study area. Therefore, parameter values for the model are based on the average of the ranges used by Seibert, (1997)(Table 11).

TT (°C)	CFMAX ($m°C^{-1} h^{-1}$)	CFR (-)	CWH (-)
0	0.0055	0.05	0.10

Table 11 The parameters for sub model used to calculate the amount of snow based on the averages of the ranges used by Seibert (1997).

3.5 Climate input

Besides the soil and vegetation input parameters, the model is fed with meteorological data. No free hourly climate data was available for the study area. Precipitation, temperature, wind velocity, relative humidity and incoming short wave radiation were measured with a meteorological station in a nearby catchment by Lana-Renault et al. (2010) for the years 2005 and 2006. The data from this station are used as input for this study although the catchment is located several kilometers to the East. The lateral spatial variation is assumed to be negligible but the influence of elevation on climate is incorporated. Lapse rates are used to simulate the spatial distribution of the climate with elevation. Rolland (2003) states that there is a general seasonal trend in vertical lapse rates in alpine regions. For mean temperature the summer lapse rate is roughly 0.65°C per 100 m and during winter months around 0.5°C per 100 m. These values correspond well to the different lapse rates found in literature for the Pyrenean rage by López-Moreno & García-Ruiz, (2004) of 0.6°C per 100 m García-Ruiz et al., (1985), 0.56°C per 100 m (Del Barrio et al., 1990) and 0.49°C per 100 m (Lampre, 1998). For the study area a lapse rate was found of 0.53°C per 100 m García-Ruiz et al., 1985). The lapse rates of Rolland (2003) will be used since these separate the summer and winter period. Basist & Bell (1994) studied the statistical relationship between topography and precipitation. Results show that elevation, slope and exposure of mountain ranges affect on the precipitation but that the relationships tend to differ between climate regions. With a lack of a true suitable relation for the Pyrenees, a simple lapse rate of 0.55 mm km-1 change in elevation is used. This is based on Pfeffer (2003) and Fontaine et al. (2002) who use and find a change of 0.55 mm km-1 for Austrian Alps and 0.5 mm km-1 for Wyoming respectively. The used lapse rate results in a total annual precipitation of over 1.5 m in the highest regions, corresponding well with the value reported by García-Ruiz et al. (2010). Examples for simulated temperatures and precipitation at different elevations are presented in Appendix 4 and Appendix 5.

3.6 Simulation time and water stress

The catchment area is relatively large and the time steps of the model are small, which results in long computation times. Therefore the model is not run continuously from the period of abandonment until dates far in the future. Instead the model is run for one hydrological year at several intervals from the period of abandonment until years in the future. A hydrological year starts in July and ends in June. The starting year is 1950 because this is the year where the transition matrices for the vegetation model start. Subsequently, hydrological years are modeled with intervals of 25 years up to the year 2050 with the exception of the year 2000. Instead of the year 2000, the year 2005 is taken because the climate variables were measured during that year. This means that the simulated hydrological years are 1950, 1975, 2005, 2025 and 2050. In order to make sure that the initial conditions at the start of the modeling year are representative, the model will be run twice with the same climate input and the resulting soil moisture content will be used as initial condition for the second run.

Changes in future water stress will be assessed by comparing monthly reservoir inflow and outflow. Reservoir inflow is determined by extrapolation of the discharge from the sub catchment North of Jaca to the entire Yesa catchment, as explained below. Outflow from the Yesa reservoir for the hydrlogical year 2005- 2006 is obtained from the Centre of Hydrographic Studies (CEH). The residuals between reservoir inflow and outflow due to different scenarios are evaluated. This method allows for a simple way of assessing the contribution of secondary succession in abandoned fields to water stress. In order to put the influence of revegetation in perspective of the influence of climate change,

also two extra scenarios are simulate with changed climate and demand, as discussed below. This work is mainly focused on the effect of secondary succession though

3.7 Sub catchment extrapolation

Discharge totals from the sub catchment need to be extrapolated to the entire catchment of the Yesa reservoir in order to get the modeled reservoir inflow. The relative contribution from the catchment North of Jaca (study area) to the total discharge of the Aragón river is not constant for each month. Figure 12 shows long term averages of monthly discharges flowing into the reservoir obtained from CEH. During summer, discharge from the Jaca catchment represents a larger fraction of the total reservoir inflow than during winter. In order to correct for the seasonal trend, a different extrapolation factor is used for each month. The relative monthly contributions from the Jaca catchment to the total reservoir inflow for the hydrological year from 2005 to 2006 are used as extrapolation factors.

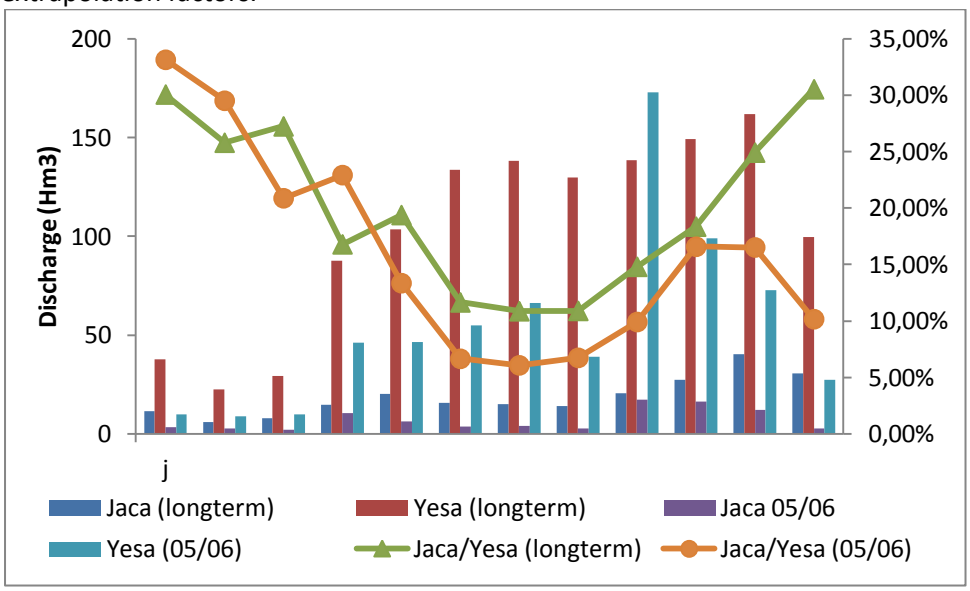

Figure 12 Measured monthly inflow of the Yesa reservoir (Yesa), contributions from the sub catchment of Jaca (Jaca) and relative contributions (Jaca/Yesa). Longterm averages and measurements for the hydrological year 2005-2006 are shown. Data from CEH.

3.8 Scenarios

3.8.1 Vegetation and soil

Different scenarios are simulated in order to find the specific contributions of soil and vegetation parameter changes due to vegetation growth (Table 12). The specific contributions of soil and vegetation parameters are determined by changing the model parameters for soil or vegetation between 1950 and 2050, while keeping other factors constant. The scenarios can be divided into three main categories (Table 12). The first scenario aims to determine the effect of vegetation change. The second is focused at the effect of changes in the soil and the final scenario combines vegetation and soil change in order to determine the total effect of vegetation growth in abandoned areas. The measured climate input from 2005 is used for all of these simulations from 1950 to 2050 in order to isolate the effect of the vegetation change.

Scenarios are indicated with codes in order to be able to point to a specific parameter setting of a certain scenario without the need of a long description. Codes for the different scenarios are presented in the overview of (Table 12). The letter S indicates changed soil parameters, V changed vegetation parameters and SV means both soil and vegetation parameters are changed. These letters

are followed by a number which gives the represented year by the parameters. When only letter (S or V) is present, it means that only these parameter values are changed while the others remain unchanged, representing abandoned land in 1950. For example, V2050 means that soil parameters for the year 1950 are used and vegetation parameters represent the year 2050.

Scenario code	Soil	Vegetation
S	+	-
V	-	+
SV	+	+

Table 12 Different scenarios with parameter settings representing a certain year (+) or parameter settings representing abandoned farmland around 1950 (-) to determine relative contributions of parameter settings to changes.

3.8.2 Future climate and demand

In addition to the above scenarios, also two extra scenarios are simulated with changing climate and demand. The effect of future climate change on reservoir water yield is assessed by changing the climate input of the years 2025 and 2050 with a hypothetical climate scenario. The results for the years 2025 and 2050 are then compared with the results of 2005 to show differences in water yield. Finally, the effect of future water demand on possible water stress is evaluated by changing the demand in 2025 and 2050 according to the results of Wada et al. (2011).

The hypothetical climate scenario assumes a constant monthly change in rainfall and temperature throughout the year compared to the measured climate of 2005-2006 (Table 13). The magnitudes of the changes in precipitation and temperature remain within the boundaries of the changes predicted for 2100 by López-Moreno et al. (2011). Despite this, the scenarios are probably not very realistic because a constant climate change for each month is unlikely. The scenario is highly hypothetical and should not be seen as an attempt to predict future climate as accurate as possible. It merely serves to study the effects of a small increase in temperature and decrease in precipitation to the system.

	Clim	
	Temperature	Precipitation
2025	+0.5	-0.5%
2050	+1	-10%

Table 13 Hypothetical climate change scenario for 2025 and 2050

Future water demand for irrigation is based on data from Wada et al. (2012). Wada et al. (2012) calculated evaporation from monthly irrigated areas with the help of the global hydrological model PCR-GLOBWB and the Pennman method with the use of crop calendars. The monthly evaporation was compared with soil moisture availability and corrected with country-specific accounts of losses during processes such as water transport (Wada et al., 2011). The data from Wada et al. (2012) is at a global scale, which means that a single pixel already covered the entire Yesa catchment. The relative increase in total yearly irrigation demand of that pixel for the hydrological years 2025 and 2050 compared to 2005 is used to estimate the increase in demand for the years 2025 and 2050 in this study. Data from the CEH showed that the outflow from the reservoir through the Aragón river remained fairly constant around 13 Hm^3 m^{-1} throughout the year. It is assumed that this component of reservoir outflow will remain constant in the future. The Yesa reservoir is mainly used for irrigation purposes (López-Moreno, 2004). Therefore, the remainder of the outflow that is not drained though the Aragón river is assumed to be the measured irrigation demand. The measured irrigation demand is increased relatively to the increases in irrigation demand from the pixel of Wada et al., (2011) for the hydrological years 2025 and 2050. The measured outflow through the Aragón river during the hydrological year of 2005 is than added to the irrigation demand of 2025 and 2050 to form the total estimated reservoir outflow for the future.

4 Results

4.1 Spatial-temporal pattern of secondary succession

The reconstructed land use map for the year 1950 is presented in Figure 13 (left). Abandoned farmlands cover 24% of elevations below 1600 m, which means 12.5% of the total study area. They are located in the valleys and cluster around arable land that is still currently in use. The valleys with low elevations generally are covered with forests and shrubs. Elevations above 2000 m are covered with grasses or bare rocks are exposed. Also shown are maps with soil depth (Figure 13 middle) and soil texture classes (Figure 13 right). Vegetation and soil parameters that correspond to the classes of the land use and texture map can be found in Appendix 1 and Appendix 3.

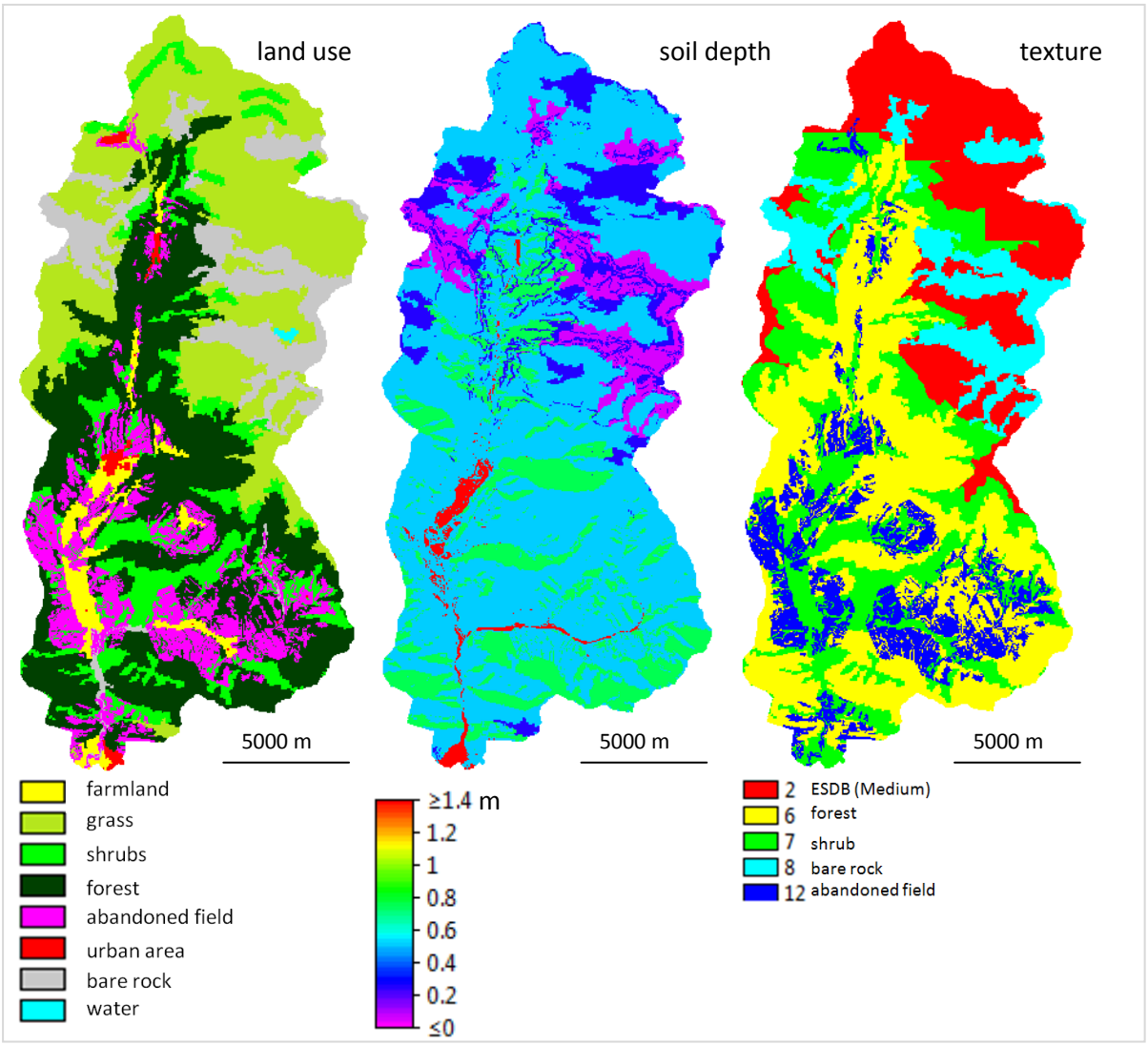

Figure 13 (Left) Reconstructed land use map of 1950 for the sub catchment. (Middle) Soil depth map (m). (Right) Texture map. Corresponding parameter values for the land use and texture map can be found in Appendix 1 and Appendix 3.

Figure 14 shows the spatial distribution of land cover at three moments during the simulation of vegetation growth in the abandoned fields. The expansion of forests in abandoned fields is shown at the moment of abandonment (1950), about halfway (2005) and at the end of the simulation (2050). Forests start to emerge rapidly after about 15 years in the most suitable places, after which the expansion of forests declines (Figure 15). Roughly 57% of the abandoned areas are covered by forest in 2005 and this increases to almost 78% in 2050. The fraction of simulated forest cover is 33% of the

entire study area in 1950 (Figure 13, Figure 15). This increases to 40% in 2005 and 42% in 2050. The results of the logistic models for the calculation of the transition probabilities in the abandoned farmlands are presented in Appendix 7. Appendix 8 shows maps with the simulated carbon densities with the same intervals that were used for the hydrological modeling.

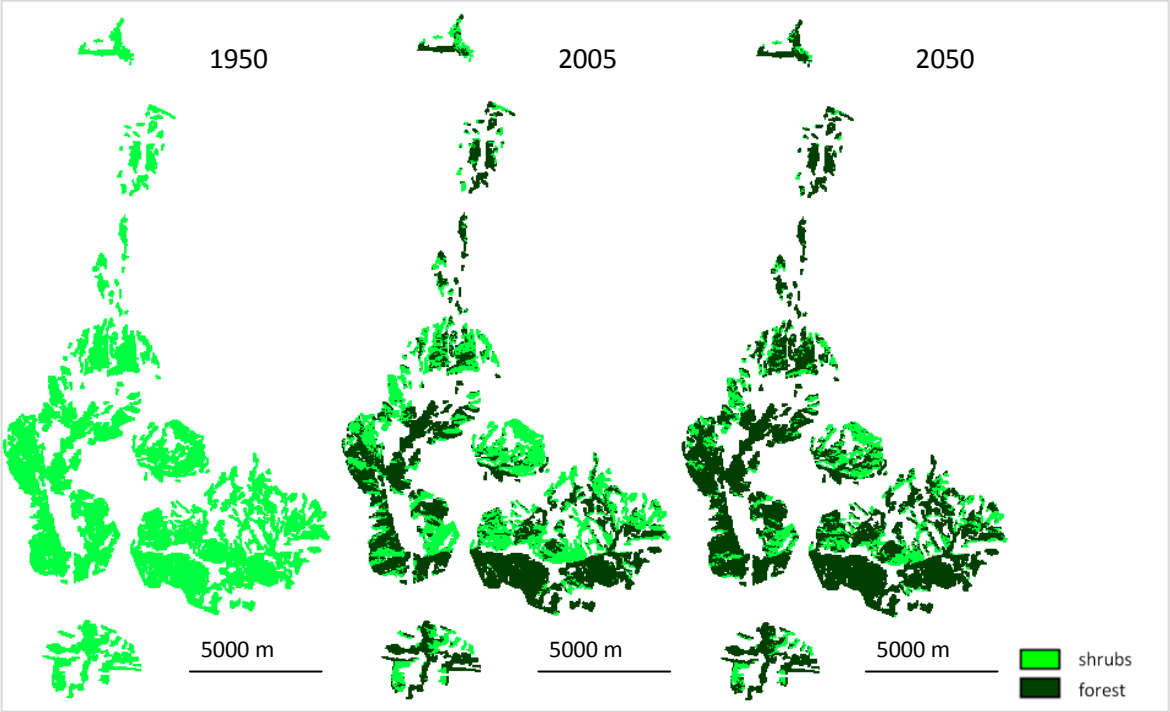

Figure 14 Maps showing land cover in abandoned fields for 1950 (left), 2005 (middle) and 2050 (right).

The performance of the vegetation model is assessed by comparing modeled land cover percentages of shrubs and forest with the Corina Land Cover map of the year 2006 (CLC 2006). The vegetation model predicts 58% of the abandoned area to be covered by forest in 2006 (Figure 15), corresponding quite well to the 63% forest cover of CLC 2006. About 61% of the cells that are predicted by the model to be forest or shrub in 2006, are also forest or shrub on CLC 2006 (Figure 15).

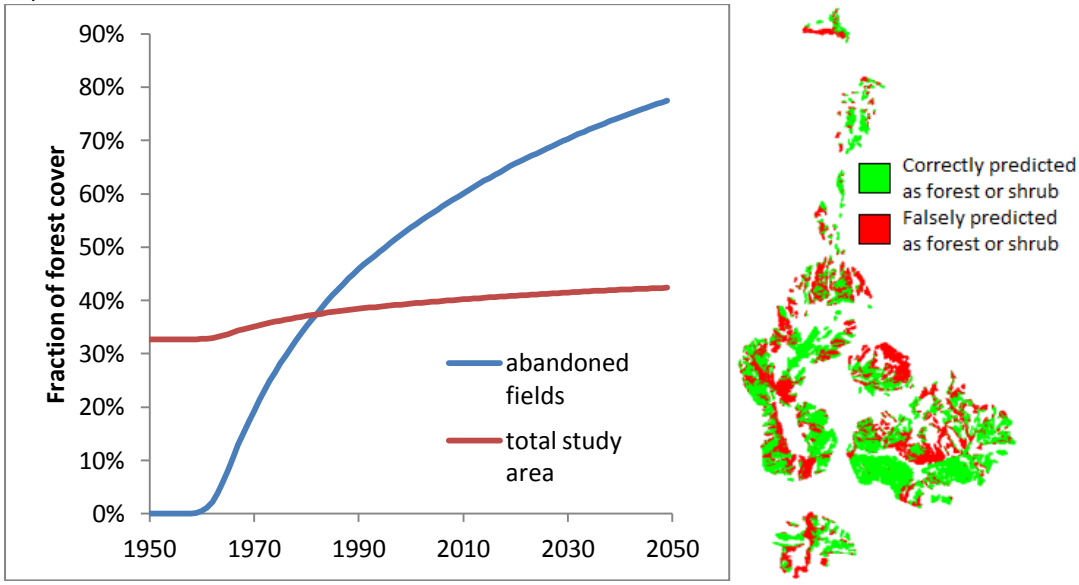

Figure 15 The graph shows the forest cover as a percentage of total cover in abandoned fields (blue) and total study area (red). The map shows the results of the success test for the vegetation model. Green (61%) indicates the vegetation model correctly predicts shrubs or forest at that location compared to the Corina Land Cover map (CLC 2006). Red (39%) means that shrubs are predicted instead of forest and vice versa.

4.2 Effect of secondary succession

4.2.1 Hydrological model performance

Measured and modeled discharges for the hydrological year 2005-2006 are compared in order to assess the performance of the hydrological model. The scenario which includes both soil and vegetation change (SV2005) is thought to represent the realistic situation in 2005 as best as possible, hence this scenario is used to determine the model performance. Measured discharge is retrieved from a river gauge from the Centre of Hydrographic Studies (CEH). The river gauge and the outflow point of the model are located roughly at the same location so discharges should be equal in an ideal situation. Figure 16 shows that the high spring discharge is overestimated by the model and the low summer discharge is underestimated. Differences for the other months are less than 30%. Total yearly water yield and the general seasonal trends are simulated quite well. This is reflected by the Pearson correlation coefficient (R^2) value of 0.89 based on monthly totals of measured and modeled discharge. For a lot of hours the discharge is zero and the monthly totals are only the result of a few high peak flows. The model predicts a total of 2854 hours with no river flow which results in 96 days with a dry river for the entire day. The measured discharge shows no days with a dry river. Daily measured and modeled discharge totals compare poorly with an R^2 of 0.38. Maximum daily discharge is overestimated by 68%.

	Measured 2005	SV2005
Total river water yield (Hm3/year)	83.4	85.1
Difference	NA	2,1%
Max discharge (Hm3/day)	3.11	5.24
Dry river (hours)	0	2854
Dry river (days)	0	96
R^2 (month)	NA	0.89
R^2 (day)	NA	0.38

Table 14 Summary of the comparison between measured and modeled (SV2005) river discharge for the hydrological year 2005-2006. The Pearson corrolation cpefficients, R^2(month) and R^2(day) are indicators of the corelation between measured and modeled monthly and daily discharge totals respectively (with 1 being a perfect relation and 0 very bad).

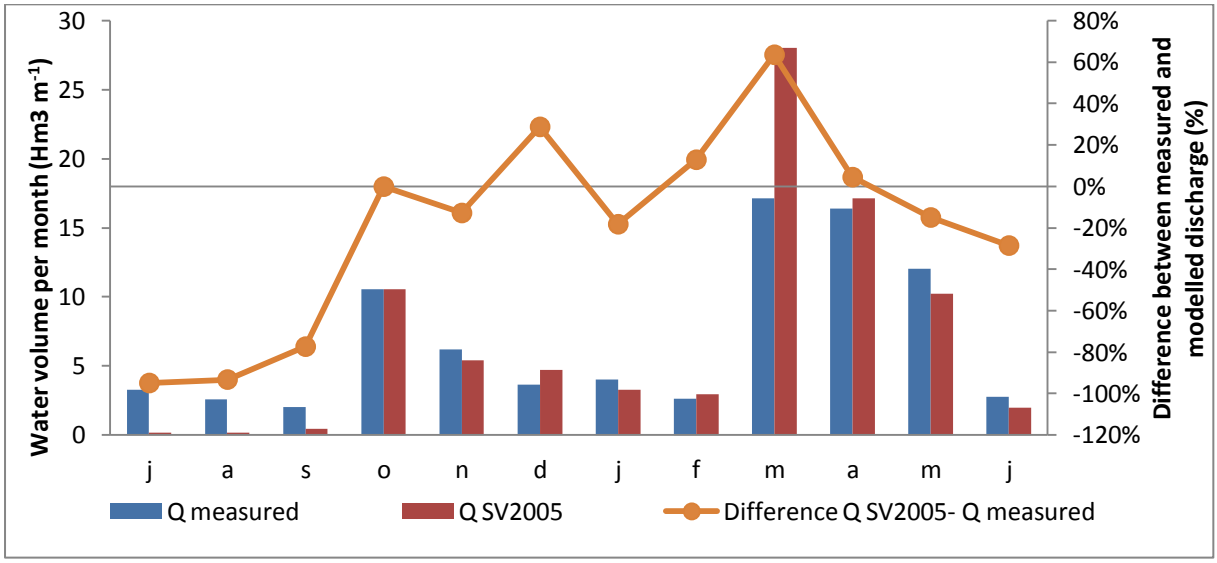

Figure 16 Measured (blue) and modeled (red) monthly river discharge for the sub catchment North of Jaca. Orange line gives the difference in percentage between the modeled and measured discharge, where a positive percentage indicates an overestimation by the model.

4.2.2 Discharge

Figure 17 shows the total yearly water yield from the sub catchment North of Jaca for the scenarios with vegetation change, soil change and combined. The net effect of soil change on river discharge is less pronounced than that of vegetation. Monthly differences between different scenarios are relatively small (Figure 18). Differences are only noticeable during winter months. Scenarios where only vegetation is changed or vegetation and soil change are both incorporated result in decrease in monthly discharge. When only soil parameters are changed, discharge even slightly increases for the months January, February and April. The combination of soil and vegetation change together results in the largest relative decrease in discharge of almost 25% during the month December. The largest change in terms of water volume occurs March with a decrease of 2 Hm^3.

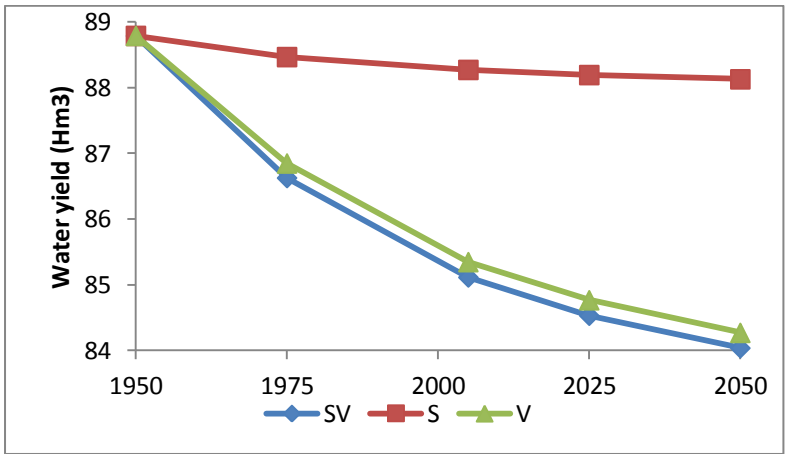

Figure 17 Total modeled river water yield from the sub catchment North of Jaca for the scenarios with only soil change (red), only vegetation change (green) and combined change (blue) due to secondary succession in abandoned farmlands from 1950 to 2050. Exact values and relative differences for the modeled discharge totals can be found in Appendix 9.

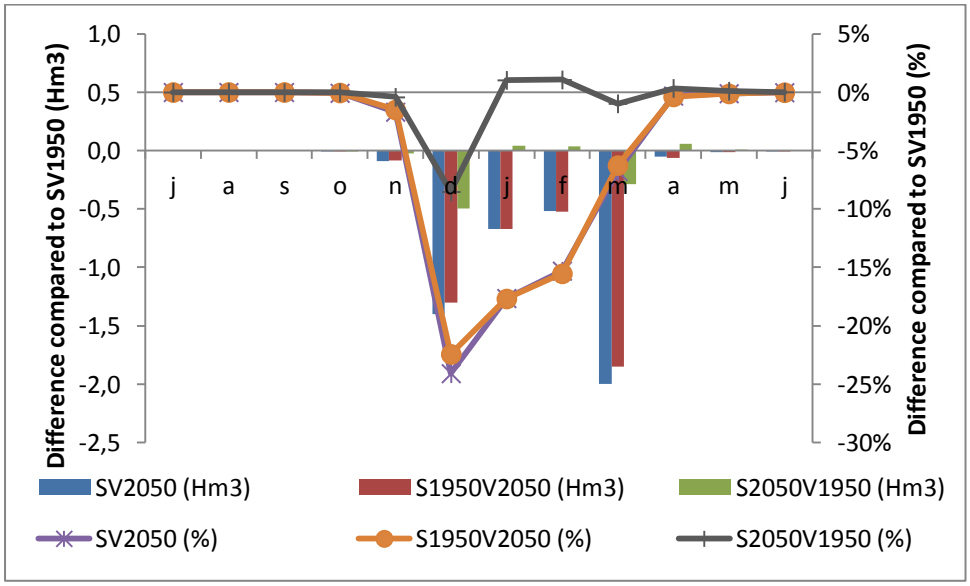

Figure 18 Differences in monthly discharge of several scenarios compared to the situation just after abandonment (SV1950). Left axis shows the effect of secondary succession in abandoned farmlands after 100 years in water volume ($Hm^3\ m^{-1}$) considering soil and vegetation change (blue columns), only vegetation change (red columns) and only soil change (green columns). Right axis shows the percentage of increase or decrease in river discharge due secondary succession in abandoned farmlands after 100 years compared to SV1950 considering soil and vegetation change (purple), only vegetation change (orange) and only soil change (black).

4.2.3 Evapotranspiration and infiltration

Rainwater can either exit the system as runoff or by evapotranspiration. In addition, runoff is influenced by infiltration rates because this determines how much water is passed directly as runoff or is first retained in the soil. Hence, changes in runoff should be reflected by changes in evapotranspiration and infiltration. It is interesting to evaluate how these fluxes change and how they relate to each other. Figure 19 (left) shows the totals of canopy (EtotIc), snow (EtotSC) and subsurface evapotranspiration (EtotSub) for the entire sub catchment during the situation just after abandonment of farmlands (SV1950). Subsequently, the effects of secondary succession in abandoned farmlands on the different evaporation components are presented. The scenarios SV2050, S1950SV2050 and S2050V1950 are used to show the combined effects of soil and vegetation change and the separate effects of just vegetation and soil change after 100 years respectively. Differences between the evaporation totals of scenarios SV2050 and S1950SV2050 are very small. Changes in vegetation cover have a larger net effect on the total yearly canopy evaporation than the total evapotranspiration from the subsurface. Evaporation from molten snow remains almost unaffected. Total yearly infiltration decreases for scenarios SV2050 and S1950SV2050, while it decreases for S2050V1950. Changes are relatively small though (Figure 19, right).

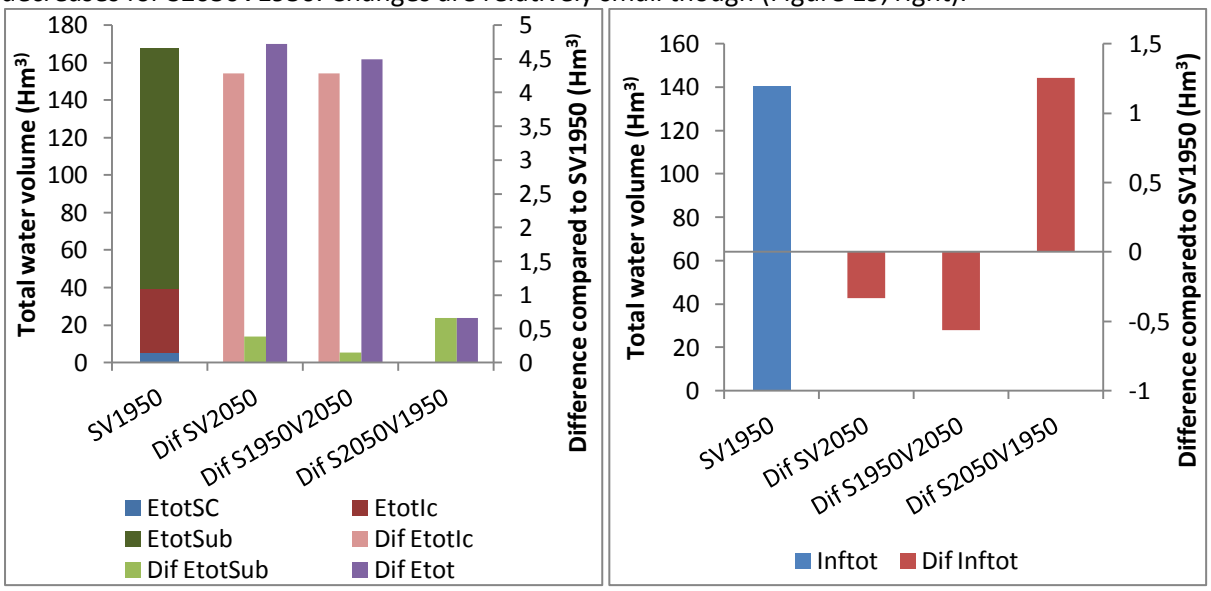

Figure 19 (Left) Graph shows totals of evapotranspiration from snow cover (EtotSC), canopy (EtotIc) and subsurface for the hydrological year just after abandonment (SV1950). Subsequently, the effects of secondary succession on the different evapotranspiration components are shown for 100 years of soil and vegetation change (Dif SV2050), only vegetation change (Dif S1950V2050) and just soil change (Dif S2050V1950). Changes in evaporation from snow did not occur. (Right) Graph shows the total infiltration in the sub catchment for the SV1950 scenario. Subsequently the differences in infiltration totals between SV1950 and scenarios SV2050, S1950V2050 and S2050V1950 are shown. Positive differences indicate increase compared to SV1950. Exact values and relative differences for the modeled evapotranspiration and infiltration totals can be found in Appendix 10.

Figure 20 presents the monthly changes in the different evapotranspiration components for the scenario with vegetation and soil change after 100 years of abandonment (SV2050) compared to the situation just after abandonment (SV1950). The changes for SV2050 and the scenario with only vegetation change (S1950SV2050) are almost identical, hence only the changes for SV2050 are presented. For scenario SV2050, evaporation increases from October to April and decreases from March to September compared to SV1950. The monthly evapotranspiration differences between the scenario with only soil change (S2050V1950) and SV1950 are negligible for the majority of the year. Only during the months June and July, the evapotranspiration totals increase. These increases are exclusively the result of changes in evapotranspiration from the subsurface. Since there are no differences to observe for other evapotranspiration components of the S2050V1950 scenario, only the subsurface component is shown in the figure.

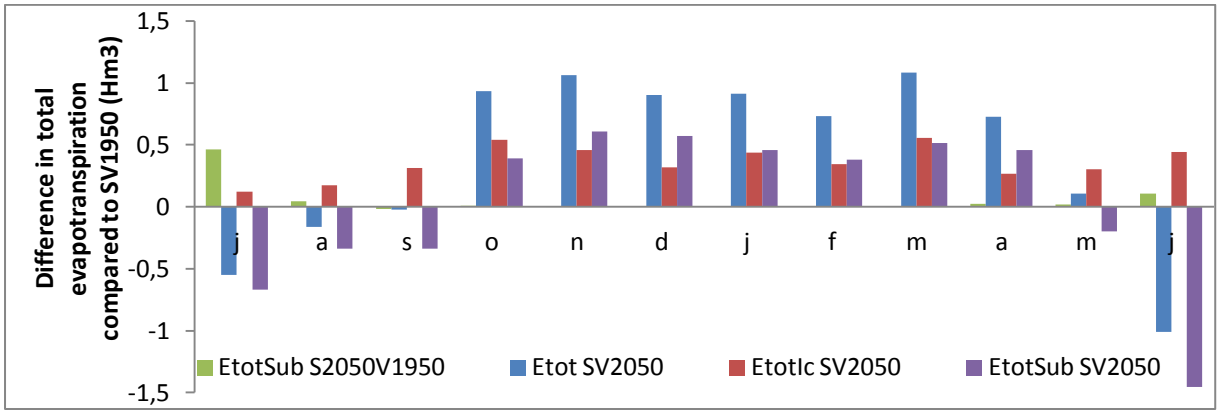

Figure 20 Differences in monthly totals of evapotranspiration components between scenario SV1950 and scenarios S2050V1950 and SV2050 (see text above for further explanation). Positive values indicate increase in evapotranspiration compared to SV1950.

Figure 21 shows monthly totals of infiltration (InfTot) and surface water (SW) for the entire sub catchment for the SV1950 scenario. Surface water is the combination of melt water and rainfall that has passed the canopies. Also changes in monthly infiltration totals are shown for the three scenarios, showing the influence of changes in soil, vegetation and combined change due to secondary succession after 100 years. Monthly infiltration totals follow the same trend as surface water, except for the months March, April and May, when the difference between surface water and infiltration is larger than during the rest of the year. From spring to autumn, infiltration totals for the scenarios SV2050 and S1950V2050 decrease compared to the SV1950 scenario. During winter months, vegetation change results in the opposite effect and infiltration increases. The increases are less substantial during the winter months with little surface water. The S2050V1950 scenario only shows increases during winter, infiltration during the other seasons remains similar to SV1950.

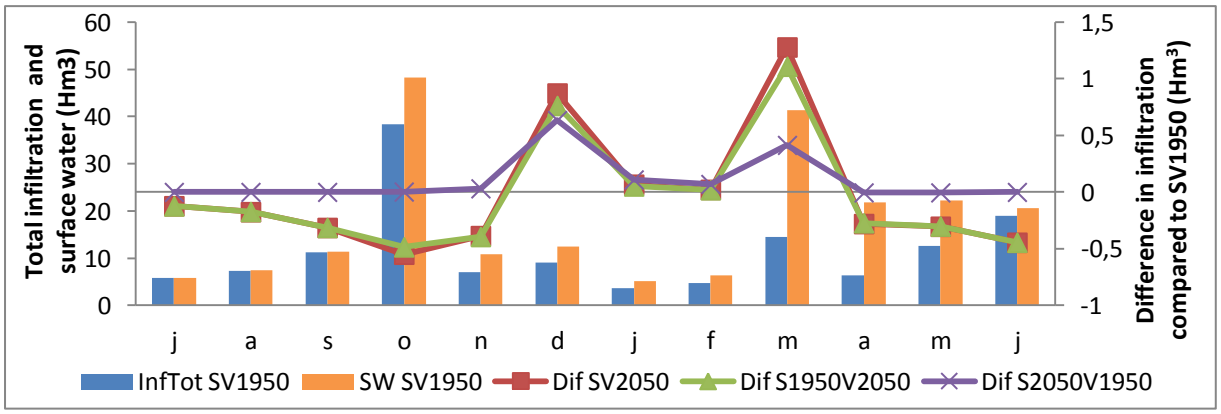

Figure 21 Columns give the total monthly infiltration (InfTot SV1950) and surface water (SW SV1950) for the hydrological year just after abandonment. Lines show the difference in monthly infiltration totals compared to the SV1950 scenario for 100 years of vegetation and soil change (SV2050), just vegetation (S1950V2050) and just soil change (S2050V1950) due to secondary succession.

Figure 22 presents the changes due to vegetation growth in abandoned areas in monthly infiltration (Dif Inf SV2050) and canopy evaporation (Dif EtotIc SV2050) totals compared to the SV1950 scenario. It shows that the above mentioned decreases in infiltration change from April to November due to vegetation (Figure 21), are equal to the increases in canopy evaporation during the same months (Figure 20).

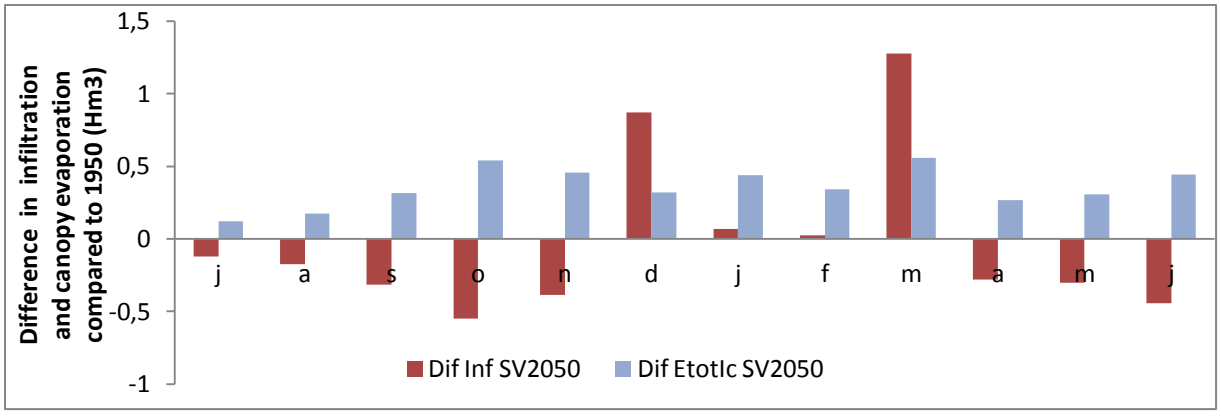

Figure 22 Differences in monthly totals of infiltration (Dif InfSV2050) and canopy evaporation (Dif EtotIc SV2050) between scenario SV1950 and scenario SV2050.

4.3 Effect of future climate change

Figure 23 shows the total yearly discharge for the hypothetical climate scenario with constant vegetation and soil parameters of 2005 (Clim) and the combination of hypothetical climate and changing vegetation and soil (SV Clim). Climate change has a larger impact on the total river water yield than the effect of secondary succession. The combination of soil and vegetation change causes a decrease in yearly discharge of only little over 1 Hm^3 from 2005 to 2050, while adding the hypothetical climate scenario causes a decrease of over 15 Hm^3. Also the monthly trends in discharge due to changes in soil and vegetation in combination with the hypothetical climate compared to constant vegetation and climate for 2005 (Dif SV2025 Clim 2025 and Dif SV2050 Clim2050), are presented in the same figure (Figure 23). A climate change towards less rain and higher temperatures leads to decrease in discharge during autumn and spring, while discharges during the winter months increase.

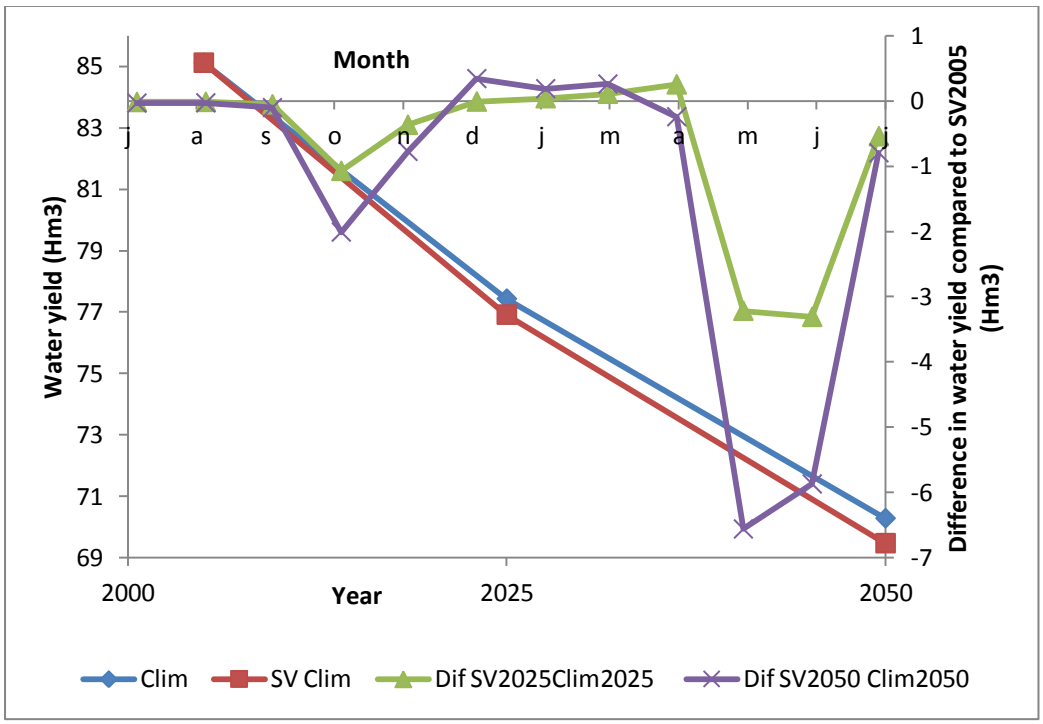

Figure 23 Left y axis gives the total river modeled discharge for the hydrological years 2005, 2025 and 2050 for the hypothetical climate scenario (Clim) and combination of secondary succession and climate change (SV Clim). Right y axis gives the difference in monthly discharge totals between the SV2005 scenario with climate input of 2005 and the scenarios with hypothetical climate and secondary succession in 2025 (Dif SV2025 Clim 2025) and 2050 (Dif SV2050 Clim2050). Exact discharge totals for the different scenarios can be found in Appendix 11.

4.4 Water stress

4.4.1 Sub catchment extrapolation and demand

Figure 24 shows measured and modeled inflow for the year 2005. The modeled discharge from the sub catchment had to be extrapolated to the entire Yesa catchment in order to get the modeled reservoir inflow (section 3.7). A simple method was applied, by using a correction factor for monthly discharge based on the ratio between measured reservoir inflow and the measured discharge at Jaca. This correction changed each month, based on monthly relative differences between measured discharge at Jaca and measured inflow at the reservoir. Despite the large overestimation in March, the monthly changing correction factor resulted in a R^2 of 0.94. Figure 24 also includes measured outflow from the Yesa reservoir for the year 2005 and estimated outflow for the year 2050 based on the results of Wada et al. (2012) (section 3.8.2).

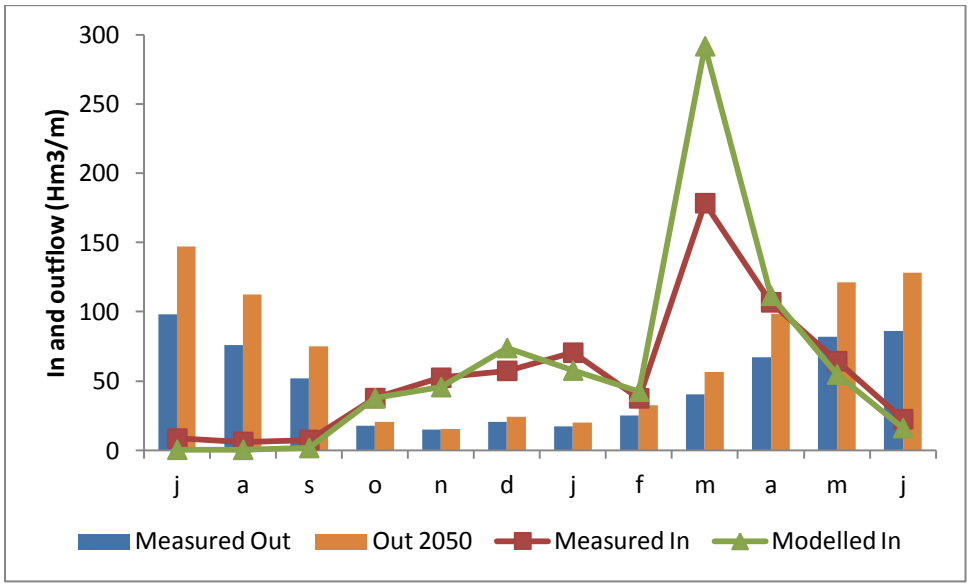

Figure 24 Blue columns give the measured outflow from the Yesa reservoir for the year 2005 and orange columns the estimated outflow for the year 2050. The red and green lines indicate the measured and modeled inflow for the year 2005 respectively.

Table 15 shows the estimated total water demand for the future, based on relative increase in demand for irrigation, obtained from the model of Wada et al. (2012). Model results of Wada et al. (2012) showed increase in water demand for irrigation of 21 and 37% for the years 2025 and 250 respectively. If all other factors would remain unchanged, this results in a shortage of 64 and 202 Hm^3 for the years 2025 and 2050, while in 2005 there was a surplus of 53 Hm^3.

	Total Demand	Increase (%)	Difference with 2005 measured inflow
2005	597	0%	53
2025	714	20%	-64
2050	851	43%	-202

Table 15 Total water outflow from the Yesa reservoir as measured in the hydrological year 2005 and estimated for 2025 and 2050. Measured outflow was retrieved from Centre of Hydrographic Studies (CEH) and future estimations were made based on data from Wada et al. (2012).

4.4.2 Water stress

Table 16 shows the changes in differences between reservoir inflow and outflow during the filling season for the simulated scenarios with changing vegetation (SV), vegetation and climate (SV Clim) and vegetation climate and demand (SV Clim Dem). The filling season is the period during which the water storage of the reservoir increases. It assumed to start in October and end in May. A minus sign indicates a relative decrease in water availability compared to the scenario where vegetation, climate and demand all represented the conditions of 2005 (SV2005).

	SV	SV Clim	SV Clim Dem
2025	-8	-41	-89
2050	-14	-78	-182

Table 16 Differences in residue between reservoir inflow and outflow between the year 2005 and future estimations for 2025 and 2050. Residual differences in Hm^3. Negative values indicate that the residue between inflow and outflow is smaller than in 2005. The measured residue in 2005 was about 53 Hm^3.

Figure 25 shows the monthly differences between reservoir inflow and outflow for the scenario SV2005. The reservoir is drained during the summer months and is filled during winter months. The monthly trends in changes in residue due to the different scenarios are shown in the graph as well. The effects of changes in vegetation, climate and demand can be recognized. Vegetation change leads to less water during winter months. Climate change means a decrease in discharge during autumn and spring and the negative effect of vegetation change during the winter is outweighed by the positive effect of climate change. Increased demand by irrigation is mostly noticed from spring to autumn.

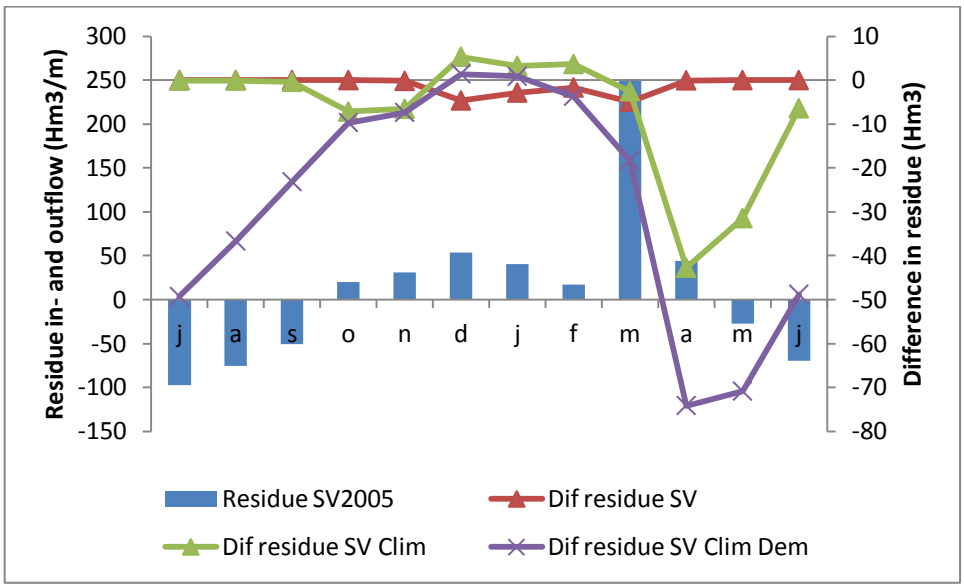

Figure 25 Columns give the residue between monthly reservoir inflow and outflow for the scenario with modeled vegetation and soil for 2005 and measured climate for 2005 (Residue SV2005). Positive values indiciate a surpluss of water supply to the reservoir. The lines (right y axis) give the monthly differences between Residue SV2005 and residues for scenarios SV2050 (Dif residue SV), SV2050 with hypothetical climate scenario 2050 (Dif residue SV Clim) and SV2050 with hypothetical climate scenario 2050 and estimated demand for 2050 (Dif residue SV Clim Dem). Positive values indicate increases in monthly residuals.

5 Discussion

5.1 Spatial-temporal pattern of secondary succession

5.1.1 Objective and approach

In order to assess the effect of secondary succession in abandoned farmlands on river discharge from 1950 to 2050, first the transition in vegetation cover in these fields had to be reconstructed for that period. A land use map representative for the situation of 1950 was created based on descriptions in literature. This study is focused at the effect of land abandonment, hence the reconstruction of land use only considers the locations of former farmlands, while any other possible changes in land use were ignored. All fields were considered to be abandoned at the same moment in 1950 for convenience. The locations of areas which have the highest potential to be formerly abandoned fields were determined using specifications on elevation, slope, current land use and distance to nearest settlement. Subsequently, a logistic Markov-chain model with spatially varying transition probabilities (Pueyo & Beguería, 2007) was used to simulate the succession of the vegetation in the abandoned fields. The probability for a cell to transform from shrub (abandoned land) to forest was made dependent on terrain characteristics in order to represent the effect of terrain suitability on vegetation growth. Aboveground carbon density and organic matter fraction were used to express the state of the vegetation and soil characteristics for a given stage in the succession from abandoned field to forest. Subsequently, vegetation and soil parameters were related to carbon and organic matter with equations from literature.

5.1.2 What is the reconstructed vegetation cover in abandoned farmlands from 1950 to 2050?

Formerly abandoned fields are located on gentle slopes below elevations of 1600 m, mostly in the Southern part of the study area where also most of the settlements can be found. After farmlands are abandoned, vegetation initially expands rapidly after which growth rates decline as the succession continues. About 15 years after abandonment, the first forests are already starting to rise. Forests spread out quickly but this expansion becomes less as the most suitable locations become occupied. After about 55 years of abandonment (2005), roughly 60% of the abandoned area is covered with forest. This is expected to increase to 78% of the area by 2050, which is a considerable change compared to the situation of 1950. Although the vegetation cover in abandoned areas changes dramatically, this areas covers only about 24% of the elevations below 1600 m and only 12.5% of the total study area, meaning that the influence of the changes on the entire system are limited. Simulated forest cover increases from 33% of the entire study area in 1950 to 40% in 2005 and 42% in 2050.

5.1.3 Model performance and validation

The success test (Figure 15) only checks whether a cell is correctly assigned as forest or no forest. About 63% of the abandoned area is covered by forest on the Corina Land Cover map. One has to keep in mind that this implies that when a Monte Carlo simulation is performed where 63% of the area is randomly assigned as forest, the expected success rate would be 53%. This follows from the fact that when 63% would be randomly assigned as forest, the expected success rate for cells that are assigned forest would be 63% of 63%, being almost 40% of the abandoned area. When 63% of the area is covered with forest, 37% is considered to be left as shrub. This means that the expected success rate for the cells that are left as shrubs is 37% of 37%, which is about 13% of the abandoned area. Hence, the combined expected success rate for the forested and not forested cells together is 53% of the total abandoned area. The 61% success rate of the vegetation model with spatially varying transition probabilities gives an improvement of 8% over a model with a spatially constant transition probability. The success rate of 61% is comparable with the success rate of 67%, obtained with the original model by Pueyo and Beguería (2007). The hydrological impact of the cells that are wrongly assigned with shrub or forest covers can be relatively small, as long as the fractions of shrub

and forest covers in the area is predicted correctly. The vegetation model predicts 58% of the abandoned area to be covered by forest in 2005, corresponding quite well to the 63% forest cover of the Corina Land Cover map. The model is thought to work sufficiently.

Validation of the modeled vegetation growth rate over time and the corresponding change in soil and vegetation parameter values remains a problem. All that can be said is that is that the shapes of the carbon growth curves in single locations seem plausible and that the minimum and maximum vegetation and soil parameters values remain within extremes found in literature. A more elaborate discussion on this subject can be found in Appendix 13.

5.2 Effect of secondary succession

5.2.1 Objective and approach

The goal of this study is to determine the effect of secondary succession in abandoned farmlands on river discharge. Discharge is simulated with an existing hydrological model (Lana-Renault et al., 2010) that was expanded with a snow routine. Climate input was obtained from measurements in a nearby catchment (Lana-Renault et al., 2010) and extrapolated to different altitudes with the use of lapse rates. The model was run several times with different soil and vegetation parameter settings that represented different stages in the succession between 1950 and 2050. Both the separate and the combined effect of soil and vegetation change from 1950 to 2050 were simulated. The modeled runoff, evapotranspiration and infiltration fluxes for the different stages in the succession were analyzed to determine trends on both monthly and decadal scale.

5.2.2 What is the hydrological response of the system to vegetation growth in terms of infiltration, evapotranspiration and runoff?

First of all it has to be noted that the observed changes in fluxes due to vegetation growth are relatively small. This is not surprising as only a small fraction of the total study area (12.5%) is affected by land abandonment and the conditions in the remainder of the area are assumed to be constant.

The runoff from the sub catchment is gathered in streams which eventually converge into a river. Secondary succession in abandoned farmlands causes river discharges to decrease during winter months. The vegetation growth in abandoned fields is estimated to be responsible for a decrease of 4.14% in total yearly water yield from 1950 to 2005 (Figure 17, Appendix 9). The continuing vegetation growth in the future is expected to cause a decrease of another 1.25% by 2050. Based on the results of this study it can be concluded that these decreases are dominantly caused by the change in vegetation cover, the effect of change in soil characteristics is less pronounced. Decreases in water yield are caused by increases in total yearly evapotranspiration due to changed vegetation characteristics in revegetated abandoned fields. This effect of vegetation growth on evapotranspiration is not constant throughout the year because evapotranspiration increases during winter months, but decreases from July to September. The influences of the changes in parameters is discussed more elaborately further on (section 5.2.2.1). In short, albedo and stomatal conductance both decrease as the vegetation cover makes a transition from abandoned land to forest and vegetation height increases. This results in an increase of net radiation and stomatal resistance, where the change in net radiation is beneficial to evapotranspiration and the change in stomatal resistance means less evapotranspiration. The influence of the decrease in stomatal conductance is dominant over the influence of albedo when solar radiation is abundant and soils are dry. During periods with less abundant solar radiation and more water availability, the influence of the lower albedo becomes more dominant. Potentially the vegetation change should be beneficial for the infiltration rates and more water should be infiltrated in the soil (discussed more elaborately in section 5.2.2.2). During summers this positive effect on infiltration is overshadowed by the increase

in canopy evapotranspiration. This is because dry conditions cause changes in water availability to be the dominant factor for infiltration, instead of a change in storage capacity.

5.2.2.1 Evapotranspiration

The transition from shrubs to forest in abandoned lands results in higher vegetation with an increased surface of leaves and stems. This implies more interception of rainfall and a higher aerodynamic surface resistance (Breurer et al., 2003). Forests are also characterized by a lower albedo (Breuer et al., 2003). The higher aerodynamic surface roughness means more advection at the evaporation surface and lower albedo means less solar radiation is reflected, both implying that more energy is available for evapotranspiration (Gay, 1991). In addition, the higher interception capacity means more water is exposed to open air and directly available for evaporation from the surface of the vegetation. These effects of vegetation growth are beneficiary to evapotranspiration. However, the transition from shrubs to trees implies a decrease in canopy stomatal conductance (Breuer et al., 2003). This means an increase in canopy resistance against evapotranspiration (Robinson & Ward, 2000). Hence, the changes in vegetation parameters due to vegetation growth actually have both a positive and a negative effect on evapotranspiration. The general observed effect of forest growth is that evapotranspiration increases (Zhang et al., 2001).

Vegetation growth indeed results in more evapotranspiration (Figure 19). However, total evapotranspiration actually decreases during summer months for the scenarios where the vegetation is changed (Figure 20). The decrease in summer evapotranspiration from the subsurface is not noticeable for the scenario with only soil parameter change. Also, the decrease during summer months is caused by the decrease in evapotranspiration from the subsurface, because canopy evaporation increases throughout the year and evaporation from melt water remains constant. Hence, the decreases in summer evapotranspiration are caused by changes in evapotranspiration from the subsurface due to altered vegetation parameters. Vegetation parameters are constant throughout a year, which means that a mechanism is needed to explain the different effect of vegetation growth on evapotranspiration in summer and winter. The explanation for the different effect during winter and summer follows from the fact that evapotranspiration is water limited when soils are dry and energy limited when soils are wet (Wetzel & Chang, 1987; Calder, 1998). Transpiration by vegetation decreases when soils become very dry and strong suction in the root zone is needed to subtract water from the soil (Wetzel & Chang, 1987). In the model this relation between soil moisture and evapotranspiration is represented by a reduction factor that is linear function of soil moisture content (Brolsma et al., 2007; Feddes et al., 1978). When the soil moisture drops below limiting point, this reduction factor increases the canopy resistance against evapotranspiration. When the soil moisture content is above limiting point, canopy resistance is only depending on stomatal conductance. Soils are dry during summers (below limiting point), which implies that changes in soil moisture content cause changes in canopy resistance. On the other hand, during winters soils are wet (above limiting point) and canopy resistance remains unchanged.

Vegetation growth results, as discussed above, in increased rainfall interception and more available energy for evaporation. This means more canopy evaporation and less water reaching the soil throughout the year. The result of increased canopy evaporation during summer months is that the soil moisture content is lowered further below limiting point and evapotranspiration from the subsurface is reduced. During winters, soils are wet and evapotranspiration is energy limited, meaning that the change in soil moisture content has no effect on evapotranspiration but the availability of energy is the determining factor. In this case not just canopy evaporation but also subsurface evapotranspiration increases due to the increased availability of energy caused by lower albedo and higher surface roughness. Apparently the increased canopy interception capacity and positive effects of albedo and vegetation height due to vegetation growth outweigh the negative effect of a decrease in stomatal conductance.

5.2.2.2 Infiltration

Forest growth causes infiltration totals to increase during the winter months from December to March, while infiltration decreases during the rest of the year (Figure 21). In addition, Figure 22 shows that the monthly decreases in infiltration are equal to the increases in canopy evaporation from April to October. The infiltration conductivity parameter was not altered for any scenario, which means that the changes in infiltration are caused by other parameters. Infiltration can either be affect by changing the properties of the soil, or by changing the availability of water for infiltration. Properties of the soil are altered because forest growth leads to an increase in soil porosity and saturated conductivity, meaning that the storage capacity of the soil is increased and soil water is drained faster. This means that the soil is altered in such a way that more water can infiltrate. Water availability is decreased by the increase in canopy evaporation because this causes less rainwater to reach the surface of the soil. Hence the changes is vegetation cover in abandoned farmlands can cause both an increase in infiltration due to higher storage capacity and a decrease in infiltration due to more canopy evaporation. The moisture content of the soil determines whether the positive or the negative effect of vegetation growth is dominant. This is because when the soil is saturated, no more water can infiltrate and a decrease in water availability has no effect. However, increasing the storage capacity means that more water can infiltrate. On the other hand, when soils are dry, storage capacity is not the limiting factor and decreasing the water availability will mean less infiltration.

5.2.3 Comparison with literature

Differences in hydrological response of a system to vegetation change are site specific and depend largely on climate factors (Gallart & Llorrens 2002). This makes it rather complicated to compare the results of this study with results in literature. Factors such as climate, vegetation types and the fraction of total area that is subject to vegetation cover change have to be considered for studies before differences in results can be assessed.

Lasanta et al. (2006) and García-Ruiz et al. (2010) used experimental plots to determine the effect of different land uses on runoff coefficient (runoff as a percentage of annual precipitation). These experimental plots are located in the Aísa valley, roughly 5 km from the sub catchment of this study. This means that the climatic conditions and effect of vegetation change on runoff can be assumed to be similar in this study. Based on the results of Lasanta et al. (2006) and García-Ruiz et al. (2010) , the average difference in runoff coefficient between recently abandoned arable land (cereal or shifting culture) and plots with dense shrubs (abandoned more than 40 years), is about 6%. Sadly no studies have been found that compared the runoff from recently abandoned plots with runoff from areas with forest cover in the vicinity of the study area. Still the decrease of 6% in runoff coefficient due to a change from abandoned farmland to dense shrubs should provide a good indication for the effect of secondary succession. Based on a global analysis of studies in 26 different catchments, Farley et al. (2005) conclude that afforestation can be expected to result in a reduction of 15% of the annual runoff coefficient (runoff as a percentage of precipitation). This result of Farley et al. (2005) can only be used as a general indication because climate conditions of the catchments are unknown. However, afforestation means that the complete area is vegetated by forest, while secondary succession in abandoned farmlands sometimes only results in shrubs. Therefore, it seems unlikely that secondary succession results in a larger reduction of the runoff coefficient than 15%. Based on the above, a vegetation change from abandoned farmland to forest can be expected to cause a decrease in runoff coefficient of at least 6% and not much more than 15%. In this study, vegetation is only changed in abandoned farmlands which represent 12.5% of the study area. This means that the runoff coefficient is only expected to change in 12.5% of the area. The runoff coefficient for the entire hydrological year and total sub catchment area is about 30%. Based on the results of the studies above, total runoff in this study can be expected to decrease between roughly 2.5 and 6%.

Molinillo et al. (1997) used experimental plots to study the effects of a change in land cover from meadows to shrubs. The study area is close to the study area of this study so conditions can be

assumed to be similar. A change from 85% grass cover to 100% shrub cover resulted in a reduction in runoff coefficient from 23% to 2%. When this result is converted to a vegetation change in only 12.5% of the area, this would mean a change of almost 9% in runoff.

Bosch & Hewlett (1981) analyzed 94 catchment experiments and showed that clear cutting of forest has the opposite effect of afforestation on water yield. This means that results of clear cutting experiments can also be used to evaluate the effect of vegetation change from abandoned land to forest on water yield. If results from Bosch & Hewlett (1981) are converted to represent changes in water yield after 12.5% of the catchment areas were deforested, clear cutting caused decreases between around 2% and 6% in total water yield. Only results of catchment experiments with mean annual precipitation totals between 800 and 1000 mm were considered because these annual totals resemble the rain in the abandoned farmlands of this study.

Cognard-Plancq et al. (2001) used a modeling approach to study the role of forest cover on streamflow down sub-mediterranean mountain watersheds (Cevennes, France) with relatively similar climatic and topographic conditions to this study. Cognard-Plancq et al. (2001) conclude that the difference between dominantly broom vegetation cover (shrubs) and mostly spruce forest in terms of change in runoff is about 10%. When this result is converted to a shift in vegetation cover in only 12.5% of the study area, the vegetation change is responsible for a change in runoff of just over 4%.

The results of the above studies suggest that a change from abandoned farmlands to forest in 12.5% the study area can be expected to have caused a reduction in water yield between about 2 and 9%. The result of this study is that secondary succession has been responsible for a decrease of little over 4% in discharge from 1950 to 2005. Considering that the model is thought to slightly underestimate the effect of vegetation growth on discharge (section 5.2.5), the results seem to compare quite well to the results of other studies.

The conclusion of Beguería et al. (2003) is that vegetation growth has been responsible for a reduction 30% in river discharge in the Pyrenees, which is considerably more than the 4% found in this study. This could mean that the effect of secondary succession in this model is strongly underestimated, or the effect of vegetation change is overestimated by Beguería et al. (2003). An important factor for the effect of secondary succession on river discharge is the total fraction of land that has been abandoned and revegetated. The sub catchment was chosen because it covered the whole range of elevations that are present in the Yesa catchment and should therefore cover all processes related to river discharge. However, high elevations are overrepresented in the sub catchment compared to the Yesa catchment (Figure 1). This means that the abandonment of 24% of land below 1600 m represents a larger proportion of the catchment area of the Yesa reservoir than of the sub catchment. The area between 750 and 1600 m represents about 80% of the Yesa catchment and only 53% of the sub catchment. This means that where abandoned lands cover 12.5% of the sub catchment, they actually cover about 19% of the Yesa catchment. Since the abandoned area is about 35% larger, discharges can also be expected to decrease by 35% more. This would mean that for the Yesa catchment, the effect of secondary succession would be a reduction of over 6% in annual discharge. The exact fraction of the total study area of Beguería et al. (2003) that has been abandoned is unknown, which makes the results quite hard to compare.

Another explanation for the seemingly different results could be the different approach of the two studies. In this study only vegetation change in abandoned farmlands below elevations of 1600 m is considered and the effect of this vegetation change on discharge is assessed. On the other hand, Beguería et al (2003) used a hydro-climate model and assumed that residuals in discharge that could not be directly explained by significant trends in temperature and precipitation were caused by vegetation change. This means that the change in discharge of 30% that is attributed to vegetation change by Beguería et al. (2003), actually incorporates all changes in the Pyrenees during the last

decades and not just vegetation growth in abandoned areas below 1600 m. Rejecting the results of this study based on the results of Beguería et al (2003) would therefore be a premature conclusion. The work of Vicente Serrano et al. (2005) indeed suggests that vegetation has expanded in areas other than abandoned fields during the last decades. Most of this vegetation growth was concluded to be related to climate changes. Biomass has also increased in cultivated fields, indicating intensification of croplands. These vegetation changes could be responsible for a considerable part of decreases in river discharge noticed by Beguería et al. (2003). Also, this study only considers changes in vegetation cover in the actual abandoned fields below 1600 m. Possible reduced human induced pressure on vegetation in other areas is not considered.

5.2.4 Hydrological model performance

5.2.4.1 Discharge simulation

The goal of this work is to study differences in monthly discharges due to vegetation growth and not to simulate discharge as accurate as possible. This does not mean that it is not important to be able to simulate discharges accurately. If measured discharges are replicated properly by the model, it can be assumed to simulate the processes in the system in a representative manner. This means that when certain parameters are changed in order to study the effects of vegetation growth, the model can be expected to produce results that are more reliable than when the model was not performing properly in the first place.

Figure 16 shows that the spring discharge is overestimated and the summer discharge is underestimated. However, the general seasonal trends are simulated quite well, reflected by the R^2 value of 0.89 based on monthly totals of measured and modeled discharge. The model accuracy at a daily scale is much worse with a R^2 of only 0.38, although not too much value is attached to this indicator. First of all it was not the goal to simulate discharge accurately on the daily scale. Moreover, it could be that the model is actually modeling daily variation quite well while the R^2 value is still low. For example, R^2 is low when maximum and minimum values are simulated correctly, but just with a small time lag compared to the measured values. Still the model would then be sufficient for the use of this study.

Several factors in this study lead to inaccuracy of the discharge simulation by the model which was originally constructed and calibrated by Lana-Renault et al. (2010) for a relatively small catchment. The study area of this study is much larger and this makes it hard to find reliable parameters estimations and climate input. Also, the study area of Lana-Renault et al. (2010) did not feature snowfall. Snow accumulation and melting was not incorporated in the model and had to be added. This snow model is not calibrated. The performance of the snow model and the effect of the climate and parameter input on the discharge simulation of the hydrological model are discussed below.

5.2.4.2 Snow model

A snow routine had to be added to the original hydrological model of Lana-Renault et al. (2010). Examples of simulated snow cover at different elevations are presented in Appendix 6. The snow model seems to work sufficiently since modeled snow cover is in line with descriptions in literature. Snow accumulates above 1600 m (López-Moreno & García-Ruiz, 2004). Snow is present in the catchment for at least 6 months each year (García-Ruiz et al., 2010). Isolated snow patches may persist in shady slopes until June and July (López-Moreno, 2005). Assuming a snow density for settled snow of 30% (Paterson, 1994), snow heights remain below the maximum measured values by López-Moreno (2005).

5.2.4.3 Climate

Weather input is modeled with a single weather station and lapse rates, hence daily variation cannot be expected to be modeled accurately. Appendix 15 shows that modeled precipitation during the summer period is slightly underestimated at low elevations. This could partly explain the underestimation of modeled discharge during summer months. Especially since these low rainfall totals and few rain days are extrapolated to the entire sub catchment. In reality the weather at lower elevations says very little about the weather in the high mountains (Appendix 14). In this study this fact is neglected, which is an important limitation to the model accuracy. Temperature lapse rates are quite common, but the precipitation lapse rate is probably not very reliable. Particularly the variation in rain days could have a substantial impact on the amount of days with a dry river, daily accuracy and the maximum daily discharge. Because there were very few rain days in July at low elevation, rainfall is assumed to have occurred only during these scarce events for the entire region. Appendix 14 shows that this is not necessarily the case and that the high elevations could provide a much more spread out supply of water. Also, rain events at different elevations do not necessarily occur at the same day, again spreading the water input.

5.2.4.4 Parameter estimation

Soil parameter values and their spatial variation are estimated based on scarce available information and some assumptions. An increase in soil depth or porosity both result in a larger storage capacity of the soil. Storage is an important factor for the amount of river discharge. A larger storage capacity of the soil means that it takes more water for the soil to be saturated and more surface water can infiltrate. The travel time of surface water is much shorter than that of infiltrated water. This means that a higher storage capacity results in a less instantaneous supply of water to the river.

When water is infiltrated in the soil, it is longer present in the system and longer subject to evaporation. Hence a higher storage capacity will result in more evaporation and less discharge (assuming infiltration rate and soil moisture fraction remain constant). Storage capacity is not the only factor influencing hydrological characteristics of the soil. Another parameter is the saturated conductivity for infiltration. This parameter restrains the rate at which surface water infiltrates in the soil. Hence it is a determining factor for the response time of the system to rainfall events and the hydrological characteristics of the slopes. Saturated conductivity for infiltration is assumed to be constant for the entire area, which is very unrealistic. In reality, infiltration depends on vegetation cover and soil type. Runoff from bare zones infiltrates in vegetated zones (Cerdà, 1998). Furthermore, infiltration rates vary significantly with different plant species (eg. Dunne at el., 1991; Dadkha & Gifford, 1980), rock cover and soil compaction (Dadkha & Gifford, 1980). The latter two mentioned factors are related to vegetation cover again (e.g. Morgan, 2005). Soil type is a determining factor for the infiltration rate as well. Sets of average infiltration parameters have been developed for different textural classes (Rawls et al., 1983). However, no detailed information on the spatial variation of soil texture is available in the area and texture is therefore assumed to be constant. Vegetation cover is described in more detail, but varying infiltration rates with vegetation cover without reference values for different covers is pointless.

Changes in storage and infiltration capacity of the soil have a large impact on the response time of river discharge to rainfall events. Field measurements and an extensive calibration of the relevant model parameters was not possible in this study due to time constrains, but it probably would have resulted in an improvement of the model performances.

5.2.5 Effect of model shortcomings on results

The model is, apart from the underrepresentation of abandoned area (section 5.2.3), expected to slightly underestimate the effect of vegetation growth in abandoned fields on discharge. This is because not all processes related to vegetation growth are considered in the model and some conditions are not assumed to be simulated correctly.

The differences in discharge between 1950 and 2050 are minimal (Figure 17). Also, during summer months, a lot of times the river is dry in 1950. Especially the fact that the river is predicted to be dry for several periods means that it is impossible to determine the full effect of secondary succession on discharge. This is because a decrease in water availability cannot be reflected by a decrease in discharge when the river is already dry. This explains why the decrease in evapotranspiration and increase in infiltration during the summer months are not reflected by an increase in discharge. During winter months the river is not dry and effects of secondary succession on evapotranspiration and infiltration are reflected by a decrease in discharge.

The effect of vegetation growth on evapotranspiration is dependent on the moisture content of the soil (section 5.2.2). Vegetation growth only causes evapotranspiration to decrease when soil moisture content is low. In fact, the model only predicts evapotranspiration to decrease in months during which it also predicts rivers to be dry. River discharge is never zero in reality, hence it can be concluded that the model predicts too dry conditions. If the model would have been able to simulate wetter conditions during the summer months, probably no decrease in evapotranspiration would have been noticed. Instead, the beneficial effect of the albedo change would have been dominant and evapotranspiration would have increased. Since rivers would not have been dry, the changes in evapotranspiration would also have been reflected by larger changes in water yield. Of course the above is not necessarily the case, because the runoff contribution from abandoned areas to the downstream discharge could actually be zero during dry summers in reality. It is merely something that has to be kept in mind when evaluating the results of this study. In addition to the above, another side note has to be made about the response of evapotranspiration to vegetation growth. One of the effects of vegetation growth that has not been considered in the model is the increase of rooting depth. During dry periods, deeper roots may allow trees to transpire water from deep soils, while shallow soils are already dry and prevent transpiration of shallow rooted herbaceous plants (Canadell et al., 1996; Llorens et al., 1997). This could mean that forest growth results in more summer evapotranspiration and less discharge. However, the potential effect of increased rooting depth is considered to be minimal in this study because soils of abandoned areas are generally not deeper than 50 cm and the rooting depths of crops and shrubs generally already exceeds this depth (Breuer et al., 2003).

Several soil processes related to vegetation change are, as explained in the introduction, not incorporated in the model. Section 5.2.4.4 already addressed the impact of soil depth and infiltration capacity on storage capacity and hydrological behavior of a catchment. Soil depths can change due to lateral transport and soil production due to bedrock weathering. Lateral sediment transport is related to vegetation cover because dense vegetation covers can prevent erosion and lead to accumulation of sediment (Lasanta et al., 2006). The presence of vegetation and roots is beneficial for bedrock weathering and soil production (Kosmas et al., 2000). Hence, the changes in vegetation cover should imply changes in soil depth, but this is not considered in the model. In section 5.2.4.4 it is also described that infiltration capacity is dependent on vegetation cover. This means that the infiltration capacity should actually increase over time in the abandoned fields, instead of remaining constant. Not incorporating the above mentioned effects probably causes the differences between modeled river discharges to be smaller for different vegetation scenarios than what they would be if all processes were included.

5.3 Reservoir inflow and water stress

5.3.1 Objective and approach

The objective of this study was not just to determine the effect of vegetation growth in abandoned fields on river discharge, but also to estimate its contribution to future changes in reservoir inflow and water stress. The catchment area of the Yesa reservoir was too large for the model, so reservoir inflow could not be modeled directly. Instead, the modeled discharges of a representative sub catchment had to be extrapolated to the entire Yesa catchment. This was done with the help of a correction factor, which was based on the relative contribution of the monthly measured discharge at Jaca to the total measured reservoir inflow. Changes in water stress were assessed by studying changes in monthly residuals between reservoir inflow and measured outflow.

With the results of this study it is not really possible to accurately predict future water stress for a full hydrological year since future climate is uncertain and the model is incapable of simulating realistic discharge during summer months. However, monthly discharge totals and changes due to vegetation growth are simulated quite well from autumn to spring. This is the period that is used for filling the reservoir. Hence the model can be used to evaluate the effect of secondary succession and climate change on the water availability during the filling season. The filling season is assumed to start in October and end in May. Summer discharge in the Jaca sub catchment is relatively high compared to the summer inflow of the Yesa reservoir (Figure 12). Reservoir inflow during summers is actually quite low anyway and does not contribute much to the supply for the water demand (Figure 24). This makes the shortcomings of the model during summer relatively unimportant. The results of this study can be used to draw conclusions on the effect of secondary succession on reservoir inflow during the filling season.

5.3.2 What is the effect of secondary succession on monthly residuals between reservoir inflow and outflow?

The results of this study indicate that secondary succession in abandoned fields leads to a decrease in reservoir inflow. These decreases are most profound in the months December and March, which are also the months with the highest surplus of reservoir inflow compared to outflow (Figure 18 and Figure 25). However, the total decrease in residual between reservoir inflow and outflow for 2025 and 2050 due to secondary succession are only 8 and 14 Hm^3 respectively, while there was a surplus of 53 Hm^3 inflow in 2005. This means that, although less water can be stored during December and March, changes in vegetation due to secondary succession are not likely to cause major water stress in the future. In the introduction (section 2.4) it was already mentioned that maximum reservoir storage is not reached during the winter, but a safety margin is kept as a precaution against flooding (López-Moreno et al., 2004). Also, during the last decades, storage regimen changed to a more gradual filling during the entire filling season. This means the safety margin during winters has already decreased in the past decades. The decrease in spring discharge will require more reservoir filling during winter months and this will push the reservoir more to its limits.

5.3.3 Quality and weaknesses

The calculation of reservoir inflow required the extrapolation of the modeled discharge from the sub catchment to the Yesa catchment. High elevations are, as already discussed (section 5.2.3), overrepresented in the sub catchment. Since the abandoned area in the Yesa catchment is about 35% larger than in the sub catchment, discharges can also be expected to decrease by 35% more. This would mean that the total decreases in residuals between inflow and outflow would be 12 and 22 Hm^3 in 2025 and 2050. This does not change the fact that the contribution of secondary succession in farmlands below 1600 m is still not causing water stress in the future.

The used correction factor was based on the relative contribution of the monthly measured discharge at Jaca to the total measured reservoir inflow. It was decided to use a monthly changing

correction factor because the relative contribution of the sub catchment to the reservoir inflow changed each month (Figure 12). The differences in the monthly contribution from the Jaca sub catchment to the reservoir can be explained by the fact that elevations of sub catchments that contribute to the Yesa reservoir inflow are not equal. This means the contribution of melt water from snow is not equal. The Jaca sub catchment has relatively high elevations and thus precipitation is stored as snow instead of being passed as runoff. During spring, this snow melts, which results in the discharge peaks. High elevations receive more rainfall than low elevations. Because during summer the rain is not retained as snow, the contribution of the Jaca sub catchment is relatively large.

The simple extrapolation method results in a relatively good simulation of the measured 2005-2006 reservoir inflow with a Pearson correlation coefficient of 0.94 for monthly inflow totals (Figure 21). Therefore it is assumed that the effects of vegetation change on modeled discharge that were found in the sub catchment are translated relatively well to the larger scale effects of the reservoir inflow. An exception is the month March during which the reservoir inflow is overestimated quite profoundly. This means that the changes in reservoir inflow due to vegetation growth for this month are expected to be exaggerated compared to the other months.

5.4 Future climate and demand

5.4.1 Objective and approach

In addition to the effect of vegetation growth on river discharge, also two scenarios are studied which consider future changes in climate and water demand. This way the changes in water stress due to land abandonment can be put in perspective of the changes due to climate variations. In order to assess the effect of climate change on fluvial discharge, a scenario was run with higher temperatures and less precipitation than was measured during the hydrological year of 2005-2006. Temperatures were increased by 0.5 and 1 ℃ and precipitation decreased by 5 and 10% in order to represent the years 2025 and 2050 respectively. Future demand was estimated based on modeled future irrigation by Wada et al. (2012). The measured outflow from the reservoir in 2005 was increased proportionally to the relative increase in irrigation demand for 2025 and 2050 as modeled by Wada et al. (2012).

5.4.2 What is the effect of climate change on reservoir inflow in the future?

The small change in climate to warmer and drier conditions has a drastic influence on the river discharge compared to the effect of vegetation growth in abandoned fields. The total modeled river discharge from the sub catchment for the year 2050 is 14 and 15 Hm^3 for the scenarios with just climate change (Clim) and the combined scenario of vegetation and climate change (SV Clim) respectively. When the modeled discharges from the sub catchment are extrapolated to the Yesa catchment, the impact of climate change on reservoir inflow can be compared with the impact of vegetation growth in abandoned fields. It becomes clear that the contribution of climate change to problems with water availability is much larger than the contribution of secondary succession. Vegetation growth in abandoned fields alone (SV) is, as mentioned above not expected to cause major problems with water stress. The hypothetical scenario in combination with vegetation change (SV Clim) leads to a total reduction of 78 Hm^3 in residuals between reservoir inflow and outflow for 2050. Since the residual between total inflow and outflow in 2005 was only 53 Hm^3, this means that future water demand has to decrease to assure that enough water will be available for irrigation.

Not just the total yearly inflow changed, also the seasonality of inflow changes due to the hypothetical climate scenario. Warmer temperatures and less rain throughout the year result in a decrease in autumn and spring inflow, while inflow during winter months actually increases (Figure 23 and Figure 25). The decrease in autumn and spring inflow is mainly caused by the decrease in precipitation. When rain totals are the highest, a small change in terms of percentages still means a

large change in terms of absolute volume. During winters the rain totals are less high and then a reduction by a small fraction actually is a small reduction in terms of volumes of water. The increase in temperature is noticed most during winter, when higher temperatures mean less precipitation is retained in the form of snow and more water is available for runoff. Again changes during summer discharge are not noticed because the river is dry.

5.4.3 What is the effect of changes in water demand?

The scenario with increased future water demand for irrigation results in massive water shortage, mainly during summer months (Figure 25). The combination of vegetation growth in abandoned fields, hypothetical climate scenario and increased future demand result in decrease of over 180 Hm3 in residuals between reservoir inflow and outflow. Since the surplus in 2005 was only 53 Hm3, this means a total shortage of about 130 Hm3 water.

5.4.4 Quality and weaknesses

The estimations for future irrigation demand are based on the results of a large scale global model of Wada et al. (2012). A very simple method is used to translate the results of one pixel of this global model to relatively small Yesa reservoir. It cannot be expected that the global model perfectly simulates the regional conditions in the study area. The scenario merely serves as a general indication of the future trend in water demand. Also the climate and demand scenarios and results are not realistic because the predicted situation of a shortage of 130 Hm^3 water in 2050 can never happen. A shortage of 130 Hm^3 water in 2050 means that problems have already arisen before that year and the system must have made adjustments to the conditions. In a drought year people can decide to change crops, so crops that are present now may not be representative of crops that are grown in a dry year. This makes future water demand in irrigation districts hard to determine. Another complicating factor is the impact of the economy on crop prices which determine the types of crops that are grown. The results of this study can be seen as a warning that when things continue to go as expected, there will be problems.

6 Conclusions

What is the reconstructed vegetation cover in abandoned farmlands from 1950 to 2050?

Formerly abandoned fields represent about 24% of elevations below 1600 m and 12.5% of the total study area and are located on gentle slopes below elevations of 1600 m. Vegetation initially expands rapidly after which growth rates decline as the succession continues. The most suitable locations are covered by forests after about 15 years, while the forest state is not reached within 100 years in the most unsuitable sites. Roughly 57% of the abandoned area is covered with forest by 2005 and by 2050 this has increased to 78%. This means forest cover of the study area increase from 33% in 1950 to 40% in 2005 and reaches 42% in 2050.

What is the hydrological response of the system to vegetation growth in terms of infiltration, evapotranspiration and runoff?

Secondary succession from 1950 is estimated to be responsible for a decrease in total yearly runoff of over 4% by 2005 and over 5% by 2050. Changes in runoff were only noticed during winter months. These decreases are mostly caused by changes in vegetation properties and to a lesser extent by changes in soil characteristics. The decreases in total yearly river discharge due to vegetation growth are reflected by a net increase in total yearly evapotranspiration. Evapotranspiration is increased during winter months, but decreases from July to September. This is because the negative effect of decreased stomatal conductance on evapotranspiration from the subsurface is dominant over the positive effects of decreased albedo and higher vegetation during dry and hot summer months. When soils are wetter during winter months, the positive effects of vegetation growth on evapotranspiration from the subsurface are dominant. Evaporation from the canopy is increased throughout the year. Vegetation growth results in increased storage capacity and faster drainage of the soil, which means that more water can infiltrate. However, during summer months the soils are dry and infiltration is limited by water availability, which is lower due to the increased canopy evaporation. This results in a decrease in infiltration during summer months. During winter months soils are wet and the increased storage capacity and faster drainage of the soil due to vegetation growth allow more water to infiltrate.

What is the effect of secondary succession on monthly residuals between reservoir inflow and outflow?

Secondary succession in abandoned fields leads to a decrease in reservoir inflow. This decrease is mainly observed during December and March, which are months with high surpluses of reservoir inflow compared to outflow. The total modeled decreases of 8 and 14 Hm^3 in residual between reservoir inflow and outflow for the respective years of 2025 and 2050 do not exceed the surplus of 53 Hm^3 inflow in 2005. This means that, although less water can be stored during December and March, changes in vegetation due to secondary succession are not likely to cause major water stress in the future. However, the decrease in reservoir inflow during spring will require more reservoir filling during winter months and this will push the reservoir more to its safety limits.

The results of this study are expected to underestimate the effect of vegetation growth and the decreases in river discharge should actually be more profound. This is because the abandoned area in the sub catchment is underrepresented compared to the Yesa catchment. Also, not all processes related to vegetation change are considered in the model and summer discharges are underestimated.

7 References

1. Allen, R.G., L.S. Pereira, D. Raes et al. (1998). Crop evapotranspiration - guidelines for computing crop water requirements. FAO Irrigation and Drainage Papers drainage paper 56 ed., FAO. http://www.fao.org/docrep/X0490E/X0490E00.htm
2. Álvaro-Fuentes, J., Easter, M., Cantero-Martinez, C., Paustian, K., 2011. Modeling soil organic carbon stocks and their changes in the northeast of Spain. European Journal of Soil Science. 62. 5. 685–695.
3. Arora V.K., Boer G.J., 2005. A parameterization of leaf phenology for the terrestrial ecosystem component of climate models. Global Change Biology 11:39–59
4. Ayuda M. A., Pinilla V,. 2002. El proceso de desertización demográfica de la montaña pirenaica en el largo plazo: Aragón. Ager 2:101–138.
5. Basist A., Bell G.D., Meentemeyer V., 1994. Statistical relationships between topography and precipitation patterns. J Clim 7:1305–1315
6. Beguería, S., López-Moreno, J.I., Lorente, A., Seeger, M., Garcia-Ruiz, J.M., 2003. Assessing the effect of climate oscillations and land-use changes on streamflow in the Central Spanish Pyrenees. Ambio 32, 283–286.
7. Beniston M., 2006. Mountain weather and climate: a general overview and a focus on climatic change in the Alps. Hydrobiologia, 562, 3–16.
8. Bosch, J.M. and J.D. Hewlett. 1982. “A review of catchment experiments to determine the effect of vegetation changes on water yield and evapotranspiration.” J. Hydrol. 55: 3-23
9. Bravo F., Bravo-Oviedo A., Diaz-Balteiro L., 2008. Carbon sequestration in Spanish Mediterranean forests under two management alternatives: a modeling approach. Eur J For Res 127(3):225–234
10. Breuer, L., Eckhardt, K., & Frede, H. G., 2003. Plant parameter values for models in temperate climates. Ecological Modeling, 169, 237−293
11. Brolsma, R. J., and M. F. P. Bierkens., 2007. Groundwater–soil water–vegetation dynamics in a temperate forest ecosystem along a slope, Water Resour. Res., 43, W01414, doi:10.1029/2005WR004696.
12. Calder, I.R 1998. “Water Resource and Land Use issues.” SWIM Paper 3. Colombo, Sri Lanka: Water management Inst. http:/ /www.cgiar.org/iwmi/pubs/SWIM/swim03.pdf
13. Canadell, J., R.B. Jackson, J.R. Ehleringer, H.A. Mooney, O.E. Sala, and E.D. Schulze. 1996. “Maximum rooting depth of vegetation types at the global scale.” Oecologia 108: 583- 595.
14. CEH. Centre of Hydrographic Studies, http://hercules.cedex.es/anuarioaforos/default.asp
15. Cerdà, A., 1998. The influence of geomorphological position and vegetation cover on the erosional and hydrological processes on a Mediterranean hillslope. Hydrol. Process., 12: 661–671. doi: 10.1002/(SICI)1099-1085(19980330)12:4<661::AID-HYP607>3.0.CO;2-7
16. Chauvelier, F., 1987. Reboisement et amenagement de l’espace. l’example de la province de Huesca (Espagne) (647 pp). Doctoral thesis, Université of Burdeaux III.
17. CNIG. Centre of Geographical Information: http://centrodedescargas.cnig.es/CentroDescargas/buscadorCatalogo.do
18. Cognard-Plancq, A.L., Marc, V., Didon-Lescot, J.F. and Normand, M. 2001. The role of forest cover on streamflow down sub-Mediterranean mountain watersheds: a modelling approach. J. Hydrol. 254, 229–243.
19. Corina Land Cover. gisdata (\\clarke.geo.uu.nl).
20. Cox P.M., 2001. Description of the TRIFFID Dynamic Global Vegetation Model. Technical Note 24 Hadley Centre, Met Office
21. Dadkhah, M., and G. F. Gifford. 1981. Influence of vegetation, rock cover, and trampling on infiltration rates and sediment production. Water Resources Bulletin 16:979–985.

22. Davis, M.A., Wrage, K.J., Reich, P.B., Tjoelker, M.G., Schae□er, T. & Muermann, C., 1999. Survival, growth, and photosynthesis of tree seedlings competing with herbaceous vegetation along a water-light-nitrogen gradient. Plant Ecology, 145, 341-350.
23. De Jong, S. M. and Jetten, V. G. 2007. Estimating spatial patterns of rainfall interception from remotely sensed vegetation indices and spectral mixture analysis.. International Journal of Geographical Information Science, 21(5): 529–545. [Taylor & Francis Online],
24. Del Barrio, G., Creus, J. & Puigdefábregas. J., 1990. Thermal seasonality of the high mountain belts of the Pyrenees. Mountain Res. Devel. 10, 227–233.
25. Dunne, T., W. Zhang, and B. F. Aubry ., 1991, Effects of Rainfall, Vegetation, and Microtopography on Infiltration and Runoff, Water Resour. Res., 27(9), 2271–2285, doi:10.1029/91WR01585.
26. SAIH Ebro. Ebro river basin authority, (http://195.55.247.237/saihebro/index.php?url=/historicos/peticion)
27. ESDBv2 Raster Library - a set of rasters derived from the European Soil Database distribution v2.0 (published by the European Commission and the European Soil Bureau Network, CD-ROM, EUR 19945 EN); Marc Van Liedekerke, Arwyn Jones, Panos Panagos ; 2006.
28. FAO/IIASA/ISRIC/ISSCAS/JRC, 2012. Harmonized World Soil Database (version 1.2). FAO, Rome, Italy and IIASA, Laxenburg, Austria.
29. Farley, K. A., Jobbágy, E. G. and Jackson, R. B., 2005. Effects of afforestation on water yield: a global synthesis with implications for policy. Global Change Biology, 11: 1565–1576. doi: 10.1111/j.1365-2486.2005.01011.x
30. Feddes R A, Kowalik P J and Zaradny H 1978 Simulation of field water use and crop yield. Simulation Monographs, Pudoc, Wageningen, The Netherlands.
31. Florinsky, I.V., Kuryakova, G.A., 1996. Influence of topography on some vegetation cover properties. Catena 27 (2), 123–141.
32. Fontaine T.A., Cruickshank T.S., Arnold J.G., Hotchkiss R.H., 2002. Development of a snowfall–snowmelt routine for mountainous terrain for the soil water assessment tool (SWAT). Journal of Hydrology 262(1–4): 209–223.
33. Gallart F, Llorens P, Latron J, Regüés D. 2002. Hydrological processes and their seasonal controls in a small Mediterranean mountain catchment in the Pyrenees. Hydrology and Earth System Sciences 6(3): 527– 537. http://hal.archives-ouvertes.fr/hal-00304709
34. Garcia Ruiz, J. M., Lasanta-Martinez, T., 1990. Land-use changes in the Spanish Pyrenees. Mountain Research and Development 10, 267–279.
35. Garcia-Pausas, J., Casals, P., Camarero, L., Huguet, C., Sebastià, M.-T., Thompson, R., Romanyà, J., 2007. Soil organic carbon storage in mountain grasslands of the Pyrenees: effects of climate and topography. Biogeochemistry 82, 279–289
36. García-Ruiz J M, Lana-Renault N, Beguería S et al., 2010. From plot to regional scales: Interactions of slope and catchment hydrological and geomorphic processes in the Spanish Pyrenees.Geomorphology, 120(3—4): 248–257. doi: 10.1016/j.geomorph.2010.03.038
37. García-Ruiz, J. M., Puigdefábregas, J. & Creus, J., 1986. La acumulación de la nieve en el Pirineo Central y su influencia Hidrológica (Snow accumulation and its hydrological influence in the Central Spanish Pyrenees) Pirineos 127, 27– 72.
38. García-Ruiz. J. M., Puigdefábregas, J. & Creus, J., 1985. Los recursos hídricos superficiales del Alto Aragón (Surface water resources of the High Aragón). Instituto de Estudios Altoaragoneses. Huesca, Spain.
39. Gauquelin, T., Jalut, G., Iglesias, M., Valle, F., Fromard, F. and Dedoubat, J. J., 1996. Phytomass and carbon storage in the Stipa tenacissima steppes of the Baza basin, Andalucia, Spain. Journal of Arid Environments, 34: 277–286.
40. Gay, L. W., 1991: Enhancement of evapotranspiration by advection in arid regions. Hydrological Interactions between Atmosphere, Soil and Vegetation, G. Kientz et al., Eds., Publ. 204, IAHS, 147–156.

41. Gessler, P.E., Chadwick, O.A., Chamran, F., Althouse, L., Holmes K., 2000. Modeling soil-landscape and ecosystem properties using terrain attributes Soil Science Society of America Journal, 64, pp. 2046–2056
42. Haverkort, A. J., Uenk, D., Veroude, H., and van de Waart, M., 1991. Relationships between ground cover, intercepted solar radiation, leaf area index and infrared reflectance of potato crops. Potato Res. 34:113-121.
43. Jobbágy, E. G. & Jackson, R. B., 2000. The vertical distribution of soil organic carbon and its relation to climate and vegetation. Ecol. Appl. 10, 423–436.
44. Karssenberg, D., De Jong, K. and Van der Kwast, J., 2007, Modeling landscape dynamics with Python. International Journal of Geographical Information Science, 21, pp. 483-495
45. Kosmas, C., S. Gerontidis, and M. Marathianou. 2000. The effect of land use change on soils and vegetation cover over various lithological formations on Lesvos (Greece). Catena 40:51–68.
46. Lampre, F., 1998. Estudio geomorfológico de Ballibierna, Macizo de la Maladeta, Pirineo Aragonés. Modelado glaciar y periglaciar (Geomorphologic study of Ballibierna, Maladeta Sector, Aragonés Pyrenees. Glacial and periglacial forms). Consejo de Protección de la Naturaleza de Aragón. Zaragoza, Spain.
47. Lana-Renault, N., Latron, J., Karssenberg, D., Serrano, P., Regüés, D. & Bierkens, M. F. P., 2011. Differences in streamflow in relation to changes in land cover: a comparative study in two sub-Mediterranean mountain catchments. J. Hydrol. 411, 366–378.
48. Lasanta T., Beguería S., García-Ruiz J.M., 2006. Geomorphic and hydrological effects of traditional shifting agriculture in a Mediterranean mountain area, central Spanish Pyrenees. Mountain Research and Development 26(2): 146–152.
49. Lasanta-Martínez, T., S. M. Vicente-Serrano, and J. M. Cuadrat-Prats. 2005. Mountain Mediterranean landscapeevolution caused by the abandonment of traditional primary activities: a study in the Spanish Central Pyrenees. Applied Geography 25:47–65.
50. Lecina, S., Isidoro, D., Playán, E., Aragüés R., 2010. Irrigation modernization in Spain: effects on water quantity and quality. A conceptual approach Int. J. Water Resour. D, 26, pp. 265–282
51. Llorens, P., R. Poch, J. Latron, and F. Gallart. 1997. “Rainfall interception by a Pinus sylvestris forest patch overgrown in a Mediterranean mountainous abandoned area. I. Monitoring design and results down to the event scale.” J. Hydrol. 199: 331-345.
52. López Moreno J. I., 2005. Recent variations of snowpack depth in the Central Spanish Pyrenees. Arctic Antarctic and Alpine Research37: 253–260.
53. López Moreno J.I., García Ruiz J.M., 2004. Influence of snow accumulation and snowmelt on streamflow in the Central Spanish Pyrenees. International Journal of Hydrological Sciences 49: 787–802.
54. Lopez Moreno, J. I., 2004. The Management of a Large Mediterranean Reservoir: Storage Regimens of the Yesa Reservoir, Upper Aragon River Basin, Central Spanish Pyrenees.
55. López-Moreno JI, Vicente-Serrano SM, Morán-Tejeda E, Zabalza J, Lorenzo-Lacruz J, Garcı´a-Ruiz JM., 2011. Impact of climate evolution and land use changes on water yield in the Ebro basin. Hydrol Earth Syst Sci 15:311–322
56. Lopez-Moreno, J.I., Goyette, S. & Beniston, M., 2008. Climate change prediction over complex areas: spatial variability of uncertainties and predictions over the Pyrenees from a set of regional climate models. Int. J. Climatol., 28, 1535–1550.
57. Molinillo, M., Lasanta, T. and García-Ruiz, J.M. 1997. Managing mountainous degraded landscapes after farmland abandonment in the Central Spanish Pyrenees. Environ. Mgmt 21, 587–597.
58. Montané, F., Rovira, P. & Casals, P., 2007. Shrub encroachment into mesic mountain grasslands in the Iberian peninsula: effects of plant quality and temperature on soil C and N stocks. Global Biogeochem. Cycles, 21, GB4016.

59. Moore, I.D., Gessler, P.E., Nielsen, G.A., Peterson G.A., 1993. Soil attribute prediction using terrain analysis Soil Science Society of America Journal, 57 pp. 443–452
60. Morgan, R. P. C., 2005. Soil Erosion and Conservation (third edition ed.)Blackwell Publishing Ltd.
61. Morgan, R.P.C., 2001. A simple approach to soil loss prediction: a revised Morgan–Morgan–Finney model Catena, 44, pp. 305–322
62. Mottet A., Ladet S., Coque N., Gibon A., 2006. Agricultural land-use change and its drivers in mountain landscapes: a case study in the Pyrenees. Agric Ecosyst Environ 114:296–310.
63. Navas, A., Machín, J., and Soto, J., 2005: Assessing soil erosion in a Pyrenean mountain catchment using GIS and fallout 137Cs, Agr. Ecosyst. Environ., 105, 493–506,
64. Navas, A., Soto, J., Machín, J., 2002. ^{238}U, ^{226}Ra, ^{210}Pb, ^{232}Th and ^{40}K activities in soil profiles of the Flysch sector (Central Spanish Pyrenees). Appl. Radiat. Isot. 57, 579–589.
65. Ortigosa, L. M., 1990. Land reclamation by reforestation in the central Pyrenees. Mountain Research and Development 10, 281–288.
66. Paterson, W.S.B., 1994.The Physics of Glaciers,. 3rd edition. Pergamon, Elsevier Science Ltd, 1994. ISBN. 0 08 037945 1.
67. Pfeffer, K.,2003. Integrating spatio-temporal environmental models for planning ski runs.
68. Picon-Cochard, C., Coll, L. & Balandier, P., 2006. The role of below-ground competition during early stages of secondary succession: the case of 3-year-old Scots pine (Pinus sylvestris L.) seedlings in an abandoned grassland. Oecologia, 148, 373–383.
69. Poyatos R, Llorens P, Piñol J, Rubio C. 2008. Response of Scots pine (Pinus sylvestris L.) and pubescent oak (Quercus pubescensWilld.) to soil and atmospheric water deficits under Mediterranean mountain climate. Annals of Forest Science 65: 306
70. Pueyo Y., Beguería S., 2007.Modeling the rate of secondary succession after farmland abandonment in a Mediterranean mountain area. Landsc Urban Plan 83:245–254.
71. Rawls, W., Brakensiek, D., and Miller, N., 1983. "Green-ampt Infiltration Parameters from Soils Data." J. Hydraul. Eng., 109(1), 62–70. doi: 10.1061/(ASCE)0733-9429(1983)109:1(62)
72. Remón, J. L., 1997. Estructura y producción de pastos en el Alto Pirineo Occidental. Doctoral thesis, University of Navarra.
73. Richards F.J., 1959. A flexible growth function for empirical use, J. Exp. Botany 10(29) 290.
74. Rivas Martínez, S., 1987. Mapa de series de vegetación de Espanà. Madrid: ICONA.
75. Robinson, M., & Ward, R., 2000. Principles of Hydrology. Berkshire England: McGraw-Hill Publishing Company.
76. Rolland, C., 2003. Spatial and seasonal variations of air temperature lapse rates in Alpine regions. Journal of Climate 16,1032–1046.
77. Ruiz-Flaño, P., García-Ruiz, J.M. and Ortigosa, L. 1992. Geomorphological evolution of abandoned fields. A case study in the Central Pyrenees. Catena 19(3–4): 301–308.
78. Ruiz-Flano, P., T. Lasanta, J. M. García-Ruiz, and L. Ortigosa. 1991. The diversity of sediment yield from abandoned fields of the central Spanish Pyrenees. IAHS Publ. 203:103–110.
79. Schaap, M.G., F.J. Leij, and M.h . van Genuchten., 2001. Rosetta: A computer program for estimating soil hydraulic parameters with hierarchical pedotransfer functions. J. Hydrol. 251:163–176
80. Seibert J., 1997. Estimation of Parameter Uncertainty in the HBV Model. Nordic Hydrology , 28 (4/5), 247-262
81. Soane, B.D., 1990. The role of organic matter in soil compactibility: A review of some practical aspects Soil Tillage Res., 16 (1990), pp. 179–201
82. The national institute of meteorology (ftp://ftpdatos.aemet.es/series_climatologicas/
83. Van Beek et al., (in prep.). Abstract: Van Beek, L. P. H., Bierkens, M. F. P., 2012. Patterns and Pathways of Evolving Catchment Response in a Medium-Sized Mediterranean Catchment on a Millennium Scale. EGU General Assembly 2012, held 22-27 April, 2012 in Vienna, Austria., p.13081
84. Van Dam, O., 2000. POTRAD5 manual.doc

85. Van Genuchten, M.Th. 1980. A closed-form equation for predicting the hydraulic conductivity of unsaturated soils. Soil Sci. Am. J. 44:892-898.
86. Vicente-Serrano SM, López-Moreno JI. 2005. Hydrological response to different time scales of climatological drought: an evaluation of the Standardized Precipitation Index in a mountainous Mediterranean basin. Hydrology and Earth System Sciences 9: 523–533
87. Vicente-Serrano, S.M., Lasanta, T. and Romo, A., 2005: Analysis of spatial and temporal evolution of vegetation cover in the Spanish Central Pyrenees: Role of human management. Environmental Management, 34(6): 802–818.
88. Wada Y, Van Beek LPH, Bierkens MFP., 2011. Modeling global water stress of the recent past: on the relative importance of trends in water demand and climate variability. Hydrol Earth Syst Sci Discuss 8(4):7399–7460
89. Wada, Y., van Beek L. P. H., Sperna Weiland, F. C., Chao B. F., Wu Yun-Hao, Bierkens M. F. P., 2012. Past and future contribution of global groundwater depletion to sea-level rise. Geophysical Research Letters, doi:10.1029/2012GL051230, in press.
90. Wetzel, P., and J. T. Chang, 1987: Concerning the relationship between evapotranspiration and soil moisture. J. Climate Appl. Meteor., 26, 18–27.
91. Zhang, L., W.R. Dawes, and G.R. Walker. 2001. “Response of mean annual evapotranspiration to vegetation changes at catchment scale.” Water Resour. Res. 37: 701-708.

No detailed information on publications could be found of Cox (1980), Soane (1999), Chaney & Swift (1984) and Rachman et al. (2003) in Van Beek et al. (in prep.).

8 Appendices

Appendix 1 Table with interpretation of land use classes of the digital land use map Corina Land Cover 2006. Also given are the assigned aboveground carbon (C_a) (Kg m^{-3}) and stomatal conductance (g_s) (s m^{-1}) values.

#	Description CLC 2006	Land use class	C_a(Kg m^{-3})	g_s(s m^{-1})
1	Continuous urban fabric	bare soil	1E-04	1E+08
2	Discontinuous urban fabric	bare soil	1E-04	1E+08
3	Industrial or commercial units	bare soil	1E-04	1E+08
4	Road and rail networks and associated land	bare soil	1E-04	1E+08
5	Port areas	bare soil	1E-04	1E+08
6	Airports	bare soil	1E-04	1E+08
7	Mineral extraction sites	bare soil	1E-04	1E+08
8	Dump sites	bare soil	1E-04	1E+08
9	Construction sites	bare soil	1E-04	1E+08
10	Green urban areas	bare soil	1E-04	1E+08
11	Sport and leisure facilities	bare soil	1E-04	1E+08
12	Non-irrigated arable land	shrubs	3	6
13	Permanently irrigated land	shrubs	3	6
14	Rice fields	shrubs	3	6
15	Vineyards	shrubs	3	6
16	Fruit trees and berry plantations	shrubs	3	6
17	Olive groves	shrubs	3	6
18	Pastures	grass	0.3	6
19	Annual crops associated with permanent crops	shrubs	3	6
20	Complex cultivation patterns	shrubs	3	6
21	Land principally occupied by agriculture. with significant areas of natural vegetation	shrubs	3	6
22	Agro-forestry areas	forest	6.5	2.5
23	Broad-leaved forest	forest	6.5	2.5
24	Coniferous forest	forest	6.5	2.5
25	Mixed forest	forest	6.5	2.5
26	Natural grasslands	grass	0.3	6
27	Moors and heathland	shrubs	3	6
28	Sclerophyllous vegetation	shrubs	3	4
29	Transitional woodland-shrub	shrubs	3	4
30	Beaches. dunes. sands	bare soil	1E-04	1E+08
31	Bare rocks	bare soil	1E-04	1E+08
32	Sparsely vegetated areas	grass	0.3	6
33	Burnt areas	grass	0.3	6
34	Glaciers and perpetual snow	bare soil	1E-04	1E+08
35	Inland marshes	shrubs	3	6
36	Peat bogs	shrubs	3	6
40	Water courses	bare soil	1E-04	1E+08
41	Water bodies	bare soil	1E-04	1E+08

Appendix 2 Input parameters for ROSETTA for different organic matter fractions of the soil (OM).

OM (%)	Porosity %)	sand %)	silt (%)	clay (%)	Pbulk (g/cm3)
5	49.2	20.2	64.1	15.7	1.33
5.05	49.8	20.2	64.1	15.7	1.31
5.1	50.4	20.2	64.1	15.7	1.30
5.15	50.9	20.2	64.1	15.7	1.28
5.2	51.5	20.2	64.1	15.7	1.27
5.25	52.1	20.2	64.1	15.7	1.25
5.3	52.7	20.2	64.1	15.7	1.24
5.35	53.2	20.2	64.1	15.7	1.22
5.4	53.8	20.2	64.1	15.7	1.21
5.45	54.4	20.2	64.1	15.7	1.19
5.5	54.9	20.2	64.1	15.7	1.18
5.55	55.5	20.2	64.1	15.7	1.16
5.6	56.0	20.2	64.1	15.7	1.15
5.65	56.6	20.2	64.1	15.7	1.14
5.7	57.2	20.2	64.1	15.7	1.12
5.75	57.7	20.2	64.1	15.7	1.11
5.8	58.3	20.2	64.1	15.7	1.09
5.85	58.8	20.2	64.1	15.7	1.08
5.9	59.4	20.2	64.1	15.7	1.06

Appendix 3 Soil parameters for the different textural classes on the texture map.

Texture class	Description	OM (%)	θ_s (m3/m3)	$\theta_{(500)}$ m3/m3)	$\theta_{(333)}$ (m3/m3)	$\theta_{(15000)}$ (m3/m3)	Ksat (m h^{-1})	Kinf (m h^{-1})
2	ESDB medium grainsize	NA	0.45	0.27	0.29	0.15	0.01	0.041
6	for	5.9	0.59	0.29	0.34	0.09	0.04	0.041
7	shrub	5.4	0.54	0.26	0.31	0.09	0.02	0.041
8	rock	5.4	0.54	0.26	0.31	0.09	0.02	0.041
12	abandoned field	5	0.49	0.24	0.28	0.08	0.01	0.041
12	abandoned field	5.05	0.50	0.24	0.29	0.08	0.01	0.041
12	abandoned field	5.1	0.50	0.25	0.29	0.08	0.01	0.041
12	abandoned field	5.15	0.51	0.25	0.29	0.08	0.02	0.041
12	abandoned field	5.2	0.52	0.25	0.30	0.08	0.02	0.041
12	abandoned field	5.25	0.52	0.26	0.30	0.08	0.02	0.041
12	abandoned field	5.3	0.53	0.26	0.30	0.08	0.02	0.041
12	abandoned field	5.35	0.53	0.26	0.31	0.08	0.02	0.041
12	abandoned field	5.4	0.54	0.26	0.31	0.09	0.02	0.041
12	abandoned field	5.45	0.54	0.27	0.31	0.09	0.02	0.041
12	abandoned field	5.5	0.55	0.27	0.32	0.09	0.03	0.041
12	abandoned field	5.55	0.55	0.27	0.32	0.09	0.03	0.041
12	abandoned field	5.6	0.56	0.27	0.32	0.09	0.03	0.041
12	abandoned field	5.65	0.57	0.28	0.33	0.09	0.03	0.041
12	abandoned field	5.7	0.57	0.28	0.33	0.09	0.03	0.041
12	abandoned field	5.75	0.58	0.28	0.33	0.09	0.04	0.041
12	abandoned field	5.8	0.58	0.29	0.34	0.09	0.04	0.041
12	abandoned field	5.85	0.59	0.29	0.34	0.09	0.04	0.041
12	abandoned field	5.9	0.59	0.29	0.34	0.09	0.04	0.041

Appendix 4 Simulated monthly (graph) and total annual (table) precipitation for different altitudes.

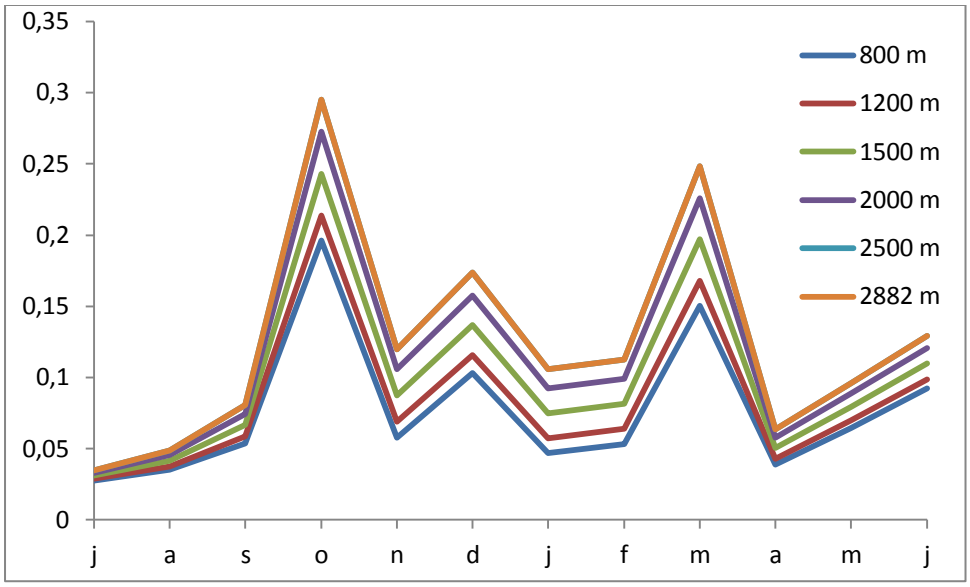

Elevation	800 m	1200 m	1500 m	2000 m	2500 m	2882 m
Annual total (mm)	78	92	102	120	137	151

Appendix 5 Modeled average daily temperature for low (800 m) and high (2882 m) elevations, tempereatures for other elevations range between these extremes.

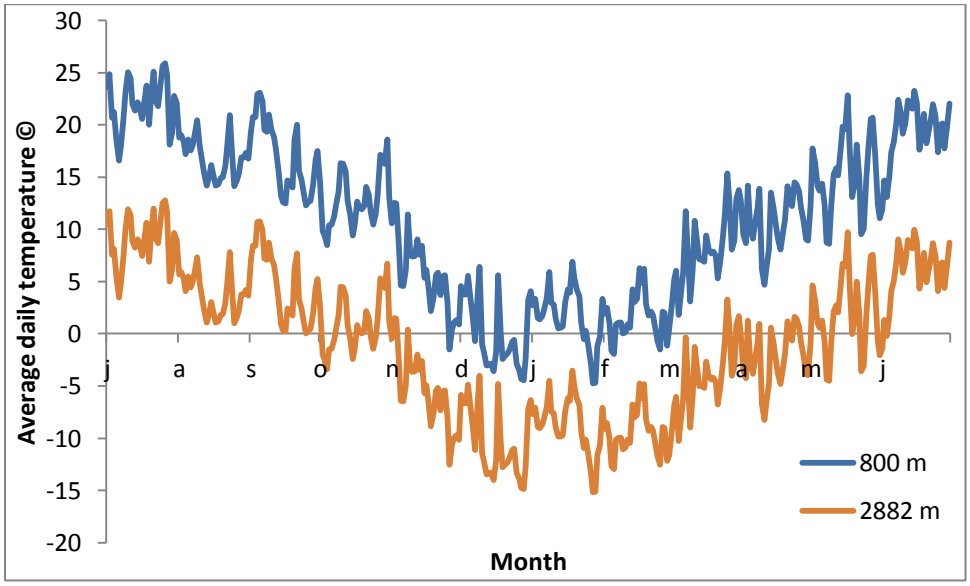

Appendix 6 Modeled water content of snow cover (m) at different elevations throughout the year.

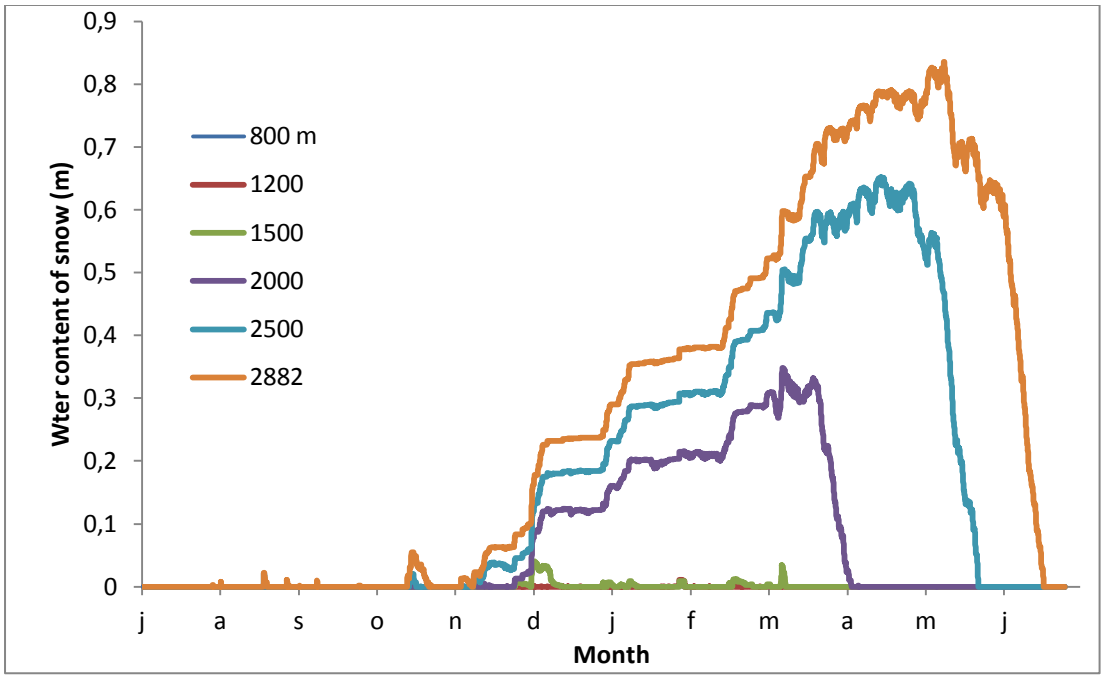

Appendix 7 Yearly transition probabilities for abandoned lands to transform to forest for the period from 1950 -1977 (logistic model b) and 1977-2050 (logistic model c). Modeled yearly transition probabilities from abandoned land to forest for the period between 1950 and 1977 vary between 0 in the most unsuitable locations and 0.069 in the most suitable locations. Transition probabilities are lower for the period from 1977 onwards, with a maximum of 0.53. Examples of modeled carbon growth curves and transitions in vegetation and soil parameter values are presented in Appendix 12. Resulting carbon densities can be found in Appendix 8.

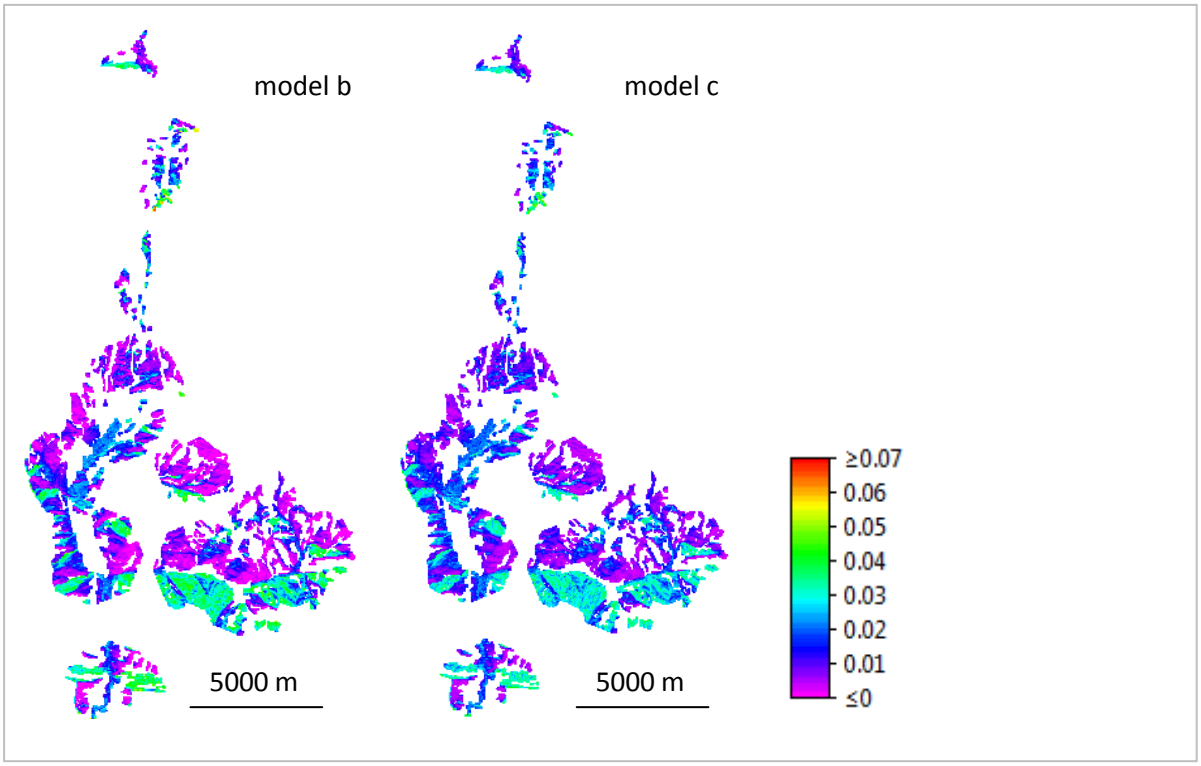

Appendix 8 Aboveground carbon densities (Kg m^{-3}) in abandoned fields as modeled for the years 1950, 1975, 2005, 2025 and 2050.

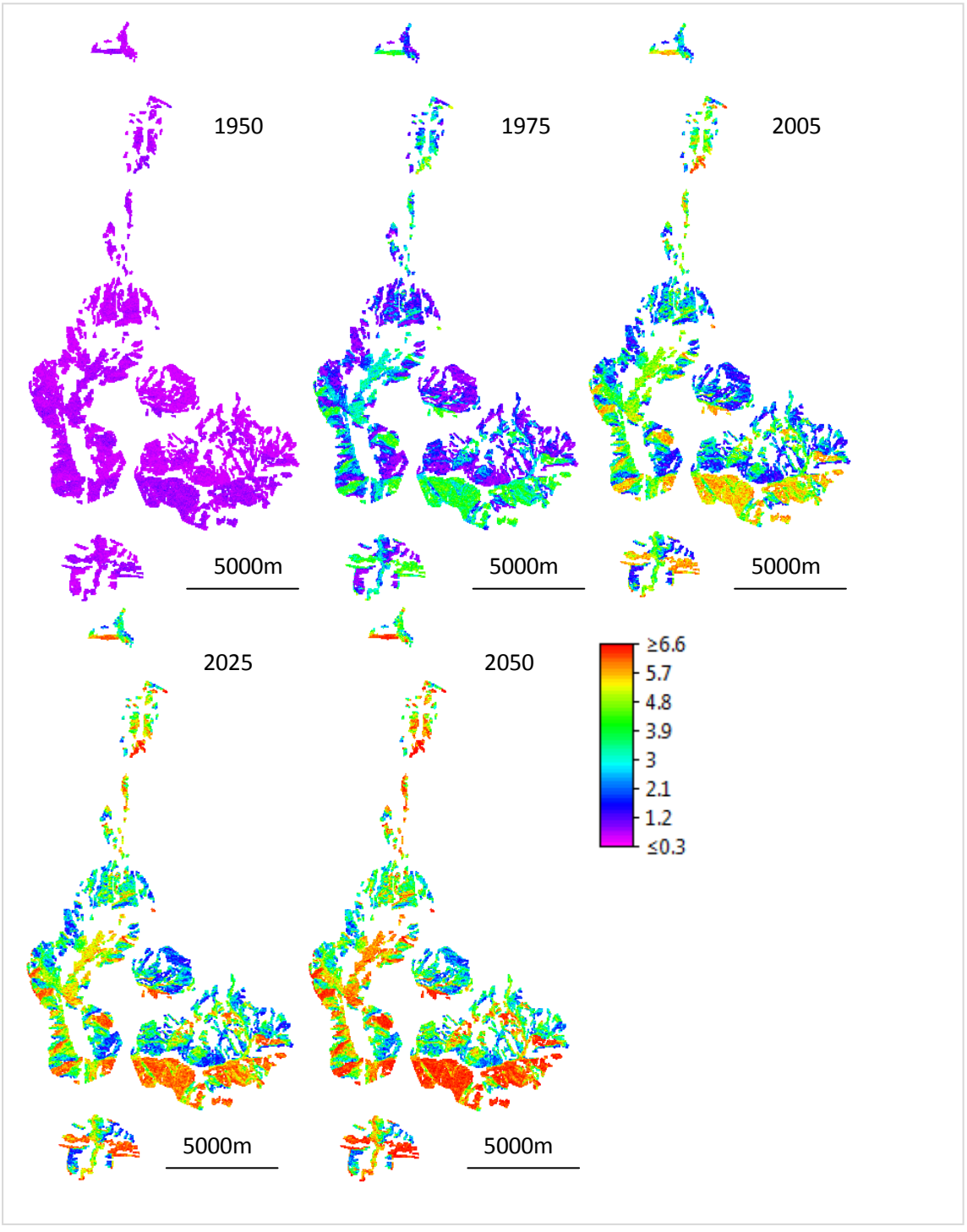

Appendix 9 Exact values of the graph in Figure 17. Dif and Dif (%) give the differences between that specific scenario and scenario SV1950, with negative values indicating discharge have decreased compared to SV1950.

		SV	S (V1950)	V (S1950)
1950	Totals	88,79	88,79	88,79
	Dif	-	-	-
	Dif(%)	-	-	-
1975	Totals	86,63	88,47	86,85
	Dif	-2,16	-0,32	-1,94
	Dif(%)	-2,43%	-0,36%	-2,19%
2005	Totals	85,12	88,27	85,35
	Dif	-3,67	-0,52	-3,44
	Dif(%)	-4,14%	-0,58%	-3,87%
2025	Totals	84,53	88,19	84,77
	Dif	-4,25	-0,60	-4,02
	Dif(%)	-4,79%	-0,67%	-4,53%
2050	Totals	84,04	88,13	84,27
	Dif	-4,75	-0,66	-4,52
	Dif(%)	-5,35%	-0,74%	-5,09%

Appendix 10 Exact values of the graphs in Figure 19. Dif and Dif (%) give the differences between that specific scenario and scenario SV1950, with negative values indicating discharge have decreased compared to SV1950.

	SV1950	SV2050	S1950V2050	S2050V1950
EtotIc	34,45	38,73	38,73	34,45
Dif	-	4,28	4,28	0,00
Dif%	-	12,44%	12,44%	0,00%
EtotSC	5,00	5,06	5,06	5,00
Dif	-	0,05	0,05	0,00
Dif%	-	1,04%	1,04%	0,00%
EtotSub	128,22	128,61	128,37	128,88
Dif	-	0,39	0,15	0,66
Dif%	-	0,30%	0,12%	0,52%
Etot	167,67	172,39	172,16	168,33
Dif	-	4,72	4,49	0,66
Dif%	-	2,82%	2,68%	0,40%
Inftot	140,01	139,67	139,44	141,26
Dif	-	-0,33	-0,56	1,26
Dif%	-	-0,24%	-0,40%	0,90%

Appendix 11 Exact values of the graphs in Figure 23. Total modeled river discharge from the sub catchment for scenarios with only vegetation change (SV), only hyptothetical climate change (Clim) and the combined effect (SV Clim).

totals	SV	Clim	SV Clim
2005	85,12	85,12	85,12
2025	84,53	66,07	65,69
2050	84,04	36,45	36,40

Appendix 12 Examples modeled carbon growth curves in suitable and not suitable locations.

Also presented are transitions in vegetation and soil parameter values, corresponding to carbon and organic matter growth in a cell with average terrain suitability (tp=0.02). Carbon density never reaches above 3 Kg m^2 in unsuitable locations. In more suitable locations, carbon growth shows an initial rapid growth which declines over time. Vegetation and soil parameters show gradual transitions with carbon density and organic matter except for vegetation height and albedo. Vegetation height and albedo show a sudden increase and decrease at the point where carbon density reaches 3 Kg m^2.

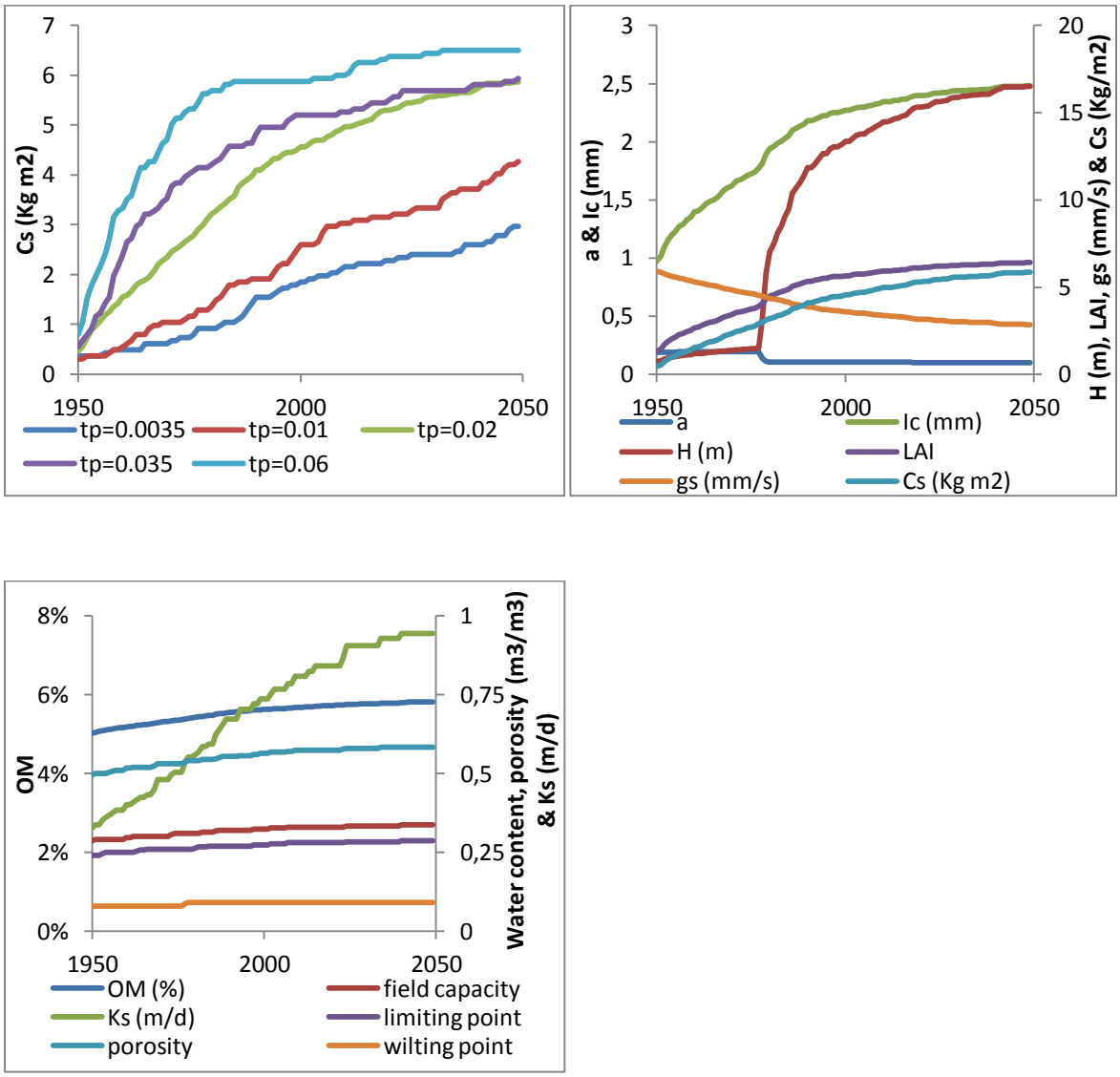

Graphs showing the transition of parameter values over time. (Top left) Aboveground carbon growth curves of five cells with different transition probabilities (tp) from shrub to forest. (Top right) Change in vegetation parameters over time for the carbon growth curve with tp=0.02. (Bottom left) Change in soil parameters over time for the carbon growth curve with tp=0.02.

Appendix 13 Vegetation growth model performance

The carbon growth curves at multiple locations initially show a rapid growth, declining as the carbon density comes closer to its maximum value (Appendix 12). The shapes of the curves compare well to the sigmoid curves of vegetation growth models in literature (e.g. Damgaard et al., 2002; Birch, 1999). These models adopt the equation first proposed by Richards (1959 in Birch, 1999). This equation consists of plant and site specific parameters that determine the shape of the curve for a certain plant in certain conditions. It cannot be used in this study since no information is available on the value of these shape parameters in the study area, let alone the spatial variation of the values. Therefore it impossible to compare the curves and the performance of the models, because the shapes are not necessarily determined by similar processes. All that can be said is that the curves show similar shapes.

With the used approach it is shown that similarly shaped growth curves can be attained without performing any fieldwork. The vegetation parameters I_c, LAI, H, g_s and a all correspond well to values from Breuer et al. (2003).This means that the shapes of the curves seem plausible and no unrealistic values are predicted. The rapid initial growth, followed by a slower transition towards the end succession stage satisfies the description of secondary succession by Molinillo et al. (1997). The sudden increase in vegetation height with carbon density at the transition from shrubs to forest (Appendix 12) is inevitable due to the shape of the equations. It is, however, the best what can be achieved and except for the kink, it resembles the vegetation height curves in Birch (1999) quite well. In both cases height initially increases slowly, reaches its maximum growth rate somewhere halfway and decreases again as the plant size reaches near the maximum asymptote. The slightly unrealistic sudden increase in this study is thought to have little effect on the results. Due to the large number of cells, the sudden increase in a few cells at a certain timestep has a negligible effect on the average increase in vegetation height during a time interval of multiple years.

Appendix 14 Monthly totals of daily precipitation measurements (columns) and total number of rain days (bars) in 2009 near villages at different altitudes spread out from North to South in the sub catchment. Villages from North to South are Candanchu at around 1500 m, Canfranc at roughly 1200 m and Albarun at about 1400 m. Rain days at different elevations and in the North and South of the study area are not the same. Also monthly precipitation totals do not increase with elevation by the same each month.

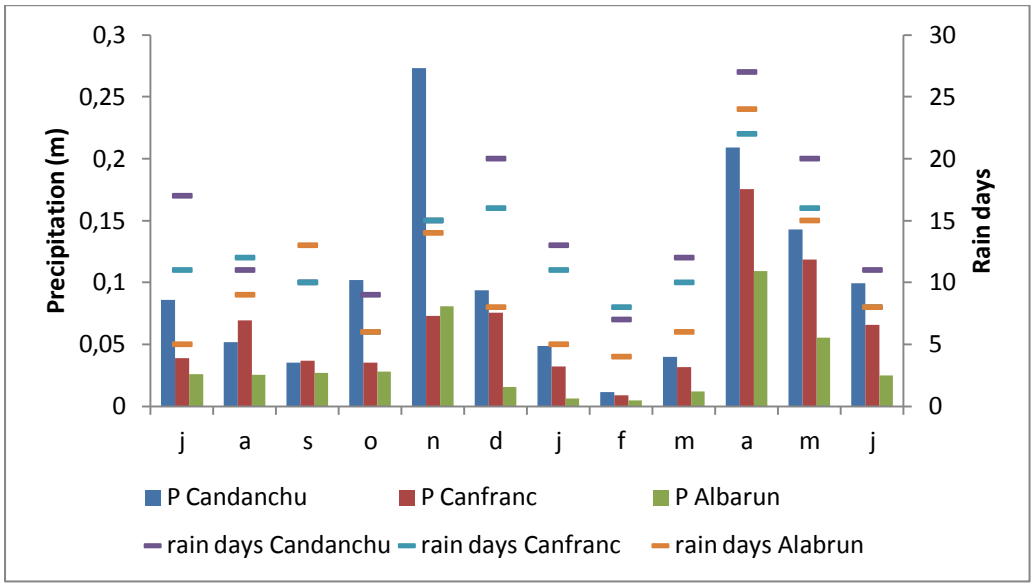

Appendix 15 Monthly precipitation totals (columns) and rain days (bars), as measured near Canfranc (1200 m) and modeled for elevations of 1200 m in this study. Rainfall totals during July and August are underestimated in the model. Also the amount of days with rain is underestimated.

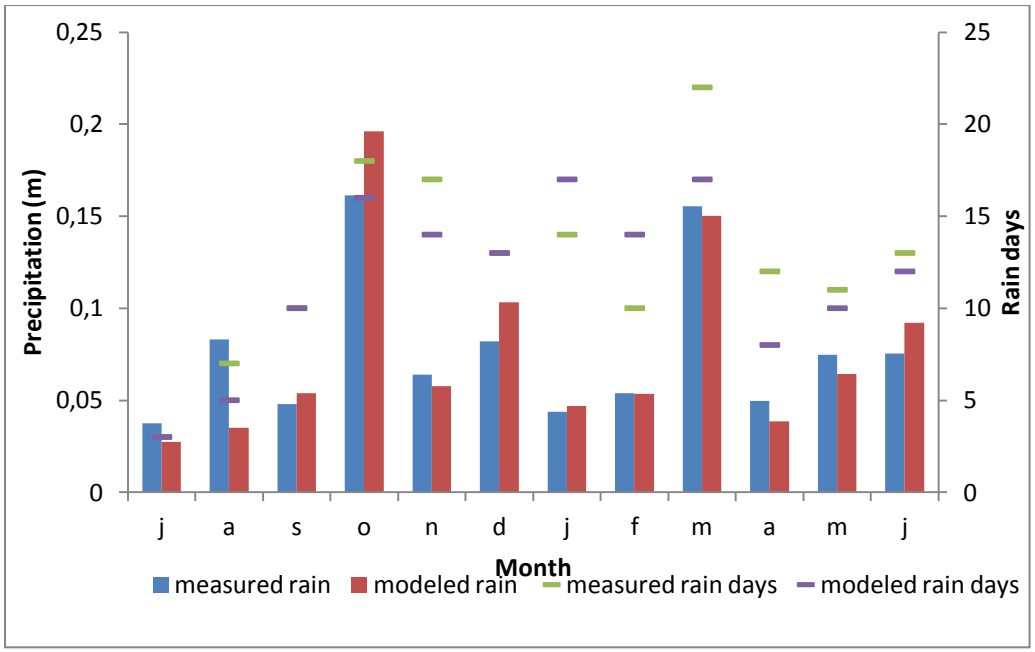

Appendix 16 Digital appendix Description

A digital file is available with model scripts, input data and map series. Contact the author or supervisors for access to this file.

Scripts

File name	Description
CarbonModel.py	Carbon simulation with Markov chain model
VegParameters.py	Linking vegetation parameters to carbon density
soil.py	Linking soil parameters to OM
soil_text_DR.txt	Construction of soil texture and soil depth maps (PCRaster script)
initial_map_script_final.txt	Construction of land use map for 1950 (PCRaster script)
potrad51.mod	Potential radiation model by drs. Oscar van Dam (2000). Note: do not use or distribute without prior approval of the author and reference to manual (POTRAD5 manual.doc). Last known contact information: oscar.van.dam@rps.nl
Main.py	Hydrological model script with added snow module. Version of Lana-Renault et al. (2012) is adapted in such a way that only .tss files are reported instead of map series. A map with all subclasses is added. Main.py should be in the same folder as all subclasses. self.Stom is multiplied by 4 in order to represent canopy stomatal conductance.
soilWaterRetention.xlsx	Excel sheet for calculation of water retention with van Genuchten (1980)
OM_porosity.xlsx	Excel sheet for calculation of change in porosity and bulk density with OM

Maps

File name	Description
dem_Yesa_catchment_25m.map	Digital Elevation Model (DEM) for Yesa catchment
dem_jaca.map	Digital Elevation Model (DEM) for sub catchment
Top_ind_jaca.map	Map with topographic index in the sub catchment for calculation of transition probabilities
Slope_jaca.map	Map with slope in the sub catchment for calculation of transition probabilities
PRadY1.map	Potential radiation map in the sub catchment for calculation of transition probabilities
catch_jaca.map	Clone map (boolean true) for the sub catchment
dr_jaca.map	Map with soil depth classes of the sub catchment
Text_jaca.map	Map with textural classes of the sub catchment
Input SV1950, SV1975, SV2005, SV2025 and SV2050	Maps with input files for different scenarios
Text_jaca_ESDB.map	Map with textural classes from the European Soil Database 2.0

Tables

File name	Description
4xairTemperatureArnaJulAugSep0506.tss	Temperature as measured by Lana-Renault et al. (2012) for the Arnás catchment between July first 2005 and August 2006.
4xincomingShortwaveRadiationArnasJulAugSep0506.tss	Incoming short wave radiation as measured by Lana-Renault et al. (2012) for the Arnás catchment between July first 2005 and August 2006.
4xrainfallFluxArnasJulAugSep0506.tss	Rainfall as measured by Lana-Renault et al. (2012) for the Arnás catchment between July first 2005 and August 2006.
4xrelativeHumidityArnasJulAugSep0506.tss	Relative humdidity as measured by Lana-Renault et al. (2012) for the Arnás catchment between July first 2005 and August 2006.
4xwindVelocityArnasJulAugSep0506.tss	Wind velocity as measured by Lana-Renault et al. (2012) for the Arnás catchment between July first 2005 and August 2006.
4xTLapse.tss	Lapse rates to translate temperature and precipitation to different altitudes
C_CLC.txt	Carbon density for different classes on Corina Land Cover map
Stom_CLC	Max stomatal conductance for different classes on Corina Land Cover map
depth_class.txt	Table containing different depth classes corresponding to soil_Text_DR.txt
landuse_class.txt	Table containing different land use classes corresponding to soil_Text_DR.txt
slope_class.txt	Table containing different slope classes corresponding to soil_Text_DR.txt
Fldcap.txt	Table containing field capacity values for different OM, belonging to soil.py
Ksat.txt	Table containing saturated conductivity values for different OM, belonging to soil.py
Limit.txt	Table containing limiting point values for different OM, belonging to soil.py
Prosity.txt	Table containing porosity values for different OM, belonging to soil.py
Wilt.txt	Table containing wilting point values for different OM, belonging to soil.py

Results

File name	Description
Carbon	Map stacks of simulated carbon density
OM	Map stacks of simulated organic matter
Results	Map containing results of the hydrological model for several scenarios